

The benefits of Post Weld Treatment for cost efficient and sustainable bridge design

Master of Science Thesis in the Master's Programme Structural Engineering and Building Technology

ANDREA MOSIELLO
KONSTANTINOS KOSTAKAKIS

Department of Civil and Environmental Engineering
Division of Structural Engineering
Steel and Timber Structures
CHALMERS UNIVERSITY OF TECHNOLOGY
Göteborg, Sweden 2013
Master's Thesis 2013:54

MASTER'S THESIS 2013:54

The benefits of Post Weld Treatment for cost efficient and sustainable bridge design

*Master of Science Thesis in the Master's Programme Structural Engineering and
Building Technology*

ANDREA MOSIELLO

KONSTANTINOS KOSTAKAKIS

Department of Civil and Environmental Engineering
*Division of Structural Engineering
Steel and Timber Structures*

CHALMERS UNIVERSITY OF TECHNOLOGY

Göteborg, Sweden 2013

The benefits of Post Weld Treatment for cost efficient and sustainable bridge design
Master of Science Thesis in the Master's Programme Structural Engineering and Building Technology

ANDREA MOSIELLO

KONSTANTINOS KOSTAKAKIS

© ANDREA MOSIELLO, KONSTANTINOS KOSTAKAKIS, 2013

Examensarbete/Institutionen för bygg- och miljöteknik,
Chalmers tekniska högskola 2013:54

Department of Civil and Environmental Engineering

Division of Structural Engineering

Steel and Timber Structures

Chalmers University of Technology

SE-412 96 Göteborg

Sweden

Telephone: + 46 (0)31-772 1000

Cover:

Material and Cost saving diagrams for railway and highway bridges – Life Cycle Cost analysis of a composite continuous bridge

Chalmers Reproservice / Department of Civil and Environmental Engineering
Göteborg, Sweden 2013

The benefits of Post Weld Treatment for cost efficient and sustainable bridge design
Master of Science Thesis in the Master's Programme Structural Engineering and Building Technology

ANDREA MOSIELLO

KONSTANTINOS KOSTAKAKIS

Department of Civil and Environmental Engineering

Division of Structural Engineering

Steel and Timber Structures

Chalmers University of Technology

Abstract

Most of the steel bridges being designed follow conventional design methods. In other words steel quality S355 is the most commonly used structural material, given its good cost to strength ratio, while other steel qualities are often not taken into consideration. A literature study is performed and focused on the advantages that high strength steel can ensure. Along with this aspect, the modern procedures of post weld treatment are investigated to determine whether they can be beneficial for bridge design. In particular, the aim of the study is to investigate a possible way to obtain advantages thanks to the combination of high strength steel and post weld treatment. With this background, four case studies and two parametric studies are performed. The case studies assess one railway and three highway existing bridges. Their designs are studied in detail and one or more alternatives are proposed and compared. The means of comparison are the total material saving and cost saving. In all cases, encouraging results are obtained with a saving range varying between 10% and 20%, in terms of cost. The projection of these detailed studies develops into two parametric studies focusing on the behavior of simply supported highway and railway bridges depending on the span length. The main outcome allowed specifying the span range that ensures the greatest benefits in terms of cost. Lastly, a brief Life Cycle Cost analysis and Life Cycle Assessment are implemented in one of the case studies, highlighting the further benefits of high strength steel bridge design.

Key words: High Strength Steel, Post Weld Treatment, Steel bridges, Highway, Railway, LCA, LCC

Contents

ABSTRACT	III
CONTENTS	V
PREFACE	IX
NOTATIONS	X
1 INTRODUCTION	1
1.1 Background	1
1.2 Purpose and aim	2
1.3 Scope and limitations	2
1.4 Methodology	2
2 HIGH STRENGTH STEEL AND ITS PROPERTIES	4
2.1 Chronology	4
2.2 Production process of HSS	5
2.2.1 Material composition	5
2.2.2 Working process	5
2.2.3 Heat treatment	6
2.3 Classification of HSS	7
2.3.1 High Strength Low Alloy Steel (HSLA)	7
2.3.2 High Performance Steel (HPS)	8
2.3.3 High Strength Weathering Steel (W)	8
2.4 Mechanical properties of HSS	9
2.4.1 Yield strength f_y and ultimate strength f_u	9
2.4.2 Fracture toughness	10
2.4.3 Ductility	11
2.4.4 Weldability	12
2.5 Examples of steel specifics	14
3 BENEFITS OF HSS IN BRIDGE APPLICATION	15
3.1 Production cost	15
3.2 Construction cost and time	16
3.3 Light weight	16
3.4 Environmental impact	16
4 APPLICATION OF HSS IN CONSTRUCTION	17
4.1 Examples of the use of HSS in the bridge industry	17
4.2 Examples of the use of HSS in other industries	19

5	INTRODUCTION TO FATIGUE AND ITS EFFECTS ON THE DESIGN OF WELDED DETAILS	21
5.1	Background of the phenomenon	22
5.2	Initiation and Propagation	23
5.3	Quantitative approach to fatigue	24
5.4	Fatigue design according to Eurocode	25
5.4.1	Details subjected to normal stresses	26
5.4.2	Details subjected to shear stresses	28
5.5	Fatigue assessment methods	29
5.5.1	Palmgren-Miner	30
5.5.2	Equivalent stress range concept	30
5.6	Fatigue life of welded details	31
5.6.1	Weld defects	31
5.6.2	Residual stresses due to welding process	32
5.6.3	Effect of steel grade on the fatigue life of a detail	33
6	INTRODUCTION AND DESCRIPTION OF POST-WELD TREATMENT METHODS	35
6.1	Classification of PWT methods	35
6.1.1	Weld geometry improvement methods	36
6.1.2	Residual stress methods	37
6.2	High Frequency Impact Treatment (HiFIT)	39
6.2.1	Description of the process	39
6.2.2	Suitability of the process	39
6.2.3	Effects of the process	40
6.2.4	Effectiveness of the process	41
7	DESIGN OF HIGHWAY AND RAILWAY BRIDGES ACCORDING TO EUROCODE	42
7.1	Models for highway traffic loads	42
7.2	Models for railway traffic loads	43
7.3	Fatigue load models for highway bridges	45
7.4	Fatigue load models for railway bridges	46
8	CASE AND PARAMETRIC STUDY OF RAILWAY BRIDGES	48
8.1	Original bridge design	48
8.1.1	Geometry and loading	48
8.1.2	Cross section verification	50
8.1.3	Results and remarks	52
8.2	New bridge design	52
8.2.1	Geometry and loading	53
8.2.2	Cross section verification	53
8.2.3	Results and remarks	54

8.3	Comparison between original and new bridge design	55
8.4	Parametric study	56
8.5	Summary	58
9	HIGHWAY BRIDGES	59
9.1	Original bridge design	59
9.1.1	Geometry and loading	59
9.1.2	Cross section verification	61
9.1.3	Results and remarks	63
9.2	New bridge design	64
9.2.1	Geometry and loading	64
9.2.2	Cross section verification	65
9.2.3	Results and remarks	66
9.3	Comparison between original and new bridge design	67
9.4	Parametric study	67
9.5	Summary	70
10	CONTINUOUS HIGHWAY BRIDGES	71
10.1	Original bridge designs	71
10.1.1	Geometry and loading	71
10.1.2	Cross section verification	73
10.1.3	Results and remarks	75
10.2	New bridge designs	76
10.2.1	Geometry and loading	76
10.2.2	Cross section verification	77
10.2.3	Results and remarks	78
10.3	Comparison between original and new bridge design	79
10.4	Summary	80
11	LONG TERM BENEFITS OF THE COMBINATION OF HSS AND PWT	82
11.1	Life Cycle Cost analysis on Bridge A	82
11.2	Life Cycle Assessment on Bridge A	84
11.3	LCC and LCA for Bridge B	85
12	BIBLIOGRAPHY	87

APPENDIX A

A.1	RAILWAY BRIDGE OVER ÖSTRA KLARÄLVEN	89
A.2	HIGHWAY BRIDGE OVER E4 IN SKULNÄS	111
A.3	CONTINUOUS HIGHWAY BRIDGE B	132

APPENDIX B

B.1	PARAMETRIC STUDY OF RAILWAY BRIDGES	180
B.2	PARAMETRIC STUDY OF HIGHWAY BRIDGES	182

Preface

This Master Thesis has been carried out in the period between January and June 2013 at the Division of Structural Engineering at Chalmers University of Technology, Göteborg, Sweden.

We would like to express our gratitude to our supervisor and examiner Prof. Mohammad Al-Emrani. His guidelines and consultations have been of great importance to the development of our study. Further, his role as a source of contacts has been extremely significant and allowed us to improve and implement the quality of the thesis, thanks to targeted comments and reviews made by experts in the field.

The experience of writing a Master Thesis has contributed to our personal growth. The process has been extremely inspiring and motivating, thus playing a meaningful role in sparking our interest concerning the field of bridge design. Having reached the end of our education as civil engineering students, we are looking forward to a future career as structural engineers.

Göteborg, June 2013

Andrea Mosiello and Konstantinos Kostakakis

Notations

Roman upper case letters

AR	As rolled
C	Carbon
CEV	Carbon Equivalent Value
C_n	Cost of painting
CO_2	Carbon dioxide
Cr	Chromium
C_{tot}	Total cost
Cu	Copper
D	Damage
E_{cm}	E-modulus of concrete
FLM1	Fatigue load model 1
FLS	Fatigue Limit State
HAZ	Heat Affected Zone
HiFIT	High Frequency Impact Treatment
HPS	High Performance Steel
HSLA	High Strength Low Alloy Steel
HSLM-A	High speed load model
HSS	High Strength Steel
K	Fracture toughness parameter
L	Length
LCC	Life Cycle Cost
LCA	Life Cycle Assessment
LM1	Load Model 1
LM71	Load Model 71
Mn	Manganese
Mo	Molybdenum
M_{ULS}	Moment in ULS
N	Number of cycles
N	Normalized
Nb	Niobium
Ni	Nickel
N_i	Crack initiation life
N_{obs}	Number of observations

N_p	Crack propagation life
PWHT	Post weld heat treatment
PWT	Post Weld Treatment
Q	Quenched and Tempered
Q_{ak}	Load of a single axle
Q_{ik}	Axle load
SCF	Stress Concentration Factor
SEK	Swedish Crown
Si	Silicon
SIF	Stress Intensity Factor
SLS	Serviceability Limit State
SW/0	Train load model
SW/2	Train load model
TIG	Tungsten inert gas
TM	Thermodynamically rolled
TS	Tandem system
UDL	Uniformly distributed load
ULS	Ultimate Limit State
V	Vanadium
V_{ULS}	Shear in ULS
W	High Strength Weathering Steel
W_{eff}	Effective sectional modulus
YR	Yield Ratio

Roman lower case letters

a	Length of a wagon
c	Spacing between wagons
f	Function of geometry and loading of the detail
f_{ck}	Concrete characteristic strength
f_u	Ultimate strength
f_y	Yield strength
m	Slope
n_i	Number of cycles
q_{ik}	Distributed car load
q_{vk}	Distributed trail load

$q_{w,bridge}$	Wind pressure
r	Discount rate

Greek upper case letters

ΔK	Stress intensity factor range
$\Delta\sigma$	Stress range
$\Delta\sigma_C$	Stress range of a detail
$\Delta\sigma_D$	Stress range at fatigue limit
$\Delta\sigma_{eq}$	Equivalent stress range
$\Delta\sigma_L$	Stress range at cut-off limit
$\Delta\tau_C$	Shear stress range at fatigue limit
$\Delta\tau_L$	Shear stress range at cut-off limit
Φ	Dynamic amplification factor

Greek lower case letters

α	Length of the crack
β_Q	Correction factor for LM2
β	Crack length and component geometry factor sufficient for a specimen
γ_D	Partial factor for distributed load
γ_g	Partial factor for self-weight
γ_o	Partial factor for occasional load
δ_{TOT}	Deflection
ρ_{S355}	Density of steel
σ	Applied stress
σ_{max}	Maximum stress
σ_{nom}	Nominal stress
ψ	Partial factor for load combinations

Others

$\frac{da}{dN}$	Crack growth rate
-----------------	-------------------

1 Introduction

1.1 Background

Nowadays, around the world, the common practice is to design both railway and highway steel or composite bridges in a “traditional way”. In other words steel quality S355 is used in most of the cases, since it ensures the best cost to strength ratio. Even though higher steel qualities have become available on the market in the last years, they have not been widely utilized in bridge design, if not for isolated details of hybrid girders.

The main reason why High Strength Steels are rarely introduced in bridge construction originates directly from the different criteria that are to be met during the design phase. All bridges should meet the main requirements listed and described in the Eurocodes in terms of *bending resistance*, *shear resistance*, *deflection* and *fatigue*, along with other instability phenomena. A closer look at the formulations given in the codes for each of the resistances abovementioned highlights that exclusively bending and shear resistances benefit from an increase of the tensile properties of the material. On the contrary, as far as deflection and fatigue are concerned, no improvement is to be expected since none of the two depends on the material properties.

As a consequence of what is stated above, there seems to be no true benefit resulting from the use High Strength Steel in bridge design, since deflection and fatigue tend to become the governing factors in the design phase. In detail, no true benefit can be achieved unless these new boundaries can be overcome.

Deflection is exclusively depending on the geometry of the section and can therefore be improved in two main ways: either by adjusting the cross-sectional dimensions of the members, or by pre-cambering the structure along its length.

Fatigue is depending on the specific resistance of critical welded details and in particular to the stress range that they are capable of withstanding. Therefore two main solutions can be found in this case as well: either avoiding welded details where suitable, or improving those that are essential. In this direction, a lot of research has been done in the last years. Post Weld Treatment methods have been developed in order to improve the weld profile and remove the residual stress concentrations originating from the welding process. This way the behaviour of the critical welds with regard to fatigue can be enhanced, along with the whole structure’s performance.

On a theoretical level it can then be concluded that great benefits can be achieved from the combinations of High Strength Steel and Post Weld Treatment. Such benefits can be counted in terms of material save, weight reduction, sustainable use of material and thus cost.

In this thesis both railway and highway bridge are assessed in detail. Different lengths and span arrangements are taken into consideration in order to cover a wide range of design cases. This is performed through both case and parametric studies. For each specific case study, the original design is compared to an improved version that is developed with the use of High Strength Steel combined with Post Weld Treatment. Possible benefits in terms of total construction cost can thus be estimated.

1.2 Purpose and aim

The purpose of the study of this master thesis is to determine in which cases the implementation of High Strength Steel and Post Weld Treatment in bridge design can result into remarkable benefits.

The aim is thus to optimize the original design of both railway and highway steel bridges in order to achieve full utilization of the material. Several existing steel bridges are assessed and a following parametric study is performed in order to investigate which span lengths show the greatest benefits in terms of material saving and thus cost.

1.3 Scope and limitations

The study focuses on steel girder bridges of different lengths.

The *railway bridges* present a welded hat profile and the relative parametric study concentrates on spans varying between 16m and 30m, since no benefit is found outside these boundaries. Only one-span simply supported bridges are studied.

The *highway bridges* present a composite structure with a reinforced concrete deck supported by steel I-girders. Both simply supported and continuous bridges are studied in detail in order to determine the differences of the behaviours. The parametric study is though limited to the simply supported bridges and in this case the span lengths vary between 16m and 44m.

The design and verifications are simplified according to the following criteria:

- the simply supported bridges are assumed to keep a constant cross-section geometry throughout the whole span
- the continuous bridges are assumed to have only two different cross-section geometries: one for the support and one for the span
- only the most critical loads are assumed to be acting on the bridges
- only the steel I-girders are verified and re-dimensioned, therefore the cost and material save refers exclusively to the above
- the concrete behavior is not considered in detail

The conclusions with regard to cost analysis and comparison are performed by taking into account just material cost and Post Weld Treatment cost. Other aspects affecting cost are thus neglected.

1.4 Methodology

The first step towards the stated purpose and aim consists of a literature study. The goal is to deepen the knowledge about the different steel qualities available, the different Post Weld Treatment methods and their benefits and the design process and verifications of steel bridges.

With this background, four different kinds of bridges are chosen and their design is studied in detail. For each of them, a Mathcad¹ template is created which includes all the different verifications to be fulfilled in accordance with the related Eurocodes,

¹ Mathcad version 15

with the exception of the fatigue verification: this aspect is evaluated through BridgeFAT².

A new version of the design is then proposed with the aim to achieve the best possible utilization of the material. The Mathcad template and BridgeFAT input are modified to suit the new design and the same verifications are performed.

Finally, the material amount defined in each original design is compared to the one utilized in its final version. This allows quantifying the eventual benefits gained with regard to construction cost.

Parametric studies depending on the span length are performed for the simply supported bridges in order to extend the study to a wider range of cases.

² BridgeFAT by Mohsen Heshmati, PhD student at Chalmers University

2 High Strength Steel and its properties

Nowadays, most existing bridges around the world are between 50 and 100 years old. This situation has sparked the interest of finding new materials for construction that are stronger, long lasting, less subject to deterioration and possibly cheaper than those available on the market nowadays. One of the most suitable candidates is High Strength Steel (HSS).

Within construction, several different qualities of steel are available. Conventional steel grades include S235, S275 and S355; the last one is the most common steel quality used within structures by far. The wide use of S355 is due to the best cost to strength ratio provided, compared to other steel qualities. This can obviously be beneficial in pursuing the need of reduction of construction cost.

Improved methods of steel production, though, have introduced the possibility to use fine steel qualities in the design of structures. These qualities have been available for about thirty years and can potentially offer great advantages for bridge design.

Compared to conventional structural steel, High Strength Steel can be regarded as a material with enhanced properties originating from a finer structure.

Such a material represents a competitive alternative to conventional steel for bridge engineering. HSS development can improve the economy of the design, as its strength can be utilized more efficiently, and can contribute to environmental benefits by saving resources. In previous studies held by the US Federal Highway Association, HSS was proved to allow lifetime cost savings up to 18% and reduce the weight up to 28%, compared to conventional steel (1).

2.1 Chronology

Japan began a specific research concerning the development of construction steel with enhanced properties already in the 1950s (2). Steels with a tensile strength of 500MPa and 600MPa were introduced and specified respectively as JIS SM50Y, SM53 and JIS SM58. These products were added to the Highway Bridge Specifications in 1967 and were used for most of the Japanese bridges designed in the 1970s.

The development of bridges designed with the use of HSS is shown in Figure 2.1.

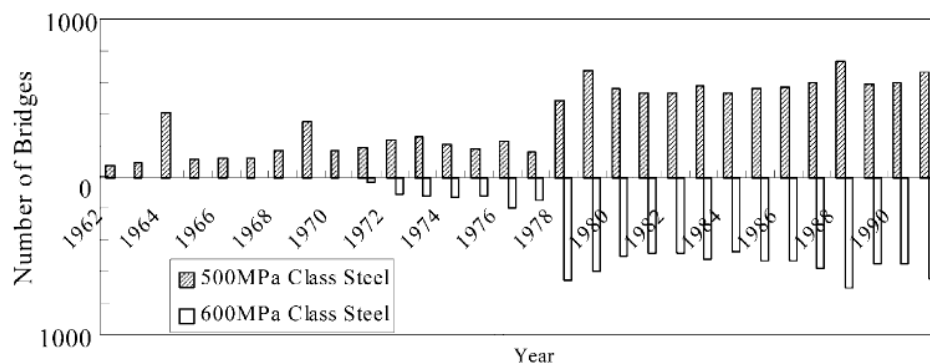


Figure 2.1 Number of bridges designed with High Strength Steel constructed in Japan over time

More recently, in 1994 (3), the American Iron and Steel Institute, the U.S. Navy and the Federal Highway Administration contributed to the development of HPS 50W (345MPa), HPS 70W (485MPa), which have been employed in the construction of several structures since. Meanwhile steel grade HPS 100W (690MPa) is being developed (4).

2.2 Production process of HSS

HSS's finer structure is achieved through a special focus on the *material composition*, the *working process* and the *heat treatment*. Each aspect is explained more in detail below (5).

2.2.1 Material composition

A specific chemical composition is fundamental in order to achieve the required qualities and it has to be adjusted directly in the mill before the steel is cast.

The strength of the material can in fact be improved drastically through the modification of its chemical composition. This consists in the addition of alloys, such as Carbon, Manganese, Niobium and Vanadium during the production process. Such addition is to be done in the liquid phase either while tapping or secondary steel making. Later on the cleanness of the final product is assured through secondary metallurgy, ladle refinement and vacuum degassing.

It is to bear in mind that the addition of such alloys can influence other properties of the material, so the composition needs special attention in order to obtain a good balance between the effects.

2.2.2 Working process

Structural steel can be manufactured both in plates and rolled sections, such as beams, L-shaped profiles and so on. Traditionally, steel goes through a process that allows obtaining its final shape and aspect. As a first step, it is produced in a mill and cast into a slab, before it is rolled.

The rolling process allows the manufacturer to achieve two important results: scale down the product to the desired dimension and improve the molecular structure, as shown in Figure 2.2.



Figure 2.2 Cold rolling process of a steel plate

2.2.3 Heat treatment

After rolling, the heat treatment takes place: the last step of the production process. This procedure is performed in order to assure that the steel reaches the required mechanical properties; the tensile properties for example are highly affected by the cooling rate. During the rolling process, steel cools down, and this temperature decrease can be controlled to obtain different steel qualities (6). Figure 2.3 below illustrates different procedures to control the temperature during the cooling process: each process is further explained later in the chapter.

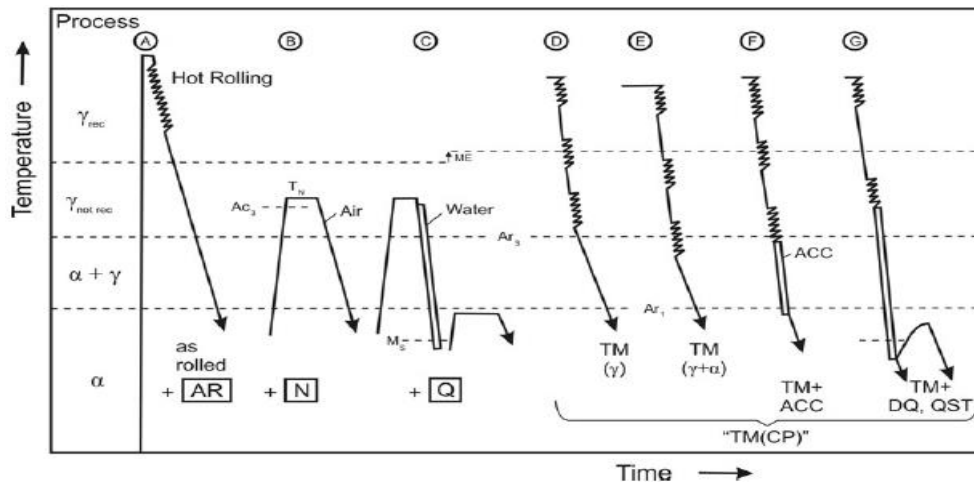


Figure 2.3 Temperature variation during the different possible heat treatment processes of High Strength Steel

The different processes contribute to the production of different steel grades:

- *Conventional steel*: a tensile strength up to 420MPa can be obtained through methods AR and N.

AR (As-rolled) - During the rolling process, the temperature of the material reaches 1100°C and then cools down to 750°C , in calm air, towards the end of the treatment.

N (normalized) - In this case the steel is, after the end of the process, reheated back and held to a temperature of about 900°C before it can cool down in calm air.

- *High strength steel*: a tensile strength up to 1100MPa can be obtained both through Q and TM.

Q (quenched and tempered) - The process starts just like N but, after the reheating process, the steel is cooled down in water or another medium (quenching). This way the cooling process is performed much faster and there is no risk of formation of ferrite and perlite. Finally the steel is heated one more time up to 600°C before it can cool down naturally (tempering).

TM (thermodynamically rolled) - In this case, the steel has a slightly different composition, which lowers the final temperature to about 700°C before the steel cools naturally. This requires, though, a more advanced rolling process since the required force is larger.

The different processes lead to the creation of different microstructures, which contribute to the production of different steel qualities. Figure 2.4 below shows the molecular structure more closely.

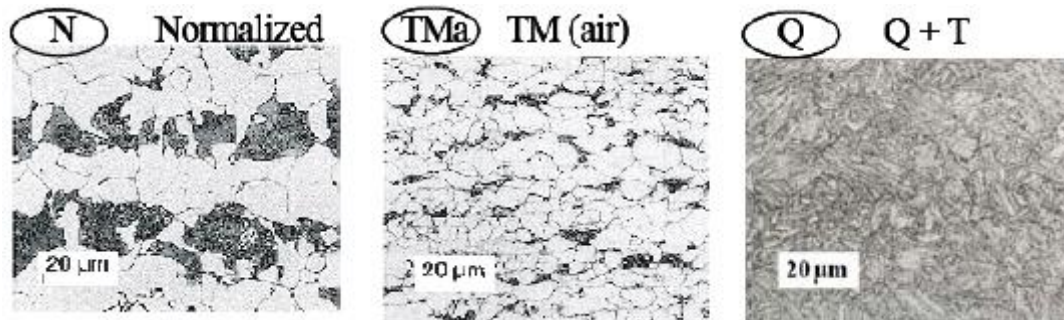


Figure 2.4 Molecular structure of different steel qualities

Each process of fabrication has dimension restrictions due to the machinery needed for the manufacturing process. For this reason only certain thicknesses and sizes are available for different steel grades. These limitations are summarized in Table 2.1.

Table 2.1: Steel processing routes for production of high strength steels

Normalized	Usually <460MPa for 50mm plate
Thermomechanically controlled rolled (TM)	Thickness restriction especially at higher strengths – usually less than 550MPa at 40mm
Quenched & Tempered (Q)	(a) Alloyed route - no real thickness restriction but expensive and costly to weld (b) Microalloyed route – thickness and strengths required offshore can be produced
Castings	Usually alloyed because of lack of processing capability

2.3 Classification of HSS

According to the different chemical composition, steels with different properties can be manufactured. Generally, three main categories of steel can be found. In this chapter they are presented in detail.

2.3.1 High Strength Low Alloy Steel (HSLA)

High strength low alloy steel is designed in order to ensure improved mechanical properties and a better endurance against corrosion, compared to conventional carbon steel. This is possible thanks to the reduction of carbon content to 0,05%-0,25%,

which improves the formability and weldability, and a manganese content limited to 2%. In addition, several other elements are added in different combinations (7).

Such combinations contribute to six different HSLA categories:

1. Weathering steels
2. Microalloyed ferrite-pearlite steels
3. As-rolled pearlitic steels
4. Acicular ferrite (low-carbon bainite) steels
5. Dual-phase steels
6. Inclusion-shape-controlled steels

Among the advantages of using HSLA steel are thickness reduction, weather resistance, formability and weldability. Of even greater importance for bridge design is the favourable strength to weight ratio, which allows a reduction of the material need.

2.3.2 High Performance Steel (HPS)

High Performance Steel has a nominal yield strength which varies between 485MPa and 900MPa. It was first developed in 1992 in the U.S. to satisfy the demand of finding a new material alternative for bridge design. HPS 70W and HPS 120W were developed and contributed to a significant reduction in terms of cost and weight of the new designed structures.

This new material had a carbon content decreased by 50% and sulphur content decreased to 10% compared to the contents of conventional steel.

Such a chemical composition results in improved welding and toughness properties, as well as in better corrosion resistance, ductility, fatigue resistance, formability and strength (8). Moreover, HPS can be manufactured with reduced cost, as no preheating is needed and theoretically recycled up to 100%, which makes it a sustainable alternative.

One of the drawbacks is that HPS has low ductility, which affects the performance related to earthquake design.

The manufacturing process is usually made through Q&T, which limits the dimensions of the plates to lengths of 15.2m, but it can also be made through TM, which extends the dimensions of the plates to lengths of 38m and thicknesses of 50mm.

2.3.3 High Strength Weathering Steel (W)

The use of weathering steel eliminates the need of coating protection of a structure. Such steels, in fact, can resist corrosion by the formation of a tight layer of dense rust, the so called “patina”. Its use has increased widely in the last decades as it cuts the cost of maintenance, as the bridges do not need to be inspected as frequently (9).

However, careful attention has to be paid to the environmental exposure conditions: it is hard to prove its efficiency in coastal areas with airborne salt or areas where deicing salts are used.

2.4 Mechanical properties of HSS

As stated in Section 2.2.1 steel obtains its mechanical properties depending on the chemical composition. In this section the main properties of steel are described in detail.

2.4.1 Yield strength f_y and ultimate strength f_u

Yield strength, or *yield point*, is defined as the stress over which the material, steel in this case, starts to deform plastically. For stresses below yield strength the material exhibits only elastic deformations, while over this limit part of the induced deformations will be permanent. This is the parameter which has the greatest impact on the design of structures.

Ultimate strength, instead, is defined as the highest stress a material can withstand before failure occurs. Such failure can be either ductile or brittle, depending on the material properties.

Different metals have different stress-strain curves and this applies as well to mild or high strength steels (see Figure 2.7).

Figure 2.5 represents the general stress-strain curve for steel (10):

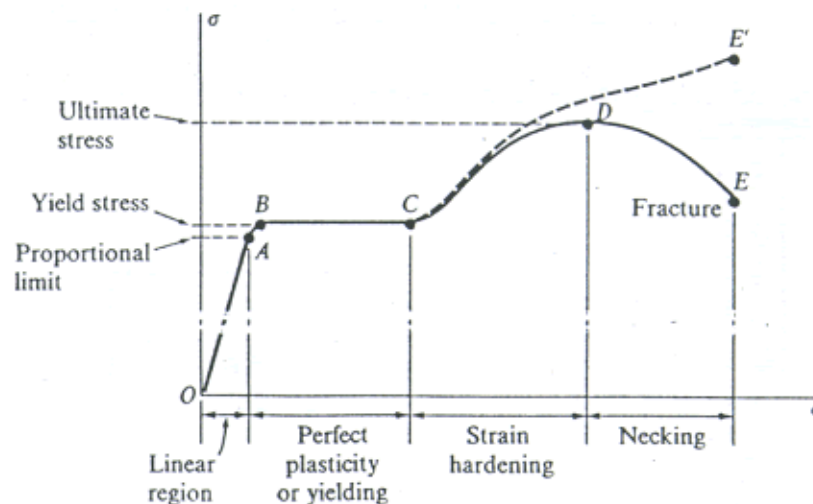


Figure 2.5 General stress-strain curve for steel

European standards define different steel grades according to the tensile strength exhibited during testing. It has to be remarked that the results of testing depend on the thickness of the specimen; in particular the yield strength decreases with increasing thickness. For this reason the Eurocode distinguishes three different thickness ranges. These categories are shown in Table 2.2 (11).

Table 2.2 Nominal values for yield strength and ultimate tensile strength for structural steel

EN 10025-6 Steel grade	Nominal thickness of the element					
	t≤50mm		50mm<t≤100mm		100mm<t≤150mm	
	f _y [N/mm ²]	f _u [N/mm ²]	f _y [N/mm ²]	f _u [N/mm ²]	f _y [N/mm ²]	f _u [N/mm ²]
S355	355	510	345	490	335	470
S460	460	570	440	550	440	500
S690	690	770	650	760	630	710

2.4.2 Fracture toughness

Steel products contain defects. It is impossible to completely avoid them during the manufacturing process and they can appear as voids or cracks. When these defects are subjected to tensile stresses, they tend to open if the material is not tough enough. *Fracture toughness* indicates the ability of the material to resist the propagation of a pre-existing defect. A good way to measure the toughness of specimens is the Charvy V-notch impact test. A notched specimen is hit by a pendulum and the energy required to break it is measured (different grades are tested at different temperatures).

Designers take this aspect into consideration by assuming that steel contains defects. The factor K is introduced to describe the fracture toughness of different materials. This parameter considers three different modes of propagation as described in Figure 2.6 (12).

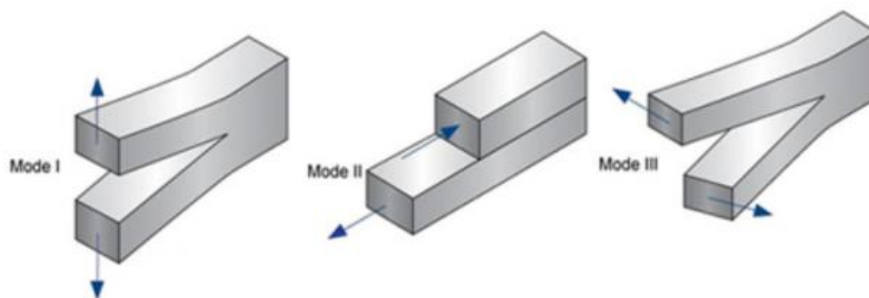


Figure 2.6 Possible modes of fracture propagation for metals

The K factor can be calculated through Equation 2.1:

$$K_i = \sigma \cdot \sqrt{\pi \cdot \alpha \cdot \beta} \quad \text{Equation 2.1}$$

Where:

K_I = fracture toughness

a = length of the crack

σ = applied stress

β = crack length and component geometry factor that is sufficient for each specimen

Eurocode separates different steel grades into subgrades depending on the fracture toughness. The categories for HSS can be found in EN 1002-6:2004.

2.4.3 Ductility

Ductility describes the ability of a material to strain or elongate between yielding and failure, which helps preventing brittle failure. It is one of the most important properties of steel and designers rely on it in many cases, among which redistribution of stresses in the ultimate limit state and reduction of fatigue crack propagation.

One measure to express the behaviour of any steel in terms of ductility is the yield ratio (YR), which is defined as the ratio between the yield strength and the ultimate strength. This parameter describes the behaviour of the material when yielding is reached. As shown in Figure 2.7 higher steel grades have a higher YR. For this reason they are considered to be less ductile than conventional mild steels.

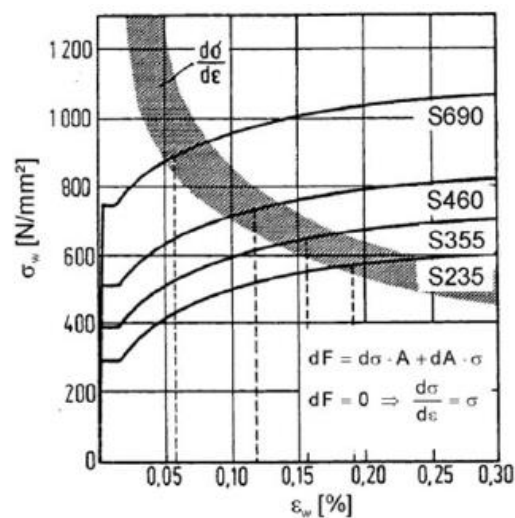


Figure 2.7 Stress-strain curves for different steel grades

Since the ductile behaviour of a structural member is of great importance for designers, as it prevents brittle failure, building codes set different limits of YR through time. Steels with a YR above a certain limit were not used in bridge design as they considered not to exhibit the necessary ductile behaviour to ensure plastic failure (13).

In Table 2.3 the YRs for the steels that will be used in the case studies below are summarized.

Table 2.3 Yield ratios for steel S355, S460 and S690

	S355	S460	S690
Yield ratio	0,69	0,80	0,90

However, recent research has shown that there are exceptions to this relation between YR and ductility, such as the case of S690, which can elongate adequately in spite of a YR=0,90. These researches are leading to changes in the modern design codes which are currently being revised.

The elongations expressed by steels with high yield strength are generally lower than those expressed by mild steels (tensile strength lower than 460MPa): steel qualities with a tensile strength between 350MPa and 460MPa usually elongate up to 35%, while those with tensile strength of 690MPa only elongate up to 18%.

For this reason, for a very long time, inelastic analysis and design methods have not been permitted and the capacity of a section was limited to the yielding values. Nowadays, extensive research and testing have resulted in the removal of many of the limitations and the construction codes are still undergoing changes.

2.4.4 Weldability

The term *weldability* describes the capacity of a material to be welded under specific conditions. One of the main goals of research is to create steel qualities with improved weldability. This way the cost of welding can be substantially reduced.

One of the most common problems while welding steel bridges is called *cold cracking* or *delayed cracking*. Such cracking can develop within days from the welding process, making it even more dangerous as it is not visible during operations. However its risk can be reduced if specific measures are taken.

For the formation of cold cracks two factors are necessary: the presence of hydrogen and tensile stresses. Tension creates microcracks where hydrogen can accumulate reducing the bond between the grains, which therefore can be separated with lower stresses. Both the welding material and the moisture in the atmosphere represent a source of hydrogen.

Since tensile stresses cannot be always avoided, the most efficient way to prevent this kind of cracking is to control the amount of hydrogen and this can be done through different measures:

- Preheating – increasing the temperature of the base metal before welding can remove dissolved hydrogen preventing embrittlement. The temperature input depends on both steel grade and thickness.
- Ensuring weld discontinuities are avoided in order to prevent the concentration of tensile stresses.
- Employ electrodes with a low amount of hydrogen in order to reduce the source.
- Soaking – a procedure of removing entrapped hydrogen by post weld heating the area for a couple of hours at a temperature between 250⁰C and 350⁰C (14).

All these procedures to avoid cold cracking during welding involve local heating of the material. When the procedure is over, the area can cool down rapidly if heat control is not performed. Such a temperature gradient can harden the so called *Heat Affected Zone* (HAZ), resulting in a decrease of toughness and enhanced embrittlement of the weld.

This material weakness depends mostly on the carbon content and on the amount of alloying elements in the base metal and can be expressed by the *Carbon Equivalent Value* (CEV). According to the latest European Standards, limits concerning the maximum CEV were introduced. See Table 2.4.

Table 2.4 Maximum carbon equivalent values according to European Standards

Element	Range for satisfactory weldability [%]	Level requiring special care [%]
Carbon	0,06-0,25	0,35
Manganese	0,35-0,80	1,40
Silicon	0,10 max	0,30
Sulphur	0,035 max	0,050
Phosphorus	0,030 max	0,040

The same values can be calculated also with a quantitative approach through Equation 2.2:

$$C_{eq} = C + \frac{(Mn + Si)}{6} + \frac{(Cu + Ni)}{15} + \frac{(Cr + Mo + V + Nb)}{5} \quad \text{Equation 2.2}$$

Steel is considered to be weldable if:

- $C_{eq} \leq 0.50\%$ and carbon $> 0.12\%$
- $C_{eq} \leq 0.45\%$ and carbon $< 0.12\%$

Another important factor when welding is the choice of the electrode. EN 1993-1-8 requires that the chosen filler metal has at least the same strength and toughness of the base metal.

However, especially for HSS, such a requirement is inadequate. In fact, the use of undermatching fillers can allow better local yielding and redistribution of the tensile stresses, which contribute to better results in terms of weld resistance (15).

Research and testing were performed on S690 steel and, based on the results, additional rules were included within EN 1993-1-12. It is now permitted to use undermatching fillers when assessing welds of HSS, but the tensile strength of the base metal has to be replaced with the one of the electrode in the calculations.

2.5 Examples of steel specifics

Further in the body of this thesis, several bridges are assessed. In particular three different steel grades are used in their design: S355, S460 and S690. Only the two latter steel grades are classified as High Strength Steel.

The detailed specifics of each are listed below. All the amounts are expressed in percentage.

- S355: generally pre-formed with standard cross-sections for specific uses in construction.

C	Si	Mn	Ni	P	S	Cr	Ti	Nb	V	Mo
0.20	0.55	1.75	0.55	0.03	0.025	0.35	0.06	0.06	0.14	0.13

- S460: fabricated both through quenching (Q) or thermo mechanical rolling (M). It can be produced in heavy carbon steel plates or fabricated sections.

C	Si	Mn	P	S	Cr	Mo	Ni	Al	Cu	N	Nb	Ti	V	Nb+V
0,14	0,15	1,65	0,02	0,01	0,25	0,25	0,7	0,015	0,3	0,01	0,04	0,025	0,08	0,09

- S690: fabricated both through quenching (Q) or tempering (T).

C	Si	Mn	P	S	N	B	Cr	Cu	Mo	Nb	Ni	Ti	V	Zr
0,2	0,8	1,7	0,025	0,015	0,015	0,005	1,5	0,5	0,7	0,06	2	0,05	0,12	0,15

The prices of each steel quality depend strictly on the availability on the market from time to time. In this thesis study, the prices have been retrieved from Ruukki³ and are listed in Table 2.5.

Table 2.5 Price of different steel qualities

Steel grade	Price per ton (SEK/ton)
S355	7000
S460	7850
S690	10600

³ Rautaruukki Corporation

3 Benefits of HSS in bridge application

In the last few years, a growing number of bridges have been constructed with the use of high strength steel. This is due to the several benefits that such a material can have under several points of view. In this section the most important ones are described further.

3.1 Production cost

Manufacturing HSS is generally more expensive than conventional steels. At the same time, the price increases at a lower rate than the increase in yield strength; i.e. a steel twice as strong is not twice as expensive. In Figure 3.1 the relative prices of steel plates, compared to S235, are shown. The data was obtained from leading European producers of steel products and the scatter among them is due to the variation of market prices and availability, from time to time.

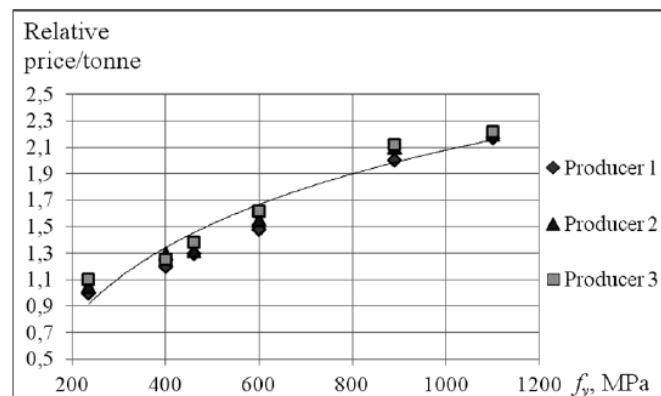


Figure 3.1 The average reference prices of HSS in function of yield limit

At the time of this study, the prices of the relevant steel qualities for the following case studies are listed in Table 2.5.

The main conclusion that can be made from both Figure 3.1 and Table 3.1 is that the production cost will decrease with increasing yield strength, with the assumption that the material can be fully utilized.

It is to keep in mind that the production cost often has a lower impact than the construction cost.

3.2 Construction cost and time

The possibility of fully utilizing the yield strength of HSS goes along with a reduction of the sections of the structural members. As a consequence, if it is assumed that the weld size is not a limit to the design, smaller welds will be necessary to connect the different plates.

Moreover, the reduction of weld sizes will contribute to decreasing the amount of electrode needed for the connection and consequently the cost of construction.

Along with the reduced need of welding process, smaller welds require shorter time to be performed.

It is worth remarking that, in some cases, the material can be exploited to its best through the use of hybrid girders, e.g. girders with different plates of different steel qualities. This way, each section can be fully utilized and the economic benefits of HSS are maximized (16).

3.3 Light weight

The stronger the material, the smaller the section needed to achieve the required resistance to stresses. For this reason HSS allows designer to dimension smaller elements compared to their conventional equivalent and it is obvious that the total weight of the structure can drop considerably.

This kind of benefit has secondary effects as well. The machines and tools needed for the construction and assembly will be chosen accordingly to the reduced dimensions of the member: smaller machines are cheaper.

3.4 Environmental impact

In modern times, the environmental impact of all kinds of structure is of great interest and importance.

In general, steel is a highly recyclable material but it is also true that it requires considerable amounts of raw material and energy to be manufactured. As explained previously, the required sized of structural members can strongly decrease where HSS is used. It is then obvious that less steel is to be produced in order to achieving the required capacities. This way a meaningful reduction in terms of raw material use, emissions and energy can be achieved, giving a valid reason to use higher steel grades.

4 Application of HSS in construction

4.1 Examples of the use of HSS in the bridge industry

With the development of new technologies and design proposals, bridge engineers are pushing more and more towards the use of high strength steels. In this section we list some of the most relevant experiences.

- Remoulins Bridge, France

Finished in 1995, it is composed of a twin girder structure combining steel grades S355ML and S460ML. The higher quality has been applied in the areas subjected to the highest stresses near the piers so to reduce the maximum thickness of the elements: from 120mm down to 80mm. This contributed to a reduction in terms of weight, leading to faster and easier fabrication and erection (17).



Figure 4.1 Remoulins Bridge, South France

- Akashi Kaikyo Bridge, Japan

When completed in 1998, it was the longest suspension bridge in the world. It has an overall length of 3911m with a centre span of 1991m.

Large amounts of steel class 800MPa were used in order to stiffen the trusses. The main goal was to reduce the dead load of the structure and the use of HSS was most appropriate.

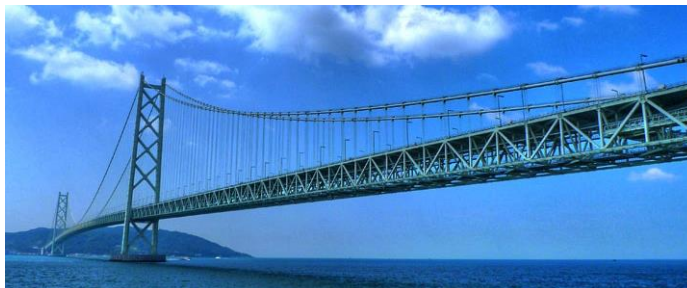


Figure 4.2 Akashi Kaikyo Bridge, Japan

- Millau Viaduct, France

Opened in 2004, this is currently the highest bridge in the world. It has a height of 343m and spans across a total length of 2460m. 18000 tons out of a total of 43000 tons are S460M. The main goal was to minimize the dead load, along with the optimization of the thickness of the welded components in order to achieve a quick construction (18).



Figure 4.3 Millau Viaduct, South France

- Tokyo Gate Bridge, Japan

First opened to traffic in 2011, it spans over the Nanboku Channel for a total length of 760m with the longest span of 440m. It was designed using BHS500 steel (nomenclature for bridge high performance steel in Japan) with a tensile strength of 500MPa.

The total amount of steel used is 3988 tons, 1143 of which are BHS500. With the use of this steel grade, the total weight of the structures was reduced by 3%, which contributed to a total cost reduction of 12%.



Figure 4.4 Tokyo Gate Bridge, Japan

4.2 Examples of the use of HSS in other industries

The benefits of HSS can be exploited in many sorts of construction industries other than bridges. Among the most common applications are offshore platforms and large scale constructions in land. In this section we list some of the most relevant experiences (6).

- Elgine-Franklin offshore field, North Sea

The structural components of the structure are designed with high strength steel with a tensile strength of 500MPa. Along with these, smaller details such as chords and bracings are designed with 700MPa steel. The use of high strength steel is instead avoided in the sea bottom area of the structure in order to prevent the risk of any hydrogen embrittlement issue.



Figure 4.5 Elgine-Franklin offshore field, North Sea

- Hutton field, United Kingdom

The floating platform presents a total of 16 tension legs. Each of them presents a pipe-like section designed with 795MPa steel in order to achieve the best integration between tensile strength and fracture toughness.

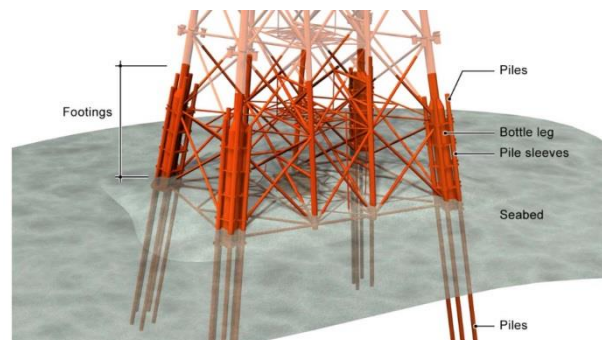


Figure 4.6 Hutton field, United Kingdom

- Airbus hangar, Frankfurt

The roof of the structure spans across 180 meters without intermediate supports. For this reason, a special truss construction was needed, which is designed with steel

quality S500ML. This improved version ensures maximum yield strength of 460MPa up to a thickness of 120mm, in accordance with the standards given by EN 10025.



Figure 4.7 Airbus hangar, Frankfurt

- World financial center, Shanghai

Many of the steel structural elements, among which truss belts and bracings, are designed with S460ML. This way a minimum tensile strength of 450MPa could be ensured.



Figure 4.8 World financial center, Shanghai

5 Introduction to Fatigue and its effects on the design of welded details

During the years, numerous steel structures have experienced failures due to loads well below the yield strength of their respective materials. In the design phase, the failure of a structure is assumed where the stresses generated by a certain load combination reach and overcome the yield strength of the materials employed. However, a fluctuating and repetitive loading of a structural member can also lead to failure: this phenomenon is known as *fatigue failure*.

The main difference between the two kinds of collapse is that the former is the result of one load cycle and the structure shows large plastic deformations, while the latter doesn't involve any relevant deformations since the stresses don't reach the elastic strength of the material and can happen after a number of cycles that can vary from a few thousands to several millions.

It is to be remarked that fatigue failure affects a large numbers of engineering materials, not exclusively steel, but composites and polymers as well. Anyway, in all cases, the phenomenon develops in a similar way. Small micro-cracks will originate from a small, confined area of a structure where, for several reasons, higher stresses develop. Weld defects and stress raisers are often two of the main reasons contributing to these high stress concentrations in the material. As a consequence, fatigue develops as a localized phenomenon. Micro cracks originate in a confined area and grow larger into a dominant crack, while the surrounding areas seem to be practically unaffected. The crack pattern will induce plastic deformations in the structural element and therefore its propagation represents an irreversible process.

An easy example to better understand this phenomenon has been performed by Dahlberg and Ekberg (19). They compared the different failures of two different teaspoons subjected to two different kinds of loading. The first spoon was gravely loaded and was unlikely to reach failure despite the significant plastic deformations observed. The second spoon instead was loaded repeatedly until a more or less brittle fracture was observed.

Such experiment summarizes the typical characteristic of fatigue failure of a material; *as a consequence of fluctuating stresses well below the yield strength of the material, small cracks will originate in a confined area subjected to high local stresses and grow into a main crack, which can propagate and lead to the brittle collapse of a structure.*

The brittle behaviour of structures prone to fatigue makes this kind of failure of primary concern for engineers. Gurney (20) assumed that up to 90% of the collapses reported in the past can be regarded as fatigue induced since it is seldom observed that a structure is loaded over its elastic capacity, while most of the engineering structures undergo cyclical loading during their life span, e.g. cranes, offshore platforms and bridges.

Fatigue failure is a very up to date issue and many studies are being performed to improve the fatigue life of structures. The optimal solution would be to avoid critical details, which are prone to fatigue, already in the design phase. Anyway, this cannot always be achieved and this is why several methods for the enhancement of the

fatigue resistance of such details are currently being investigated and will be described further in Chapter 6.

5.1 Background of the phenomenon

The initiation of a micro-crack originates at the microscopic level of the material.

Metallic alloys present an atomic structure organized in grains formed by crystals. Often such crystals present defects, which act as inhomogeneity within the material, which are referred to as *dislocations*.

As a consequence of cyclic loading, dislocations can move within a crystal and originate slip bands. This process develops at the surface grains, since the bonds between them are weaker as they are in contact with the material only on one side. Even a single stress cycle could be enough to form a micro crack.

The development of slip bands and the propagation of the micro-cracks is driven by shear stresses. For this reason, the cracks start at an angle of 45° to the surface of the material. Since it represents a surface phenomenon, the crack initiation depends mostly on the size of the grains, their orientation as well as on the elastic properties of the material.

During the loading cycle, new surfaces of the metal are exposed to the environment, and in the presence of a gaseous or liquid environment this surface will be oxidized. This results into the formation of an oxide layer, which cannot be removed from the surface, as well as a process of strain hardening.

Due to these two causes the crack cannot close during unloading and a new slip band will happen on parallel planes leading to the formation of intrusions or extrusion, as it is shown in Figure 5.1.

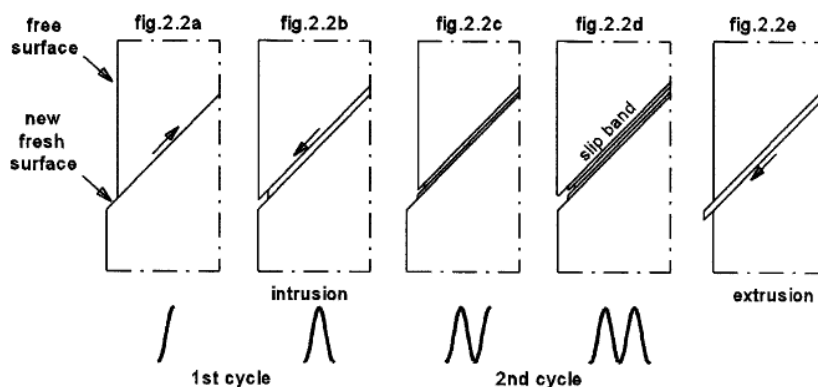


Figure 5.1 Shear stresses in the metal lead to the propagation of micro-cracks and the formation of a bond slip

As the loading cycle is repeated, new micro-cracks are formed and consequently grow together into a main crack, which propagates leaving the original 45° orientation to grow instead perpendicular to the principal stress (see Figure 5.2). During this process the cracks involve several grains, so the material properties do not play an important role any further.

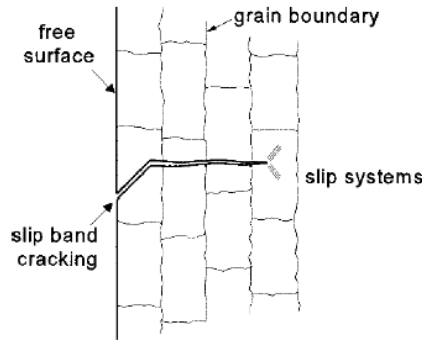


Figure 5.2 Path of a micro-crack through the cross section

5.2 Initiation and Propagation

From the detailed description of the phenomenon, it can be concluded that the fatigue life of a structural member can be divided into two different phases: *crack initiation* and *crack propagation*.

The nature of the two is different and therefore depends on different parameters. It has already been stated that the crack initiation is mostly a function of the surface characteristics of the material, while the crack propagation depends exclusively on the bulk properties. For this reason, the quantitative assessment of the two stages requires two different parameters.

The *Stress Concentration Factor* (SCF) is defined to describe fatigue crack initiation and it is expressed as K_t . It describes the relationship between the maximum stress and the nominal stress in the material. The stress that is applied to a specimen is defined as the nominal stress (σ_{nom}) acting on the section and can be calculated according to the geometry of the specimen through Navier's law, Equation 5.1.

$$\sigma_{nom} = \frac{F}{A} + \frac{M}{I} \cdot z \quad \text{Equation 5.1}$$

However, structural member are often irregular and present changes in cross section that can contribute to the development of stress concentration in localized areas of the section. In these areas the stresses change their pattern, their flow lines become denser and they therefore grow larger than the original nominal stress, thus representing maximum stresses.

The relationship between the two values is expressed through the stress concentration factor, Equation 5.2.

$$\sigma_{max} = K_t \cdot \sigma_{nom} \quad \text{Equation 5.2}$$

Figure 5.3 shows the relation between σ_{max} and σ_{nom} for a plate with a hole.

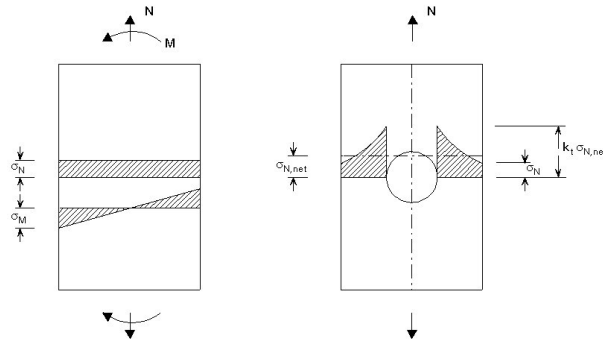


Figure 5.3 Plan view of nominal stress and geometric stress concentration of both a plain specimen and a plate with a hole

The stress concentration factor is of vital importance with regard to fatigue design but can be used only to describe the crack initiation, since it approaches infinity once a crack is opened in the material.

The Stress Intensity Factor (SIF) is then introduced to describe the way the crack propagates in the material. It has already been explained that the main crack propagates perpendicular to the main stress direction, which is often tensile (Mode I), but there are also two more possible modes of propagation (Mode II and Mode III) – these possible modes have already been described in detail in Section 2.4.2. The simplest formulation for the SIF is given in Equation 5.3:

$$K_I = \sigma_{nom} \cdot \sqrt{\pi \cdot a} \cdot f \quad \text{Equation 5.3}$$

Where:

a = crack length

f = function of geometry and loading of the detail

It is important to highlight that the different nature of the parameters is reflected in their units. The SCF is unitless, since it simply describes the geometry of the specimen, while the SIF has units $MPa\sqrt{m}$.

5.3 Quantitative approach to fatigue

The first accurate model for the estimation of the crack growth of fatigue loaded details was proposed by Paris and Erdogan (21) in 1963. They assumed that the speed of propagation of a crack can be expressed as a function of the formerly defined SIF. The equation proposed is called Paris' law, shown in Equation 5.4:

$$\log\left(\frac{da}{dN}\right) = m \cdot \log(\Delta K) + \log(C) \quad \text{Equation 5.4}$$

Where:

$\frac{da}{dN}$ = crack growth rate

ΔK = stress intensity factor range

C, m = material constants

This equation can be plotted in a logarithmic graph as a function of the growth rate and the range of the stress intensity factor. The result is a curve that expresses a different behaviour in different regions of the plot (see Figure 5.4).

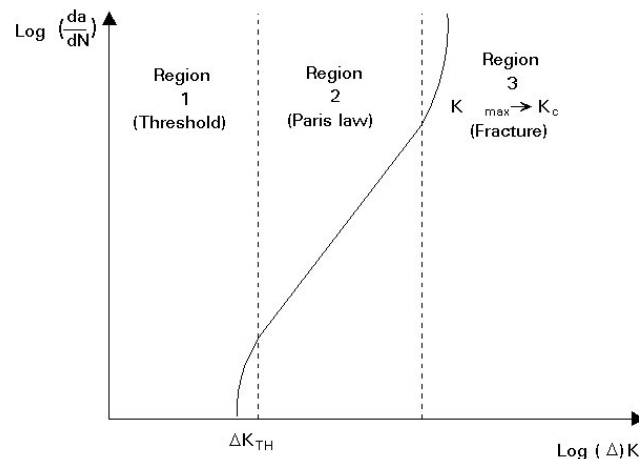


Figure 5.4 Typical fracture mechanics fatigue crack propagation behaviour

- Region 1: also called the threshold region, comprehends all those stress ranges that are not high enough to open a fatigue crack.
- Region 2: in this area of the graph Paris' law is consistent.
- Region 3: the stress range is so high that fracture is considered the cause of failure.

Paris' law highlights that the fatigue life of any detail depends directly on the *stress range* that the detail is subjected to. The stress range indicates the amplitude between the lowest and highest stresses affecting the material; in particular the wider the stress range the shorter the fatigue life. Further details about the calculation of the stress range affecting a detail will be described in Section 5.5.

5.4 Fatigue design according to Eurocode

The number of cycles n_i needed to reach failure is the most relevant outcome of fatigue tests on structural details, performed with a specific stress range $\Delta\sigma$.

The most common way to gather the results is by the means of a so called *S-N curve*, also known as the *Whöler diagram*. The number of cycles is plotted on the x-axis and the stress ranges on the y-axes, in a log-log scale.

The graph obtained, Figure 5.5, presents similarities with Paris law. By turning the graph 90° counter clockwise, the similarities become obvious: compare Figure 5.4 and Figure 5.5.

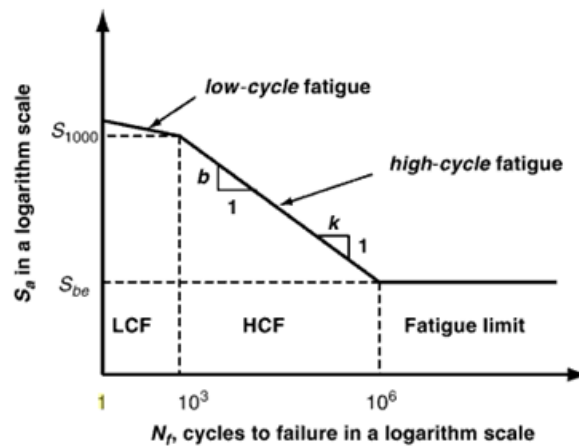


Figure 5.5 General S-N curve of a steel detail

Three regions can be identified:

- Region 1 (bottom right corner): comprehends all those stress ranges that are not high enough to lead to fatigue failure. This is known as *fatigue limit*.
- Region 2 (middle part): in this area the behavior of the detail can be expressed by a linear equation.
- Region 3 (top left corner): the stress range is so high that plastic deformations are observed. This is known as *low cycle fatigue*.

Most of the building codes, including Eurocode, use S-N curves to assess the fatigue resistance of structural details. The process of creating such curves begins with the testing of categories of details. A specific detail is tested under different stress ranges and the number of cycles at which failure is reached is recorded.

Different codes specify different amount of details to be tested before the results can be considered reliable; the Eurocode prescribes 60. Tests are in fact performed all over the world, with different size of specimens (they should be large enough to represent reality), in different environmental condition, different electrodes are used and different defects are recorded. For this reason, a large scatter in the test results is noticeable.

In order to define a single curve for each detail the Eurocode considers a probability of survival of 95%.

The most common details are listed in Eurocode EN 1993-1-9. Once the tests are performed, a *C-class* or *detail category* is assigned to each detail to describe its fatigue strength. In addition information about the load direction, load effect and the presumed cracking development are included.

5.4.1 Details subjected to normal stresses

In case of constant amplitude loading (this concept is introduced in Section 5.5) a constant slope of the S-N curve is assumed and in particular the slope, m , is equal to 3. In this case no fatigue failure is expected for a stress range below the value related to 5 million cycles.

In case of variable amplitude loading the S-N curve is defined beyond the 5 million cycles as well, but the slope is changed to $m = 5$, and a cut off limit is set at 100 million cycles. For stress ranges below the cut off limit no fatigue failure is expected, i.e. the detail can be loaded an infinite number of cycles.

Different details are assigned different S-N curves according to their resistance to fatigue. All the S-N curves are presented in Figure 5.6. The critical values for each curve are listed in Table 5.1.

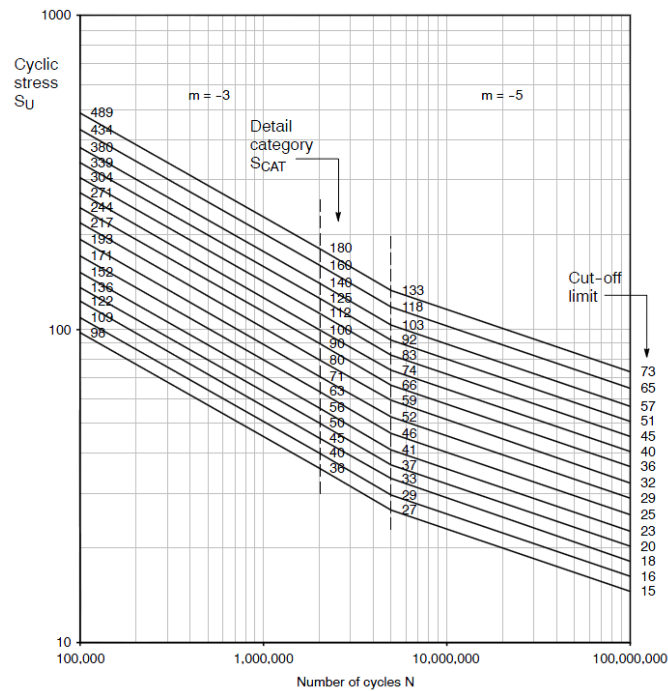


Figure 5.6 S-N curves for details loaded with normal stresses

Table 5.1 Stress ranges at fatigue limit and cut-off limit

$\Delta\sigma_C$ [MPa] at $2 \cdot 10^6$	$\Delta\sigma_D$ [MPa] at $5 \cdot 10^6$	$\Delta\sigma_L$ [MPa] at $100 \cdot 10^6$
160	118	65
140	103	57
125	92	51
112	83	45
100	74	40
90	66	36
80	59	32
71	52	29
63	46	25
56	41	23
50	37	20
45	33	18
40	29	16
36	26	15

5.4.2 Details subjected to shear stresses

For details subjected to shear stresses, the Eurocode defines only two S-N curves, one for stresses acting on the base metal and one for stresses acting on the weld profile. Moreover only one slope is assigned and taken as $m = 5$.

The cut off limit is set to 100 million cycles, see Figure 5.7 and Table 5.2.

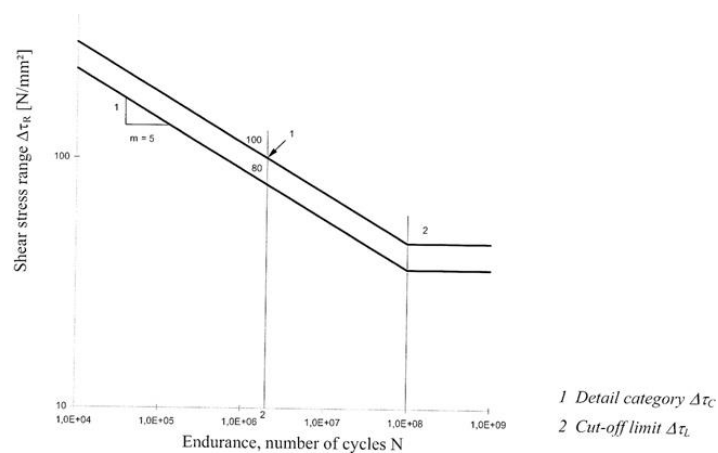


Figure 5.7 S-N curves for details loaded in shear

Table 5.2 Stress ranges at fatigue limit and cut-off limit

$\Delta\tau_C$ [MPa] at $2 \cdot 10^6$	$\Delta\tau_L$ [MPa] at $100 \cdot 10^6$
100	46
80	37

5.5 Fatigue assessment methods

In order to utilize the S-N curves when designing with regard to fatigue, the stress range affecting a specific detail needs to be calculated. Such range is a function of the maximum and minimum stresses loading a specific detail. Both values can be obtained from the same stresses, strains and loads that affect the structure through different methods. These assessment methods can be divided in *global* and *local* depending on the stress parameters taken into account (22).

Local assessment methods include the *hot spot stress method*, the *effective notch stress method* and the *crack propagation approach*.

The global assessment methods include the *nominal stress method*, which is most commonly used. In this method the average stress is calculated according to the linear elastic beam theory but finite element modelling can be used for determining the stresses of complex models as well. Any stress-raising weld defects, geometrical configurations and weld shapes are disregarded at this stage, since they are included in the detail category.

The most important parameter required by the nominal stress method is the stress range affecting a specific detail. Testing of details is usually performed under a constant stress range throughout the fatigue life. This case is referred to as a *constant amplitude fluctuating stress* but such a simplification does not describe the loading history of most structures. For example, the loads acting on a bridge vary depending on the kind and number of vehicles crossing it: this is the case of *variable amplitude loading*.

To describe varying amplitude loading history better, histograms are often used, where blocks of load amplitudes are defined (see Figure 5.8).

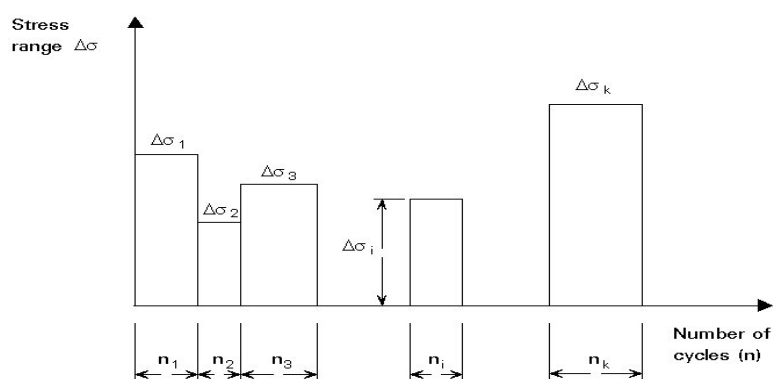


Figure 5.8 Stress histogram or stress range distribution used to simplify the loading amplitude history of a detail

The situation of variable amplitude loading appears hard to assess with regard to fatigue. For this reason a simplification of the loading history of a certain detail becomes necessary and can be achieved by the means of an equivalent constant amplitude loading. Such a simplification will lead to the definition of equivalent fatigue damage.

The first stage in the process is the utilization of cyclic counting methods, such as the *rainflow* or the *reservoir*, to transform the loading history into constant amplitude loading.

Once the loading history is simplified, the fatigue analysis can be performed, typically through the application of the so called *Palmgren-Miner rule* or the *equivalent stress range concept*.

It is to be remarked that both Palmgren-Miner and the equivalent stress range methods lead to the same results in terms of fatigue damage. Both methods are further described below.

5.5.1 Palmgren-Miner

A specific detail exhibits fatigue failure after a definite amount of cycles N , when loaded at a stress range $\Delta\sigma$. The moment it fails denotes that 100% damage is reached, or $D = 1$.

With this in mind, the damage after any amount of cycles n can be calculated through Equation 5.5:

$$D = \frac{n}{N} \quad \text{Equation 5.5}$$

From this formulation, it is possible to sum up the damages originating from different stress ranges $\Delta\sigma_i$ independently as expressed in Equation 5.6:

$$D = \sum_i D_i = \sum_i \frac{n_i}{N_i} \quad \text{Equation 5.6}$$

To conclude, the Palmgren-Miner rule enables the designer to calculate the fatigue life of any detail loaded within different stress ranges, as well as it gives the possibility to estimate the remaining fatigue life of a specific connection, where the stresses are known.

5.5.2 Equivalent stress range concept

Another way to assess the fatigue life of a detail is by the means of an equivalent stress range. In this case, it is necessary to define the stress range that, if applied the same number of cycles as the variable stress range, will lead to the same damage.

In the case of a constant slope of $m=3$ the equivalent stress range can be defined as shown in Equation 5.7:

$$\Delta\sigma_{eq} = \left[\frac{\sum_{i=1}^k (n_i \cdot \Delta\sigma_i^3)}{\sum_{i=1}^k n_i} \right]^{\frac{1}{3}} \quad \text{Equation 5.7}$$

The important feature of such formulation is that, given a fatigue load spectrum, it is straight forward for a designer to choose an adequate detail category which can withstand the stresses.

5.6 Fatigue life of welded details

Welding represents one of the most convenient, used and flexible ways for designers to connect the structural members. Along with these benefits, there are different complications arising from this practice.

Firstly, the process of welding often relies on skills of the worker assigned to the task. Nowadays, some can be performed by machines and therefore many of the imperfections can be eliminated, but this is not possible for connections to be welded on site. In this case the worker is responsible for the quality of the weld, but a perfect weld is unachievable.

Secondly, during the process, both the base metal and the electrode are heated and subsequently cool down. During the cooling period, the heated part of the material is not free to shrink since bounded to the surrounding and therefore self-balancing stresses are built up in the section.

For these reasons welded details have shown to have lower fatigue life compared to notched or plain specimens, as clearly shown in Figure 5.9.

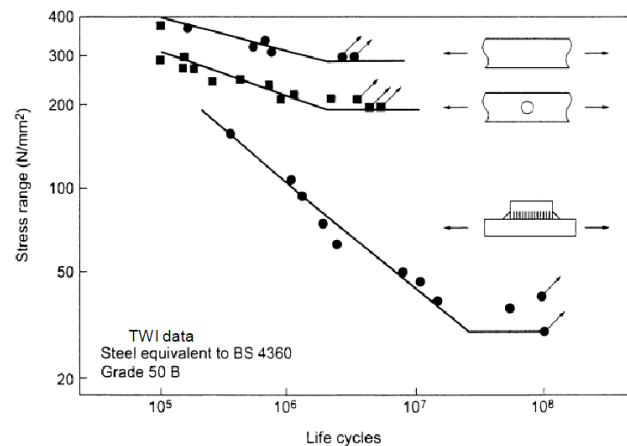


Figure 5.9 Fatigue life of plain specimens, compared to notched or welded

5.6.1 Weld defects

In general, all welds introduce a change in geometry of the section. For this reason they act as stress raisers, thus reducing the fatigue life of the detail. In addition, the welds are not perfectly uniform and homogeneous, but present imperfections, which also act as stress raisers.

The most common weld defects are listed here:

- *Undercut at weld toe*: a crack-like defect that runs perpendicular to the weld line and can also appear in the root side of butt welds.
- *Porosity*: gases can be entrapped during the welding process thus creating discontinuities in the material, where a crack is likely to start.
- *Inclusions*: appear when several runs are performed in a welded connection and the slag from the electrode is not properly removed.
- *Incomplete penetration*: results from improper penetration of the weld, which does not reach the full depth of the member.
- *Lack of fusion*: occurs when the heat input is not enough or the welding torch is moved too fast.

In conclusion, weld defects can be reduced by good workmanship, but it is not possible to eliminate them completely during the manufacturing process. Modern techniques of post weld treatment can limit the influence of weld defects to a large extent. Such techniques are presented in Chapter 6.

5.6.2 Residual stresses due to welding process

As mentioned earlier, the weld cannot shrink freely when it cools down as it is bounded by the parent metal and as a result stresses develop in both longitudinal and transverse directions, as shown in Figure 5.10.

These stresses are called *residual stresses*. Their value depends on several parameters, such as the tensile strength of the material, the size of the element, as well as the type of the weld. Both tensile and compressive stresses develop in the detail, which appear to be self-balancing to ensure equilibrium.

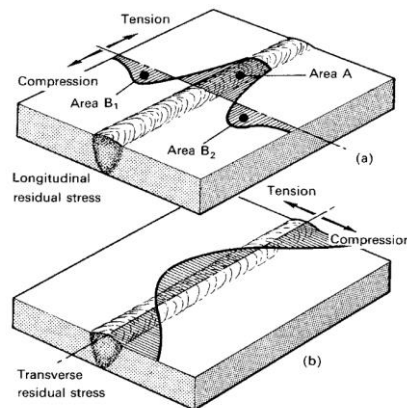


Figure 5.10 Residual stresses after welding both in longitudinal and transverse direction

Since crack initiation depends on the range of stresses and not on a single stress value, fatigue failure may occur even due to compressive stresses (see Figure 5.11). However, in this case, the crack will open but then come to an eventual stop since the residual stresses will be released, unless it still lies under the effect of tensile stresses.

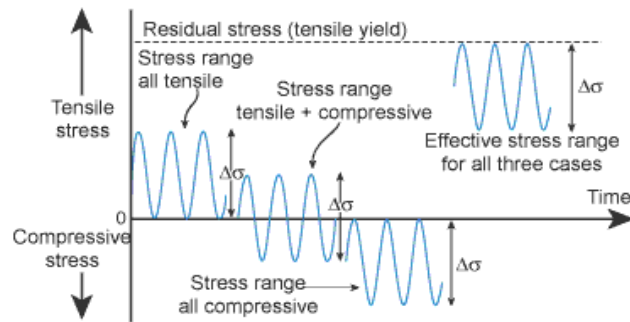


Figure 5.11 Effect of residual stresses on the position of the stress range

5.6.3 Effect of steel grade on the fatigue life of a detail

In Chapter 5, the phenomenon of fatigue failure has been explained in detail. It has been stated that the fatigue life of a specific detail is a function of the crack initiation and propagation. The former is a surface phenomenon, while the latter is strictly depending on the bulk properties of the material. It seems then obvious that an increase of material strength would have a positive influence only with regard to the crack initiation of welded details.

However, because of the aforementioned defects, welded details have shown to exhibit a similar behaviour to that of notched specimens. In other words, their fatigue life consists almost exclusively of crack propagation. Figure 5.12 clearly shows the proportion between crack initiation life and crack propagation life of two specimens, one plain and one welded one. In quantitative terms, it can be stated that:

- Plain specimen: crack initiation life $N_i = 90\%$
crack propagation life $N_p = 10\%$
- Welded specimen: crack initiation life $N_i = 10\%$
crack propagation life $N_p = 90\%$

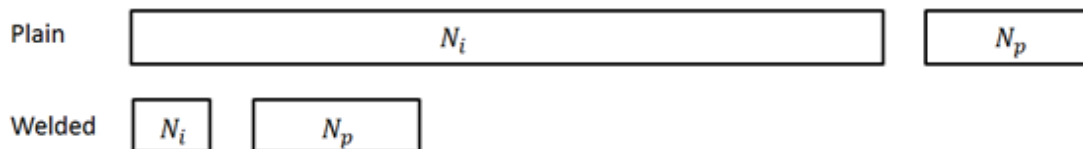


Figure 5.12 Crack initiation and propagation duration of a plain specimen compared to a welded specimen

It can then be concluded that an increase in material quality, in particular its tensile strength, would have a negligible effect on the fatigue life of a welded detail. This is clearly shown in Figure 5.13.

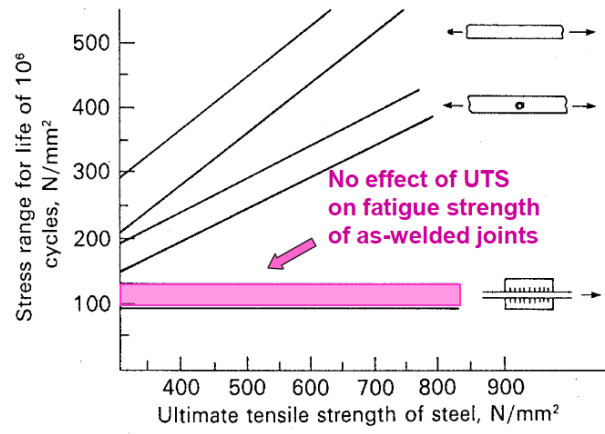


Figure 5.13 Correlation between steel quality and fatigue life

6 Introduction and description of post-weld treatment methods

The most relevant conclusion reached in the previous chapter is the following:

Since the fatigue life of welded details is almost exclusively a function of the crack propagation, no improvement in terms of fatigue resistance is achieved by increasing the strength of the material.

This conclusion is correct only to a certain extent. It is correct that the crack propagation is practically unaffected by the quality of the steel, but the benefits of a higher steel grade can be gained if the crack initiation of weld details can be restored.

The modern practice of *post weld treatment* (PWT) moves in this direction. By processing the weld, a better profile and transition can be achieved in most connections and the benefits of high strength steel can be fully exploited in the crack initiation phase. Figure 6.1 shows how PWT works with the aim of restoring the crack initiation life of a welded specimen. Nevertheless, the duration of the crack initiation that can be recovered depends strictly on the post weld treatment method, as further explained in Section 6.1.

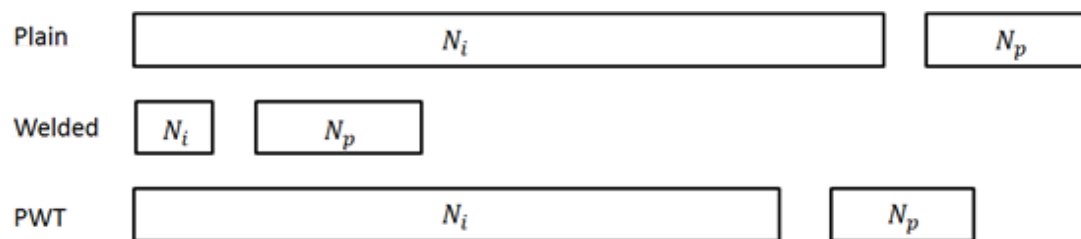


Figure 6.1 The benefit of PWT in restoring the crack initiation life of a welded specimen

Different kinds of PWT procedures are currently being performed in several industries. Among the most common applications are offshore structures, where the waves cause cyclical loading, and wind turbines, which tend to oscillate because of the wind forces.

6.1 Classification of PWT methods

The best practice in order to enhance the fatigue behaviour of a steel structure is to apply good design detailing. Anyway, in some cases critical details cannot be avoided. In this situation, the most efficient way to improve the fatigue resistance of the overall structure is to apply post weld treatment.

As mentioned in Section 5.6, the main two factors that influence the fatigue resistance of any welded detail are weld defects and residual stresses. Modern methods of post weld treatment aim to reduce the impact of the mentioned defects. For this reason it is

possible to identify two main techniques of PWT: *weld geometry improvement methods* and *residual stress methods*.

The former acts with the aim of smoothening the transition between the weld and the base metal in order to remove possible stress concentrations.

The latter act instead with the aim of introducing compressive stresses that will counteract the tensile stresses originated during the welding process.

Each of the categories can be further divided as shown in Figure 6.2.

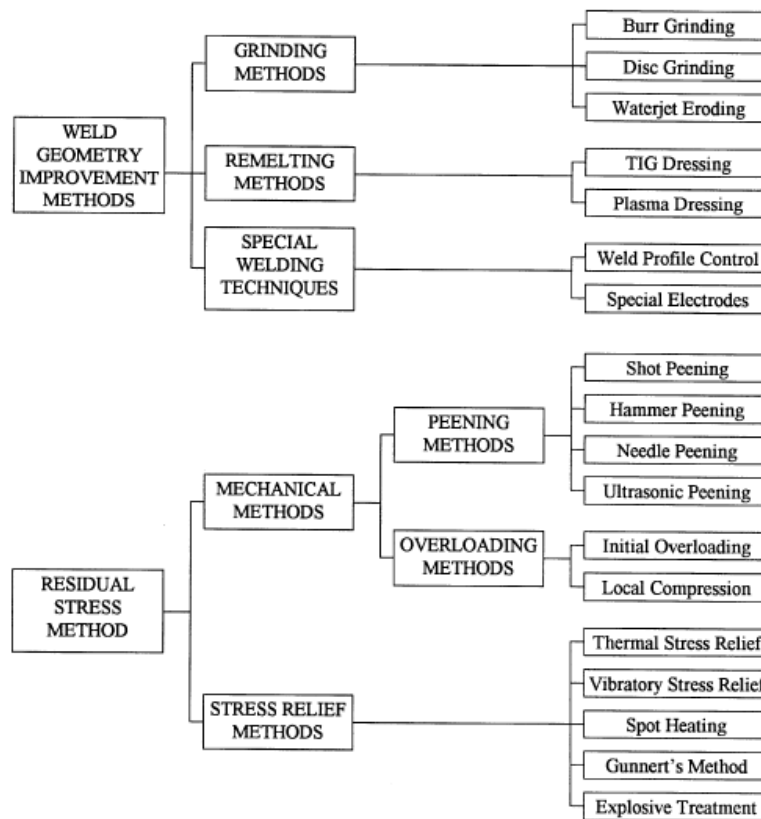


Figure 6.2 Classification of methods of post weld treatment

6.1.1 Weld geometry improvement methods

Weld geometry improvement methods can be further divided into three sub-categories which are described below.

6.1.1.1 Grinding methods

Grinding methods are far the most common method and can be performed in three different ways:

- *Burr grinding*: high speed rotary equipment is used in order to eliminate any defects which result in high stress concentrations. The surface thickness that is taken away varies from 0.5 to 2mm. It can process with the speed of 1m/h which makes it both time consuming and expensive. This method can provide

an improvement of the detail within the range of 50%-200% at 2 million cycles according to existing data.

- *Disc grinding*: considered to be less time consuming and inexpensive method but the results are not as satisfactory as burr grinding (20%-50%). Within this method, the role of the machine operator becomes very important: the amount of material that is removed might exceed the limit and could lead to the formation of a new crack.
- *Water Jet Eroding*: water containing abrasive particles is shot with high pressure on the desired area in order to erode any undercut or inclusion and provide a smooth flow of stresses. The method is very quick (10-46m/h) but requires operator training.

6.1.1.2 Re-melting methods

- *TIG dressing*: tungsten inert gas (TIG) dressing is a technique which consists into melting the weld in order to create a smoother surface. The penetration depth varies between 3 and 6 mm offering an improvement of 50%. The effectiveness of this method is highly connected with the operating conditions: the operator is responsible of controlling the geometry of the weld profile, as well as current and speed of treatment.
- *Plasma dressing*: similar to TIG dressing but double amount of heat is used to melt the surface. This results into a better transition area between the connecting materials. It is generally an inexpensive method with better improvement results than TIG, especially when working with HSS but this is outweighed by the complexity of the equipment.

6.1.1.3 Special welding techniques

- *Weld profile control*: in this method a dime (small metal plate used as tester), with a radius depending on the plate thickness, is used to check the weld profile. If any defect is detected, the weld is improved by grinding. An improvement of 25 – 30% can be expected by this method.
- *Special electrodes*: used for the final weld pass to provide a better flow of stresses between the two materials. The best results are observed in HSS with 500-800 MPa strength.

6.1.2 Residual stress methods

Residual stress methods can be further divided into three sub-categories that are described below.

6.1.2.1 Peening methods

- *Shot peening*: method through which small cast iron or steel shots are launched to the surface causing compressive stresses of 70%-80% of the yield stress. It is an inexpensive method, showing an improvement of 70% for HSS and 33% for lower class steel. Because of the need of special equipment it is mostly used for localized details.
- *Hammer peening*: performed through hammering the weld toe with hardened steel bits. It is a cold work procedure. Treating the surface four times can notch it to a depth 0.5 to 0.6mm which is enough to make the detail non critical. As with other treatment methods, better results are obtained with HSS than with conventional steel.
- *Needle peening*: it is a similar procedure to hammer peening differentiating only in the material used for the bits. The improvement that is achieved is slightly less than with the previous method.
- *Ultrasonic impact peening*: similar to hammer peening. The difference is in the materials; a peening tool with a magnetic transducer and an ultrasonic wave transmitter are used. The deformation of the weld is at around 0.5mm-0.7mm which is enough to impose compressive stresses and smooth the surface reducing the concentration of stresses. By that an improvement of 50%-200% is achieved for butt and overlap joints.

6.1.2.2 Overloading methods

- *Initial overloading*: local yielding in the range of 50%-90% of the yield stress of the steel is introduced in order to provide compressive residual stresses, improving the detail by 10%-65%.
- *Local compression*: caused by plastic deformation of the material. The detail of interest yields after being compressed between circular dies. This method offers an improvement of 70%-100% with better benefits for high strength steel.

6.1.2.3 Stress relief methods

- *Thermal stress relief*: also known as post weld heat treatment (PWHT). High temperatures are applied at the weld, which is later allowed to cool down in the air reducing therefore the residual stresses.
- *Vibration stress relief*: a way of reducing residual stresses by vibrating the weld.
- *Spot heating*: a technique through which local heating is applied in order to create local yielding. This way tensile residual stresses are formed again, and since there is a need for internal stress equilibrium, compressive stresses will grow at a close distance.

- *Gunnert's method*: performed through local heating which causes plastic deformation. The heated area is cooled down rapidly resulting in the formation of compressive residual stresses.
- *Explosive treatment*: a method through which explosive charges are placed in areas where a change has to be performed.

6.2 High Frequency Impact Treatment (HiFIT)

In the case studies that will follow in Chapter 8, 9 and 10 the fatigue assessment of the critical details will be performed referring to the improvements obtained through *High Frequency Impact Treatment* (HiFIT). This method belongs to the peening methods and aims to reduce the residual tensile stresses through building up residual compressive stresses in the detail.

A great amount of testing has been recently performed in several universities worldwide in order to quantify the benefits of HiFIT. The most relevant research project in this field is the REFRESH project conducted between 2006 and 2009, which aimed to extend the fatigues life of already existing structures.

The results were positive and an increase by 80% to 100% of the fatigue life of the analysed details was observed.

6.2.1 Description of the process

HiFIT is a high frequency impact treatment which is powered by pressurized air. The tools utilized present a metal pin which ends with a round head, with a size of 3mm in most of the applications (it can vary between 2mm and 4mm). The frequency of the treatment varies depending on the field of application and in particular between 180Hz and 250Hz.

6.2.2 Suitability of the process

The defined tool reshapes and rounds the weld toe of critical welded details. For this reason, its suitability is limited since it has no effect on root cracking, which is a pure function of the weld metal. Figure 6.3 shows the most common welded details where HiFIT is either suitable or unsuitable.

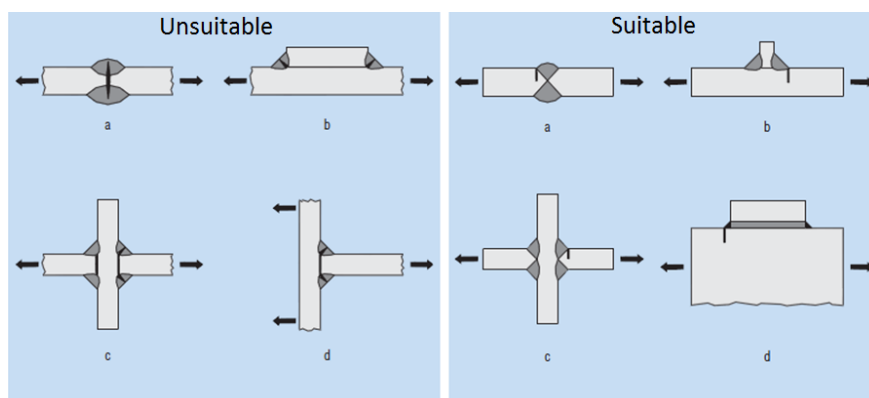


Figure 6.3 Suitability of application of HiFIT for different welded details

6.2.3 Effects of the process

Several investigations and tests have been performed recently in order to investigate the effects and improvements of the treatment on a weld. The main benefits are described in detail below.

6.2.3.1 Strain hardening

As a result of the treatment, plastic deformations are induced in the weld metal. These deformations lead to strain hardening of the material to a depth of 0,2mm to 0,3mm. Figure 6.4 shows the results of HiFIT on a weld toe.

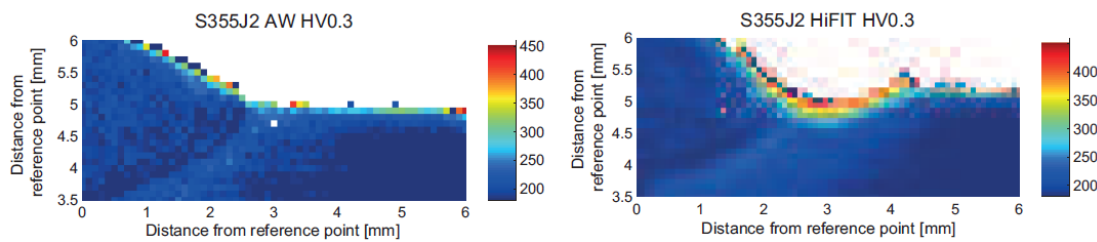


Figure 6.4 Strain hardening of the weld metal due to HiFIT

6.2.3.2 Residual compressive stresses

The plastic deformations described in Section 6.2.3.1 produce compressive stresses in the metal, which cannot be released when the treatment is over. For this reason, the stresses are kept within the material and counteract the tensile stresses originated during welding.

The amount of stress that can be induced to the material is equal to the yield strength of the base metal. It is then obvious that increasing benefits can be obtained with increasing steel quality.

The layout of the created stresses varies from case to case. It depends on many factors such as weld geometry, peening angle, pin diameter and operating conditions. However, in all cases HiFIT cannot create stresses to a depth over 2mm. The stresses vary with depth: in particular the maximum compressive stress is obtained at 0,4mm to 0,5mm. With growing depth, the stresses become tensile to ensure equilibrium.

Figure 6.5 shows the typical layout of the stresses both in transversal and longitudinal direction.

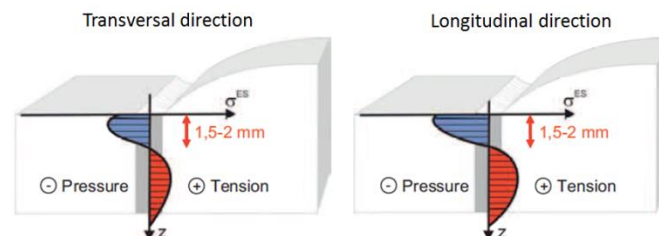


Figure 6.5 Depth distribution of stresses due to HiFIT both in transversal and longitudinal direction respectively

6.2.3.3 Changes in seams geometry

HiFIT works as a weld geometry improvement method. During the peening treatment, the pin head reshapes the transition zone between the weld toe and the base metal, resulting into a decrease of the notch factor. The 3mm pin head diameter gives the best results in this area of concern both in butt and fillet welds.

6.2.4 Effectiveness of the process

The intense testing performed recently on different categories of details showed the benefits of HiFIT. Figure 6.6 reports the test results of a transverse butt joint.

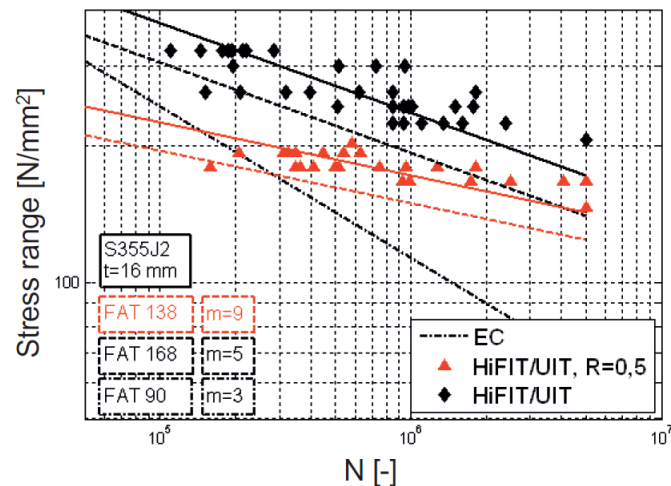


Figure 6.6 Comparison of fatigue strength between as-welded butt joints and HiFIT treated butt joints

It is clearly shown that after post weld treatment, the S-N curve of the abovementioned detail presents two main benefits:

- *Change in slope*: the slope of the line changes from $m = 3$ to $m = 5$ or 9 depending on the stresses the detail is subjected to.
- *Shift above*: the overall curve is shifted upwards in the graph, which moves the C-class from the original C90 to C138 or C168.

In the whole area of the graph where the new curves are above the original, HiFIT benefits the welded joint.

7 Design of highway and railway bridges according to Eurocode

In the case studies that follow in Chapter 8, 9 and 10, both highway and railway bridges are assessed. The design is performed in accordance with the guidelines given by the Eurocodes (each specific section is specified where relevant).

The loads models of the different bridges are presented in this chapter.

7.1 Models for highway traffic loads

Within the Eurocodes, different load models for highway traffic are presented. Each of them is described in detail:

- LM1

This model represents normal traffic. It includes both a distributed load and a concentrated pair of axles, which are to be applied in the most unfavourable positions with regard to the element being designed. The loads are displayed in Figure 7.1 and their values are listed in Table 7.1.

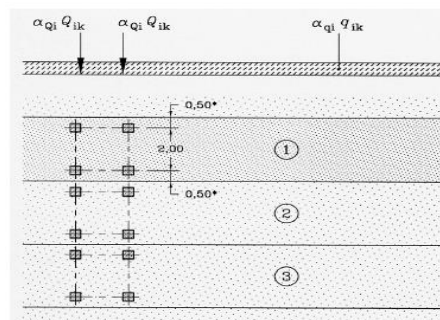


Figure 7.1 Traffic load distribution-transverse section (EN 1991-2, Figure 4.2a)

Table 7.1 Characteristic values of loading for LM1

Location	Tandem system TS	UDL system
	Axle loads Q_{ik} (kN)	q_{ik} (kN/m ²)
Lane Number 1	300	9
Lane Number 2	200	2,5
Lane Number 3	100	2,5
Other lanes	0	2,5
Remaining area	0	2,5

- LM2

This model includes the load from a single axle. The value of the load is taken as $Q_{ak} = 400kN$ (multiplied by a factor β_Q) and is to be applied in any place of the carriageway. The contact area of each tire is shown in Figure 7.2.

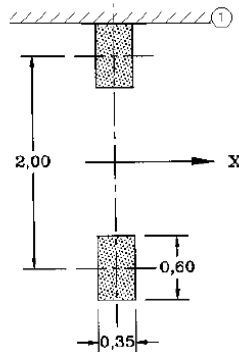


Figure 7.2 Tire size for LM2 (EN 1991-2, Figure 4.2b)

- LM3

This model assesses the case of abnormal vehicle transit. Since it is not used in any of the case studies, it is not described in detail but can be found in EN1991-2 Annex A.

- LM4 (crowd loading)

This model considers a distributed load of $5 kN/m^2$ acting in the relevant areas of the carriageway. It is allowed for transient design situations.

7.2 Models for railway traffic loads

Within the Eurocodes, different load models for railway bridges are presented. Each of them is described in detail:

- LM71

This load model is meant to describe the typical traffic conditions occurring on a simply supported bridge of the standard gauge European Railway Network. The load arrangement should be taken in accordance with Figure 7.3:

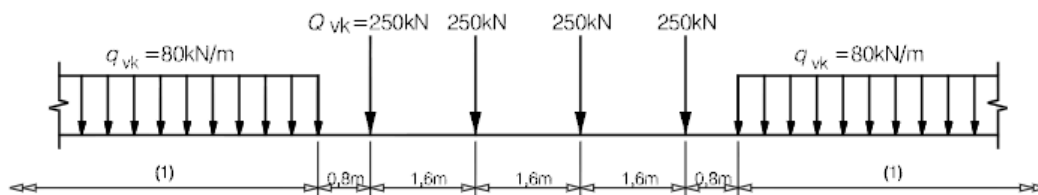


Figure 7.3 Arrangement and values of loading for LM71 (EN 1991-2, Figure 6.1)

- SW/0

This combination describes the acting loads due to normal traffic load on continuous spans. The load distribution can be taken as in Figure 7.4 and the characteristic values are listed in Eurocode as in Table 7.2.

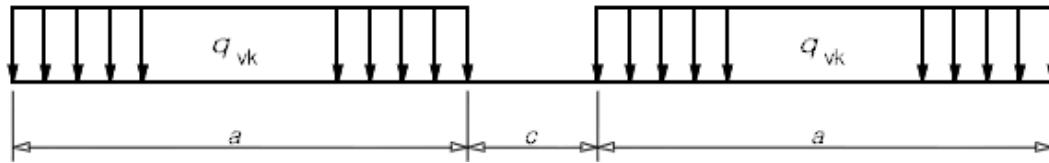


Figure 7.4 Load arrangement for SW/0 and SW/2 (EN 1991-2, Figure 6.2)

Table 7.2 Values of loading for SW/0

Load Model	q_{vk} [kN/m]	a [m]	c [m]
SW/0	133	15,0	5,3

- SW/2

This combination describes the acting loads due to the transportation of heavy equipment, such as turbines, machines, etc. In this case the loads are known and the speed of the train is often limited.

The load distribution is the same as applied in SW/0 and can be taken as in Figure 7.4. The characteristic values are different though and listed in Eurocode as in Table 7.3.

Table 7.3 Values of loading for SW/2

Load Model	q_{vk} [kN/m]	a [m]	c [m]
SW/2	150	25,0	7,0

- HSLM

This model is to be applied for trains travelling at a speed higher than 200 km/h. For such trains a dynamic analysis is required and it is performed through two different models: HSLM-A and HSLM-B (EN 1991-2 part 6.4.6). Together the models represent the dynamic effects originating from a conventional high-speed passenger train.

- Unloaded Train and Real Train

The first model is used for stability check and consists of a uniformly distributed load of 10kN/m.

The second model is used for special fatigue checks and for making assumptions about the fatigue damage of a structure (EN 1991-2 Annex D).

7.3 Fatigue load models for highway bridges

The transit of vehicles on a bridge can cause a stress spectrum which can cause fatigue problem in the structure, even though the stresses are well below the resistance of the members. The Eurocode defines five different fatigue load models in Section EN 1991-2.

- FLM1

FLM1 has exactly the same configuration as LM1 but the loads are reduced by factors of 0,7 and 0,3, unless else specified.

- FLM2 (frequent lorries)

In this case different ideal lorries are defined in Table 4.6 in the Eurocode. The stresses are to be calculated by assuming the worst possible combination of loads, separately considered.

- FLM3 (single vehicle model)

Four different axles of 120kN are taken into account. Two vehicles are to be combined where relevant.

- FLM4 (set of standard lorries)

Sets of standard lorries are taken into account to resemble the conditions of standard European roads. For this load model, it is necessary so specify the number of observations per year, N_{obs} , and the set of equivalent lorries. All these can be found in Eurocode EN 1991-2 and are here reported in Table 7.4 and Figure 7.5.

- FLM5 (recorded road traffic)

In this case, the road traffic is monitored and the data is used in the design. In some cases, statistical projections are also included.

Table 7.4 Number of observations per year-FLM4

Traffic categories		N_{obs} per year and per slow lane
1	Roads and motorways with 2 or more lanes peer direction with high flow rates of lorries	$2,0 \cdot 10^6$
2	Roads and motorways with medium flow rates of lorries	$0,5 \cdot 10^6$
3	Main roads with low flow rates of lorries	$0,125 \cdot 10^6$
4	Local roads with low flow rates of lorries	$0,05 \cdot 10^6$

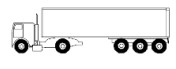
VEHICLE TYPE			TRAFFIC TYPE			
1	2	3	4	5	6	7
	Asle spacing (m)	Equivalent axle loads (kN)	Long distance Lorry percentage	Medium distance Lorry percentage	Local traffic Lorry percentage	Wheel type
	4,5	70 130	20,0	40,0	80,0	A B
	4,20 1,30	70 120 120	5,0	10,0	5,0	A B B
	3,20 5,20 1,30 1,30	70 150 90 90	50,0	30,0	5,0	A B C C C
	3,40 6,00 1,80	70 140 90 90	15,0	15,0	5,0	A B B B
	4,80 3,60 4,40 1,30	70 130 90 80 80	10,0	5,0	5,0	A B C C C C

Figure 7.5 Set of equivalent lorries-FLM4 (EN 1991-2, Table 4.7)

7.4 Fatigue load models for railway bridges

The fatigue assessment of a bridge is carried out through LM71 with the addition of a dynamic amplification factor Φ which is defined in Equation 7.1. It takes the dynamic effects on the structure into account.

$$\Phi = \frac{1,44}{\sqrt{L_\Phi} - 0,2} + 0,82 \quad 1,0 \leq \Phi \leq 1,67 \quad \text{Equation 7.1}$$

In the case studies, the railway bridges that are analysed are subjected to a *heavy traffic mix* (EN 1991-2 annex D). In this case, the distribution of the axle loads is described in Figure 7.6.

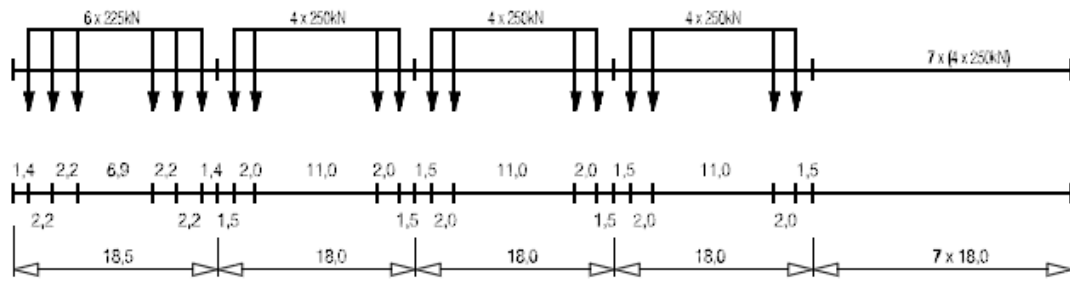


Figure 7.6 Heavy traffic mix - Locomotive-hauled freight train (EN 1991-2)

The traffic mix described above considers a total traffic of about $25 \cdot 10^6$ tonnes per year, distributed as shown in Table 7.5.

Table 7.5 Volume of traffic according to heavy traffic mix

Train type	Number of trains/day	Mass of train [t]	Traffic volume [$10^6 t/year$]
5	6	2160	4,73
6	13	1431	6,79
11	16	1135	6,63
12	16	1135	6,63
	51		24,78

8 Case and parametric study of railway bridges

Railway steel bridges are known to be highly affected by fatigue. In this section a specific bridge design is assessed and redesigned with PWT.

The general aim of the study is to verify whether the benefits coming from PWT can lead to a significant reduction of the steel amount and, more importantly, a reduction of the material costs.

8.1 Original bridge design

The hereby assessed bridge is a railway bridge over Östra Klarälven in Ställdalen-Kil, km 226+285, Figure 8.1.

8.1.1 Geometry and loading

The railway bridge is a steel bridge with two simply supported spans of 24m each: since it is symmetrical, only one of the spans is taken into account. The cross-section of the bridge (Figure 8.2) is composed of two steel girders with a common upper flange forming together an open hat-shaped profile, with cross-bracing and vertical stiffeners at regular intervals. The height of the girders varies along the length, i.e. it is reduced at the supports. However, this change of the cross section is neglected in this study and the girders are considered to maintain the same cross-section through the whole span.

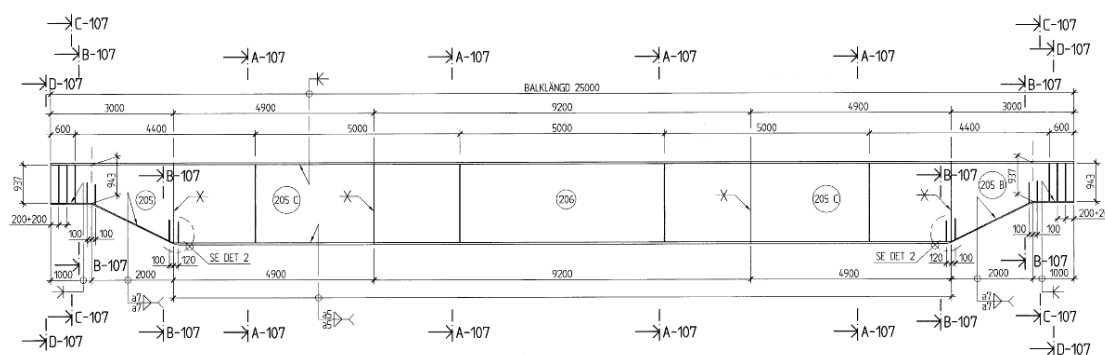
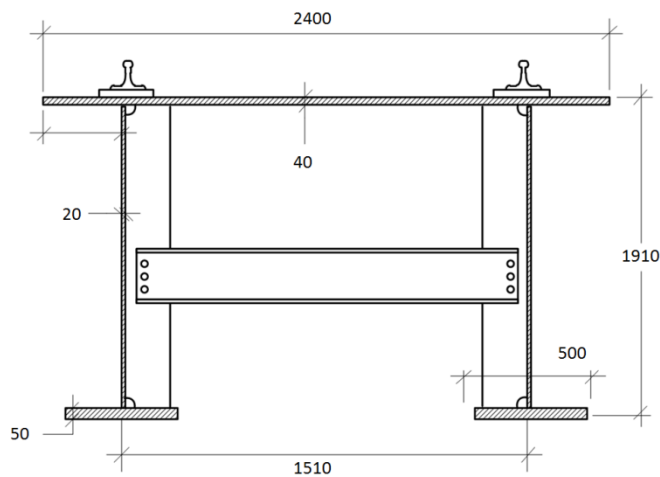


Figure 8.1 Longitudinal view of the railway bridge over Östra Klarälven, Sweden

Butt welds are used to connect the upper flange to the web as well as for the connection between the vertical stiffeners and the upper flanges. 7mm fillet welds are used for the connections at the bottom side of the girders. The steel quality used for all load-carrying parts in the bridge is S355.

In the fatigue design of the girders, the design life of the bridge is given to be 120 years and the traffic details used are the ones defined in Section 7.4.

The dimensions of the steel cross-section and the relevant dimensions are given in Figure 8.2.



L_{span}	24 m
h_{web}	1910 mm
t_{web}	20 mm
t_{top}	40 mm
b_{top}	2400 mm
t_{bottom}	50 mm
b_{bottom}	500 mm
C_{rail}	1510 mm

Figure 8.2 Bridge cross-section with dimensions

The original bridge is fabricated with steel quality S355, which has a density of $\rho_{S355} = 7700 \frac{kg}{m^3}$ and tensile characteristics which vary depending on the specific thickness of each plate: see Section 2.4.1.

In this simplified analysis, the loads taken into account are the self-weight of the structural elements (including cross-beams, stiffeners and rails), wind load and train loads.

Load combinations are given in Eurocode EN 1990:2002: Basis of structural design.

- Self-weight

The weights in Table 8.1 are considered when calculating the self-weight of the bridge. All weights are given in kg per unit length of bridge.

Table 8.1 Additional self-weights

Part	Kg/m ³
Cross-beams	10,5
Stiffeners	18
Rails	120
Screws	66

- Wind

Analysis of the load-carrying capacity of the bridge in the ULS should also consider the effect of wind loads.

1. Wind acting on the bridge, $q_{w,bridge} = 6 \frac{kN}{m^2}$
2. Wind acting on the train, $q_{w,train} = 1,4 \frac{kN}{m^2}$

- Train

The train loads are given in load model LM71 according to Eurocode EN 1991-2, see Section 7.2.

8.1.2 Cross section verification

According to Eurocode EN 1090-2, the main girders should be verified in ULS, SLS and FLS.

- ULS verification:

It includes bending and shear check, as well as their combination. The cross-sectional constants used in the verifications take the reductions due to local and global buckling of the compressed structural members into account (this explains the term W_{eff} in Equation 8.2).

These instability phenomena drastically reduce the static resistance of the section and their influence is assessed as specified in EN 1993-1-1 Section 6.3.2.

Bending:

$$M_{ULS} = \gamma_g \cdot M_{self} + \gamma_D \cdot \Phi_1 \cdot \alpha \cdot M_{train} + \gamma_o \cdot \psi \cdot M_{wind} = 11,6 \text{ MN} \quad \text{Equation 8.1}$$

$$M_{Rd} = W_{eff} \cdot \frac{f_y}{1.0} = 21,8 \text{ MN} \quad \text{Equation 8.2}$$

Shear:

$$V_{ULS} = \gamma_g \cdot V_{self} + \gamma_D \cdot \Phi_1 \cdot \alpha \cdot V_{train} + \gamma_o \cdot \psi \cdot V_{wind} = 1,97 \text{ MN} \quad \text{Equation 8.3}$$

$$V_{Rd} = V_{wRd} + V_{fRd} = 5.5 \text{ MN} \quad \text{Equation 8.4}$$

- SLS verification:

The verification for deflection includes the effects of both self-weight and train loads. The latter give the most unfavourable contribution to bridge deflection when the axle loads are symmetrically distributed around the middle section of the span.

$$\delta_{TOT} = \delta_{self} + \delta_Q + \delta_P = 21,5 \text{ mm} \quad \text{Equation 8.5}$$

$$\delta_{max} = \frac{L}{600} = 39 \text{ mm} \quad \text{Equation 8.6}$$

- Web breathing:

According to EN 1993-2 Section 7.4 we assure that such phenomenon is not an issue.

- FLS verification:

The damage accumulation method is used at this stage in order to verify the fatigue resistance of the most critical welded details along the span. Figure 8.3 shows the four different details that have been taken into account, since they are usually the most critical.

Table 8.2 gives a detailed description of the different details.

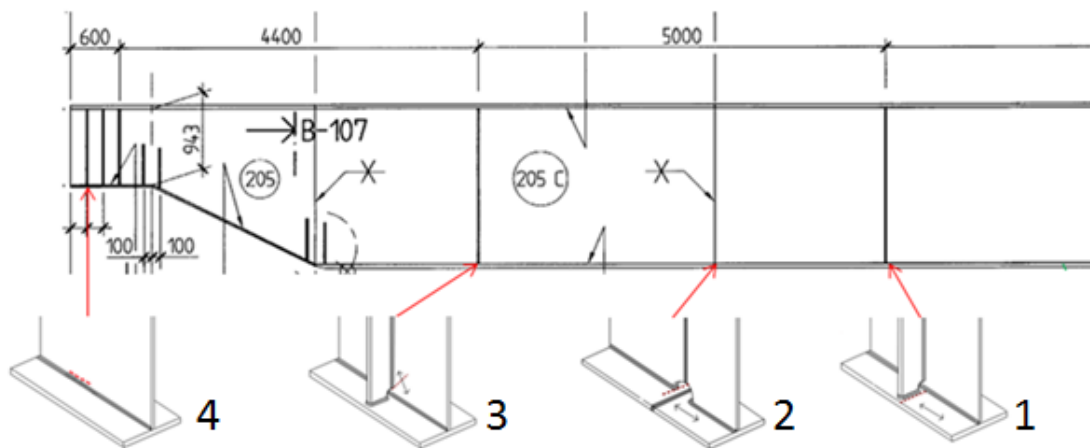


Figure 8.3 Detail view of the critical details for fatigue resistance

Table 8.2 Description of the details

Detail 1 (C80) Vertical Stiffener $x = 9,4m$	the global bending of the girder produces normal stresses in the bottom flange, which can cause a crack to start along the bottom weld of the vertical stiffener
Detail 2 (C71) Rat hole $x = 7,3m$	the global bending of the girder produces normal stresses in the bottom flange, which can cause a crack to start at the edge of the rat-hole positioned to allow the in-situ welding of the different sections of the bridge
Detail 3 (C80) Vertical Stiffener $x = 4,4m$	the combination of bending and shear stresses contribute to development of principal stresses in the web, which can cause a crack to start at the bottom edge of the vertical stiffener
Detail 4 (C80/100) Vertical Stiffener $x = 0m$	the shear stresses are highest at the support and here a crack can initiate at the bottom of the web, either along the web (C100) or the welds (C80)

The FLS analysis of the above listed details is performed with bridgeFAT, which uses the damage accumulation method in order to find the total damage of a specified detail, when the following information is given:

- Influence lines for moment and/or shear
- Sectional properties
- Detail category
- Traffic load (see Section 7.4)
- Design life

8.1.3 Results and remarks

The results of the verifications can be found in detail in Appendix A1. Their values and respective utilization ratios in ULS, SLS and FLS are summarized in Table 8.3 and Table 8.4.

Table 8.3 Design verification in ULS and SLS

	Design value	Resistance	Utilization ratio
ULS bending	11,6 MNm	21,8 MNm	0,533
ULS shear	1,97 MN	5,5 MN	0,358
SLS deflection	21,5 mm	39 mm	0,543

Table 8.4 Design verification in FLS

Detail	D _{LM5}	D _{LM6}	D _{LM11}	D _{LM12}	D _{tot}
1 (C80)	0,21	0,43	0,21	0,09	0,96
2 (C71)	0,22	0,49	0,22	0,10	1,03
3 (C80)	0,07	0,07	0,04	0,01	0,19
4 (C80)	0,07	0,19	0,07	0,02	0,35

These results highlight that the design of the bridge is governed by the fatigue resistance of details 1 and 2. The cross-section resistance cannot be fully utilized as the utilization ratios are considerably low.

8.2 New bridge design

As stated in Section 8.1.3 the cross-section resistance of the bridge is utilized only to a low degree since fatigue becomes critical.

The way of achieving a better utilization of the material is to overcome the limitation due to fatigue. In this section, a new and improved bridge design is proposed and verified, considering the positive effects of PWT on the fatigue life of critical details.

8.2.1 Geometry and loading

The cross-section dimensions of the main girders are reduced to achieve better utilization ratios in ULS. The new cross-section dimensions are listed in Figure 8.4.

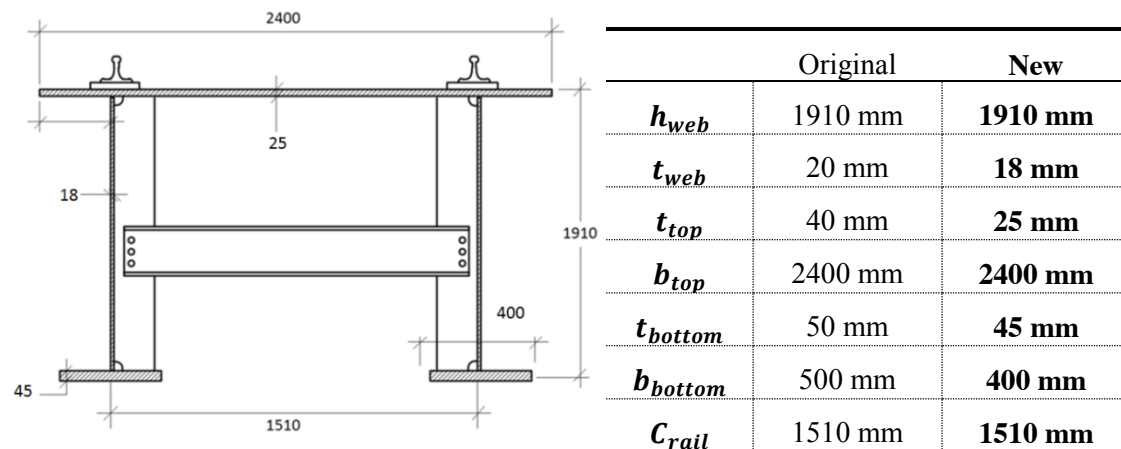


Figure 8.4 New bridge cross-section with dimensions

The steel quality S355 is kept in this new bridge design. The use of higher strength steel would not be justified since fatigue would become limiting once more, as it will be shown in Section 8.2.3.

The reduction of the cross-section results into a decrease of the self-weight of the girders. All the other loads considered in the analysis remain unaffected.

8.2.2 Cross section verification

The same cross-section verifications are performed for the new design.

- ULS verification:

In this case, since the self-weight is slightly lowered, a small decrease of the actions acting on the girders is expected, i.e. M_{ULS} and V_{ULS} will decrease.

In addition, a drastic decrease of cross-section resistance, both in shear and bending, is expected.

- SLS verification:

As the cross-section is reduced, an increase of deflection is expected, since the loading remains basically unaffected, except for the self-weight.

- Web breathing:

This verification is affected by the reduction of the web thickness. It should be verified that such a reduction doesn't result in the development of the phenomenon.

- FLS verification:

The same analysis is performed as for the original design, taking into account the reduction of the cross-sectional properties. The stresses applied on each specific detail are higher compared to the former design, which results in an increase of damage.

At this stage, PWT becomes beneficial. The C-class of those details which fail in fatigue can be enhanced so that the total damage can be kept below the limit.

The PWT described earlier in Section 6.2 can be performed in particular on detail 1 and 2. The C-classes of these details can be improved respectively to C112 and C100. As shown in Figure 8.5, the S-N curve is shifted upwards while the stress ranges remain untouched. This way the total damage is expected to decrease.

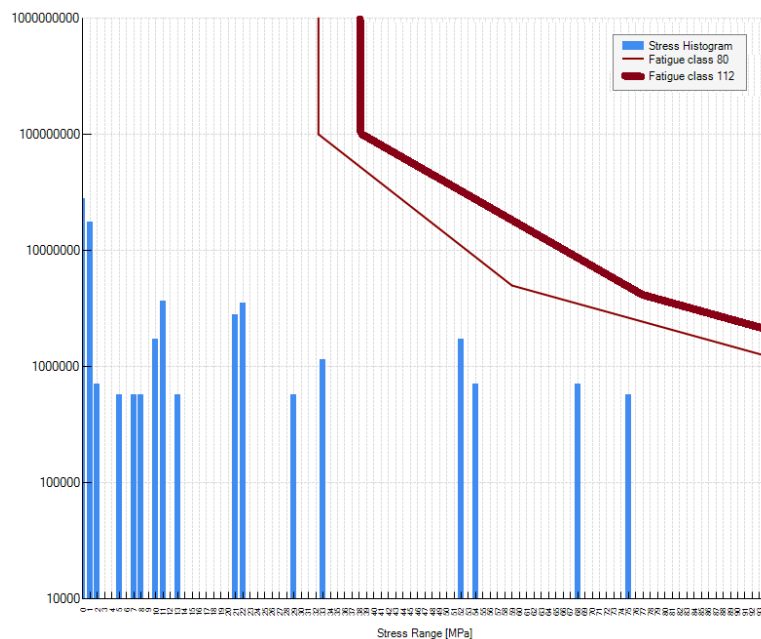


Figure 8.5 New position of the S-N curve after PWT

8.2.3 Results and remarks

The verification results for ULS, SLS and FLS are summarized in Table 8.5 and Table 8.6.

Table 8.5 Design verification in ULS and SLS

	Design value	Resistance	Utilization ratio
ULS bending	11,5 MNm	15,7 MNm	0,734
ULS shear	1,94 MN	4,4 MN	0,437
SLS deflection	29,7 mm	39 mm	0,75

Table 8.6 Design verification in FLS

Detail	D_{LM5}	D_{LM6}	D_{LM11}	D_{LM12}	D_{tot}
1 (C112)	0,19	0,36	0,18	0,07	0,81
2 (C100)	0,19	0,40	0,20	0,08	0,87
3 (C80)	0,15	0,30	0,16	0,05	0,67
4 (C80)	0,06	0,17	0,06	0,19	0,32

As for the original bridge, the design is governed by fatigue. At the same time, a much better utilization of the cross-section can be achieved.

8.3 Comparison between original and new bridge design

As stated at the beginning of the chapter, the main aim of this study is to quantify the decrease of the material costs. For this specific case study, the results are shown in Table 8.7.

Table 8.7 Cost analysis of original and new design

	Steel	$A(m^2)$	$V(m^3)$	Material cost(SEK)	PWT cost(SEK)	Total cost(SEK)
Original design	S355	0,21	5,04	269.000	0	269.000
New design	S355	0,17	4,08	221.200	1600	222.800

The table shows a significant reduction of the girder's cross-section area leading to a reduction of the material cost. The cost of PWT is evaluated by taking into consideration the amount of details to be treated and their size. The general prices and information are in accordance with the guidelines given from Dynatec⁴.

These two variables allow calculating the total cost reduction that can be achieved. For the steel girders of the bridge over Östra Klarälven a total cost saving of 46.200 SEK can be achieved, which corresponds to 17%.

It is worth remarking that even higher benefits could be obtained if the C-class of the critical details would be enhanced even further. At this stage an improvement of 3 C-classes (from C80 to C112 and from C71 to C100) is set as a boundary. Further improvement would completely remove the fatigue limitation from the design and the section dimensions could be decreased even more, until ULS or SLS utilization ratios would become the limiting factors.

⁴ Dynatec: Gesellschaft für CAE und Dynamik mbH

8.4 Parametric study

The case study performed in the previous paragraph shows that a relevant saving of total cost can be achieved thanks to the benefits of PWT. It becomes then relevant to know if the same benefits can be achieved for other span length as well. With this purpose, a parametric study is performed in order to find out how the span length of a simply supported railway bridge affects the total cost saving.

In this specific case, span length varying between 16m and 30m are studied. The shape of the cross-section is kept constant while the dimensions are adjusted to withstand the variable stresses.

For each span length the two designs are provided, where only one of them includes PWT. This way it is possible to quantify the material saving for each case. The specific data and verifications for each bridge can be found in Appendix B1.

Figure 8.6 graphically shows the variation of material and cost savings within the span range.

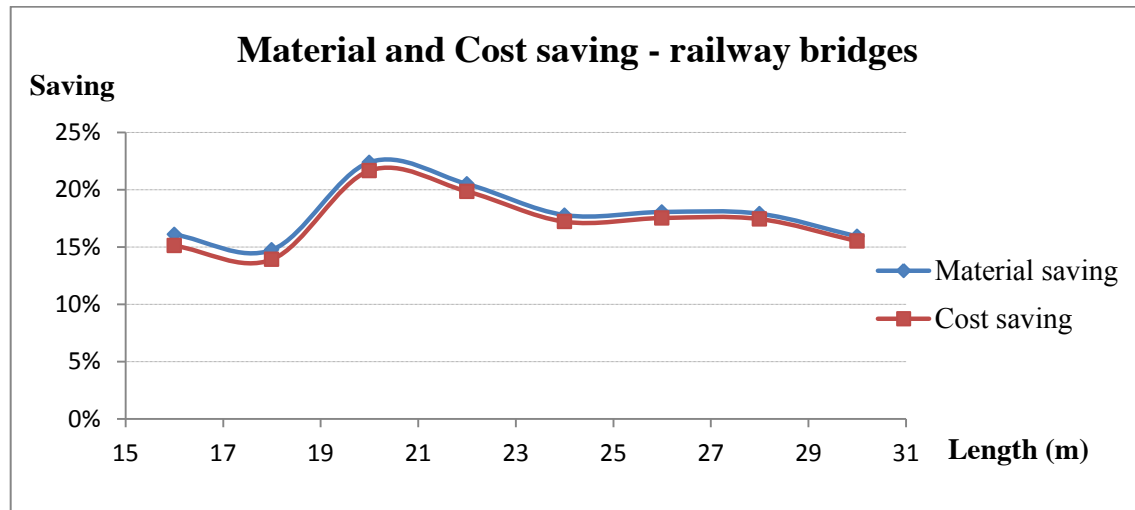


Figure 8.6 Material and cost saving achieved by the new design

The variation of cost savings within the same span range is calculated by taking into account the price of PWT needed. Longer spans present more details to be treated so the PWT cost increases slightly with the increasing spans.

It is clearly shown that the greatest benefits are obtained within the spans of 20m to 23m with a peak material saving of 22%. The values appear to be lower in the left side of the graph since fatigue is still limiting; a further improvement of the weld profiles by more advanced post weld treatment, e.g. more than three C-classes as supposed in this thesis, could higher the savings in this area by shifting the curve upwards. The other end of the graph instead cannot benefit any more by PWT since SLS is the limit to design.

In order to explain these results further, it is worth looking closer at the behaviour of the different bridges with regard to bending, deflection and fatigue. Figure 8.7 and Figure 8.8 show the variation of the respective utilization ratios with increasing span length.

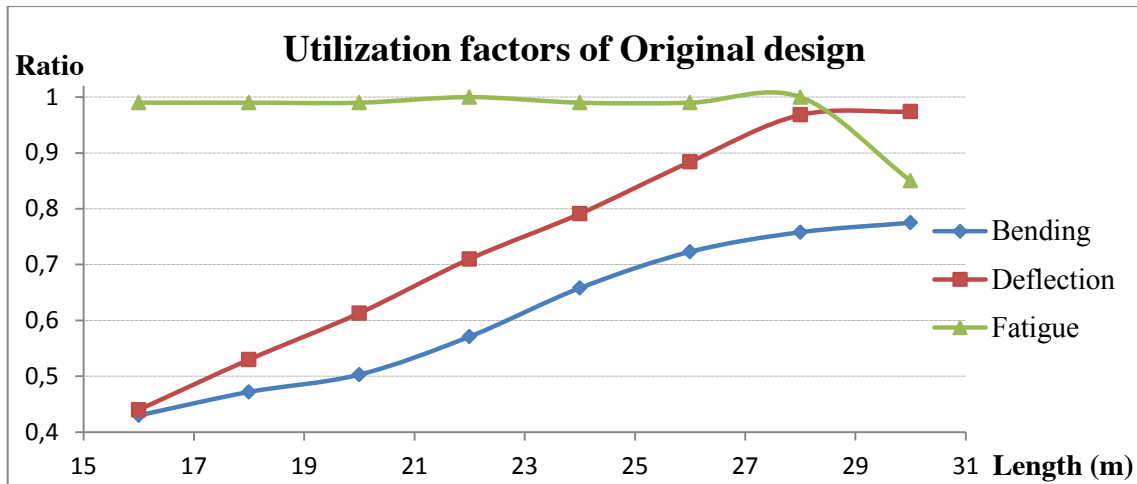


Figure 8.7 Utilization factors of Original design

The main conclusions about the original design that can be drawn from Figure 8.7 follow:

1. The original design is limited by fatigue for most of the span lengths. Only for spans over 28m it is no longer a boundary.
2. In short spans, fatigue dominates the design because of the large influence of the dynamic amplification factor (which is high for short spans). It is not possible to achieve good utilization in ULS and SLS.
3. The SLS utilization increases along with the increase of span length. Over a certain span length, SLS utilization exceeds FLS utilization and deflection becomes the limiting factor.

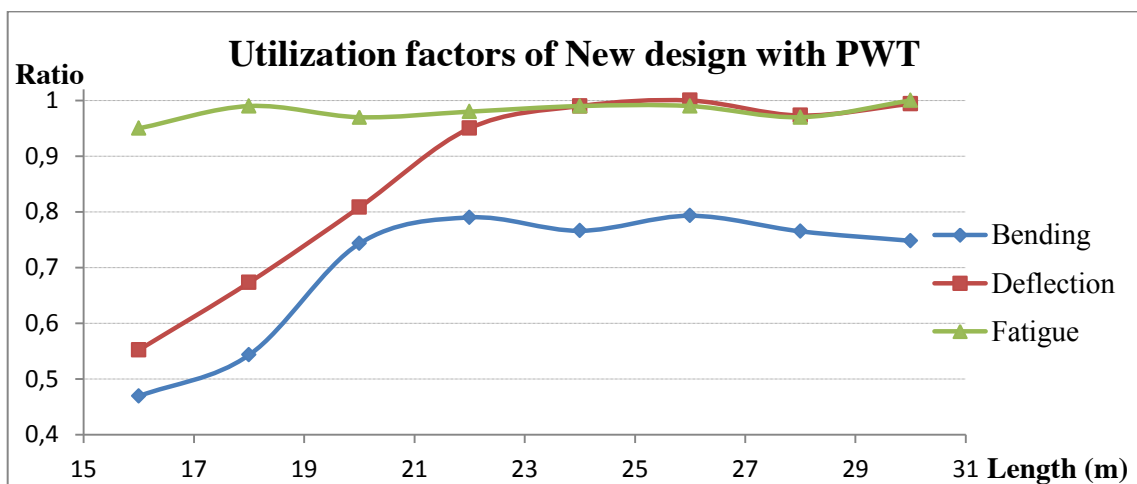


Figure 8.8 Utilization factors of New design with PWT

The main conclusions about the new design that can be drawn from Figure 8.8 follow:

1. Fatigue is still limiting the design of short span bridges, but better utilization in bending and deflection can be achieved.

2. Deflection becomes limiting much earlier since the cross-section dimensions have been decreased.
3. Overall higher utilization ratios are obtained.
4. The bending resistance cannot be fully utilized since deflection governs the design for most of the spans.
5. Compared to the original design, the trends of bending and deflection are shifted upwards.

8.5 Summary

In this chapter it has been shown that the use of PWT on critical details of steel railway bridges can have great benefits in terms of cost saving.

A case study has been performed on an existing bridge. The original design has shown to be governed by fatigue. In order to overcome this limitation, a new design has been proposed, where the critical details have been post weld treated. This enhancement of the fatigue resistance allowed a drastic reduction of the girders' cross section, leading to material and cost savings.

These positive results encouraged a parametric study to be performed. The main outcome highlighted that steel railway bridges with spans between 20m and 23m have the greatest benefits from PWT with a maximum cost saving of 22%.

9 Highway bridges

Highway composite bridges are usually less affected by fatigue than railway bridges. For this reason fatigue is less critical in highway bridge design. In this section the same procedure adopted earlier for railway bridges is performed. Unlike the former, the possible benefits of HSS will be evaluated along with PWT since the case studies will show that fatigue or deflection are not always governing.

The general scope of the study is to verify whether the benefits coming from a combination of HSS and PWT can lead to a significant reduction of the steel amount and, more importantly, a reduction of the material costs.

9.1 Original bridge design

The road bridge in this case study is a composite steel-concrete bridge over E4 in Skulnäs, with a single span of 32,0m (Figure 9.1).

9.1.1 Geometry and loading

The bridge is assumed to be straight in the horizontal plan, with a constant total depth along the entire span. The two steel girders are joined by diaphragms at each L/4. The intermediate diaphragms are made of channel profiles, while the end cross-beams are made of I-sections.

The twin steel girders are identical. Each girder is made of three segments (8,5m + 15m + 8,5m) which are assembled on site by welding.

The concrete deck is 5,0m wide, excluding the concrete edge beams. The average depth of the concrete deck is assumed to be 270mm. The dimensions of the steel cross-section and the relevant dimensions are given in Figure 9.2.

Composite action between the concrete deck and the steel girders is achieved by means of two rows of shear studs welded to the top flange of each girder.

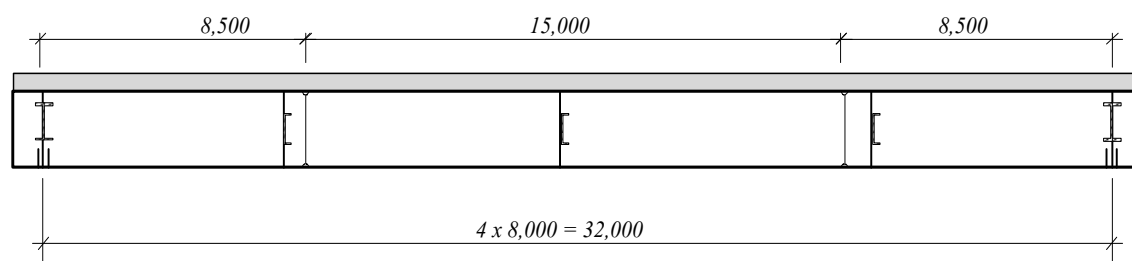


Figure 9.1 Longitudinal view of the highway bridge over E4 in Skulnäs, Sweden

Butt welds are used to connect the upper flange to the web as well as for the connection between the vertical stiffeners and the upper flanges. 7 mm fillet welds are used for the connections at the bottom side of the girders. The steel quality used for all load-carrying parts in the bridge is S355.

In the fatigue design of the girders, the design life of the bridge is given to be 80 years and the traffic details used are the ones defined in Section 7.3.

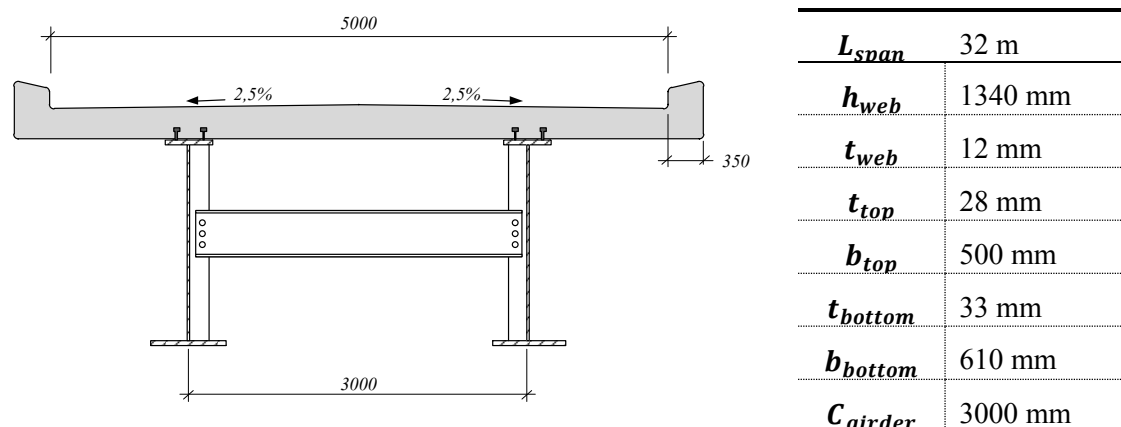


Figure 9.2 Bridge cross-section with dimensions

The original bridge is fabricated with steel quality S355, which has a density of $\rho_{S355} = 7700 \frac{kg}{m^3}$ and tensile characteristics which vary depending on the specific thickness of each plate, Section 2.4.1.

The concrete deck is made of normal concrete C35/45 which has the following characteristics:

$$f_{ck} = 35 \text{ MPa}$$

$$f_{ctm} = 3,2 \text{ MPa}$$

$$E_{cm} = 34,000 \text{ MPa}$$

In this simplified analysis, the loads taken into account are the self-weight of the structural elements (including surfacing and parapets), wind load and traffic loads.

Load combinations are given in Eurocode EN 1990:2002: Basis of structural design.

- Self-weight

The following weights are considered in calculating the self-weight of the bridge. All weights are given in kN per unit length of bridge.

Table 9.1 Additional self-weights

<i>Part</i>	<i>KN/m</i>
<i>Girders</i>	9,5
<i>Deck</i>	32,5
<i>Surfacing</i>	6,15
<i>Parapets</i>	4

- Wind

Analysis of the load-carrying capacity of the bridge in the ULS should also consider the effect of wind loads.

1. Wind acting on the bridge, $q_{w,bridge} = 6 \frac{kN}{m^2}$

2. Wind acting on the cars, $q_{w,car} = 1,4 \frac{kN}{m^2}$

- Traffic

The traffic loads are given in load model LM1 and LM2 according to Eurocode EN 1991-2, see Section 7.1.

The total carriageway width of the bridge (distance between edge beams) is 5,0 m. Thus, there is only one notional lane with a width of 3,0m and a remaining area which is 2,0m wide.

9.1.2 Cross section verification

In this case study, only the design of the main girders is relevant. At this stage, the concrete deck is neglected and only considered as a load. According to Eurocode EN 1090-2 the main girders should be verified in ULS, SLS and FLS.

- ULS verification:

The ULS verification includes bending and shear check. The cross-sectional constants used in the verifications are the action provided by the concrete deck and the reductions due to local and global buckling of the compressed structural members take into account (this explains the term W_{eff}).

These instability phenomena reduce drastically the static resistance of the section and their influence is assessed as specified in EN 1993-1-1 Section 6.3.2.

Bending:

$$M_{ULS} = \gamma_g \cdot M_{self} + \gamma_D \cdot LDF \cdot M_{LM1} + \gamma_o \cdot \psi \cdot M_{wind} = 12,1 \text{ MNm} \quad \text{Equation 9.1}$$

$$M_{Rd} = W_{eff} \cdot \frac{f_y}{1.0} = 12,7 \text{ MNm} \quad \text{Equation 9.2}$$

Shear:

$$V_{ULS} = \gamma_g \cdot V_{self} + \gamma_D \cdot LDF \cdot V_{LM1} + \gamma_o \cdot \psi \cdot V_{wind} = 1,53 \text{ MN} \quad \text{Equation 9.3}$$

$$V_{Rd} = V_{wRd} + V_{fRd} = 1,99 \text{ MN} \quad \text{Equation 9.4}$$

- SLS verification:

The deflection includes the effects of both self-weight and traffic loads. The latter give the most unfavourable contribution to bridge deflection when the axle loads are symmetrically distributed around the middle section of the span.

$$\delta_{TOT} = \delta_{self} + \delta_Q + \delta_P = 71,6 \text{ mm} \quad \text{Equation 9.5}$$

$$\delta_{max} = \frac{L}{400} = 80 \text{ mm} \quad \text{Equation 9.6}$$

- Web breathing:

According to EN 1993-2 Section 7.4 it is assured that such phenomenon is not an issue.

- Buckling during casting:

Since the concrete deck will be cast on site, there is a risk of buckling of the main girders, when they are not restrained by the deck itself. To ensure safe conditions the girders alone need to be capable to withstand the weight of the fresh concrete. This can be verified in accordance with EN 1993-1-1 Section 6.3.1.

- FLS verification:

The damage accumulation method is used in order to verify the fatigue resistance of the most critical welded details along the span. Figure 9.3 shows the four different details that have been taken into account. Table 9.2 gives a detailed description of the different details.

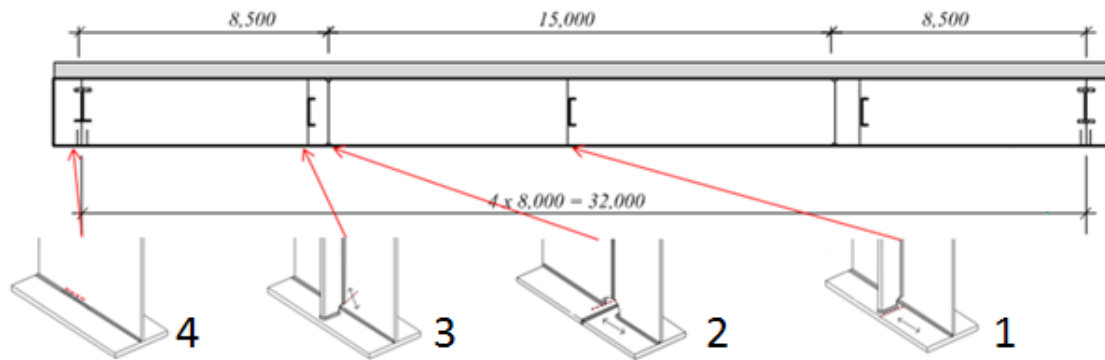


Figure 9.3 Detail view of the critical details for fatigue resistance

Table 9.2 Description of the details

Detail 1 (C80) Vertical Stiffener $x = 16m$	the global bending of the girder produces normal stresses in the bottom flange, which can cause a crack to start along the bottom weld of the vertical stiffener
Detail 2 (C71) Rat hole $x = 8,5m$	the global bending of the girder produces normal stresses in the bottom flange, which can cause a crack to start at the edge of the rat-hole positioned to allow the in-situ welding of the different sections of the bridge
Detail 3 (C80) Vertical Stiffener $x = 8,0m$	the combination of bending and shear stresses contribute to development of principal stresses in the web, which can cause a crack to start at the bottom edge of the vertical stiffener.
Detail 4 (C80/100) Vertical Stiffener $x = 0m$	the shear stresses are highest at the support and here a crack can initiate at the bottom of the web, either along the web (C100) or the welds (C80)

The FLS analysis of the above listed details is performed with bridgeFAT.

9.1.3 Results and remarks

The results of the verifications can be found in detail in Appendix A2. Their values and respective utilization ratios in ULS, SLS and FLS are summarized in Table 9.3 and Table 9.4.

Table 9.3 Design verification in ULS and SLS

	Design value	Resistance	Utilization ratio
ULS bending	12,1 MNm	12,7 MNm	0,95
ULS shear	1,53 MN	1,99 MN	0,771
SLS deflection	71,6 mm	80 mm	0,895

Table 9.4 Design verification in FLS

Detail	D _{L1}	D _{L2}	D _{L3}	D _{L4}	D _{L5}	D _{tot}
1 (C80)	0,13	0,06	0,14	0,06	0,09	0,49
2 (C71)	0,08	0,04	0,11	0,06	0,07	0,36
3 (C80)	0	0,02	0,07	0,02	0,05	0,16
4 (C80)	0	0	0	0	0	0

These results highlight that fatigue is not a limit to the design. Table 9.3 shows that the design is governed by bending and deflection.

9.2 New bridge design

As stated in Section 9.1.3 the cross-section resistance of the bridge is limited by ULS and SLS. ULS is affected by the quality of the steel employed, while deflection is mostly affected by geometrical parameters.

In this section, a new and improved bridge design is proposed and verified. Higher steel quality is adopted in order to improve the bending and shear resistance of the section, along with the appropriate geometrical adjustments in order to satisfy the requirements for deflection as well.

In addition, PWT will be performed on those details which will become critical, as subjected to higher stress ranges.

9.2.1 Geometry and loading

The cross-section dimensions of the main girders are reduced. The new cross-section dimensions are listed in Figure 9.4.

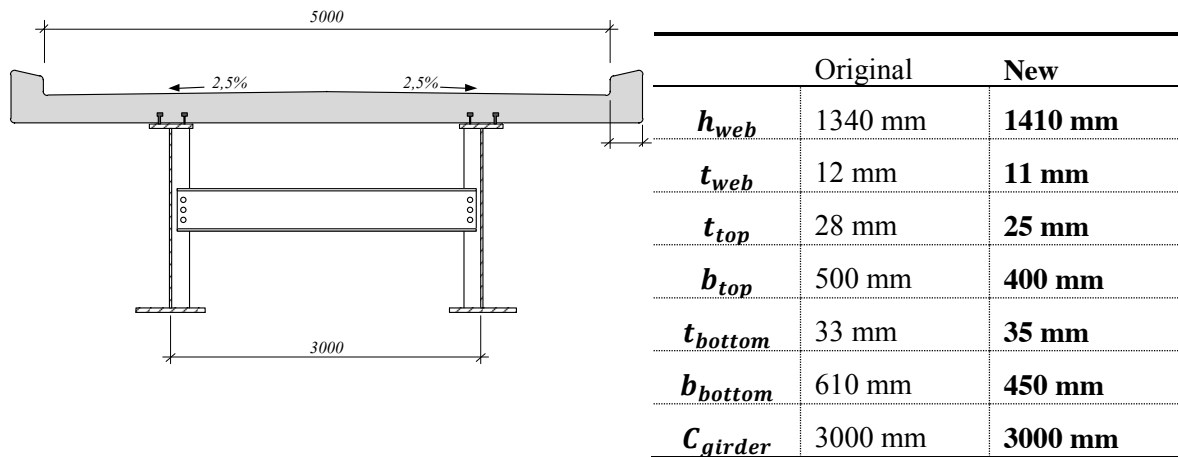


Figure 9.4 New bridge cross-section with dimensions

The steel quality is increased to S460, which allows the reduction of cross section described in the previous section.

The new steel has the same density as S355 but enhanced tensile characteristics which vary depending on the specific thickness of each plate, as listed: see Section 2.4.1.

The concrete deck's characteristics are kept constant.

The reduction of the cross-section results into a decrease of the self-weight of the girders. All the other loads considered in the analysis remain unaffected.

9.2.2 Cross section verification

The same cross-section verifications as for the original design are performed for the new design.

- ULS verification:

In this case, since the self-weight is slightly lower, a small decrease of the actions acting on the girders is expected, i.e. M_{ULS} and V_{ULS} will decrease.

The resistance of the cross section is expected to stay on a constant level. The reduction of the cross-section is, in fact, compensated by the higher tensile characteristic of the steel.

- SLS verification:

As the cross-section is reduced, an increase of deflection is expected, since the loading remains basically unaffected, except for the self-weight.

- Web breathing:

This verification is affected by the reduction of the web thickness. It should be verified that such a reduction doesn't result in the development of the phenomenon.

- Buckling during casting:

This phenomenon is affected by the size of the top flange. Its dimensions have been reduced but still in accordance with the restrictions that EN 1993-1-1 Section 6.3.1 proposes for such kind of buckling.

- FLS verification:

The same analysis is performed as for the original design, taking into account the reduction of the cross-sectional properties. The stresses applied on each specific detail are higher compared to the former design, which results in an increase of damage.

In this specific case no PWT is needed as further explained in Section 9.2.3.

9.2.3 Results and remarks

The verification results for ULS, SLS and FLS are summarized in Table 9.5 and Table 9.6.

Table 9.5 Design verification in ULS and SLS

	Design value	Resistance	Utilization ratio
ULS bending	12,0 MNm	13,3 MNm	0,90
ULS shear	1,52 MN	2,05 MN	0,74
SLS deflection	76,3 mm	80 mm	0,95

Table 9.6 Design verification in FLS

Detail	D _{L1}	D _{L2}	D _{L3}	D _{L4}	D _{L5}	D _{tot}
1 (C80)	0,27	0,09	0,22	0,11	0,15	0,85
2 (C71)	0,16	0,06	0,18	0,08	0,10	0,59
3 (C80)	0,08	0,04	0,11	0,06	0,06	0,35
4 (C80)	0,0	0,0	0,0	0,0	0,0	0,0

The new bridge design keeps a more or less constant utilization ratio for bending, which is still limiting the design.

The reduction of the cross section affects mostly SLS and FLS, since they do not gain any benefit from the higher steel quality. For this reason the utilization ratio for deflection is increased, as well as the ratios for fatigue.

FLS is affected but never reaches critical values, therefore no PWT is needed in this specific case. However, since fatigue is influenced by the bridge length, PWT might become necessary for shorter spans (see Section 9.4).

9.3 Comparison between original and new bridge design

As stated at the beginning of the chapter, the main aim of this study is to quantify the decrease of the material costs. For this specific case study, the results are shown in Table 9.7.

Table 9.7 Cost analysis of original and new design

	Steel	A(m ²)	V(m ³)	Material cost(SEK)	PWT cost(SEK)	Total cost(SEK)
Original design	S355	0,1	3,20	172.500	0	172.500
New design	S460	0,083	2,65	160.500	0	160.500

The table shows a significant reduction of the girder's cross-section area. The material saving and cost saving are directly proportional in this case as well, but unlike the railway bridge previously studied, more expensive steel is used for the new design. This results in a decreased cost saving, compared to the volume reduction.

As far as the cost analysis is concerned, in this case study no PWT is needed, therefore no additional costs appear.

All these variables allow calculating the total cost reduction that can be achieved. For the bridge over E4 in Skulnäs a total cost saving of 12.000 SEK can be achieved, which corresponds to 7%.

In this case, PWT would have no benefit. The design is in fact governed by deflection.

In this specific case study, the new design is governed by deflection. This implies that neither PWT nor higher strength steel would have any benefit.

9.4 Parametric study

The case study performed in the previous paragraph showed that fatigue was not a boundary to the design, so no benefit would have come from PWT. It becomes then relevant to know if this is the case of any span length, or if the situation changes for bridges of different sizes. In general in fact, bridges with shorter spans are affected by fatigue to a larger extent, so one might expect that PWT could play an important role there.

With this purpose, a parametric study is performed in order to find out how the span length of a simply supported highway bridge affects the total cost saving.

In this specific case, span length varying between 16m and 44m are studied. The shape of the cross-section is kept constant while the dimensions are adjusted to withstand the variable stresses.

For each span length both an original design and a new design are assessed, and only the latter includes PWT (if needed). This way it is possible to quantify the material saving for each case. The specific data and verifications for each bridge can be found in Appendix B2.

Figure 9.5 graphically shows the variation of material and cost save within the span range.

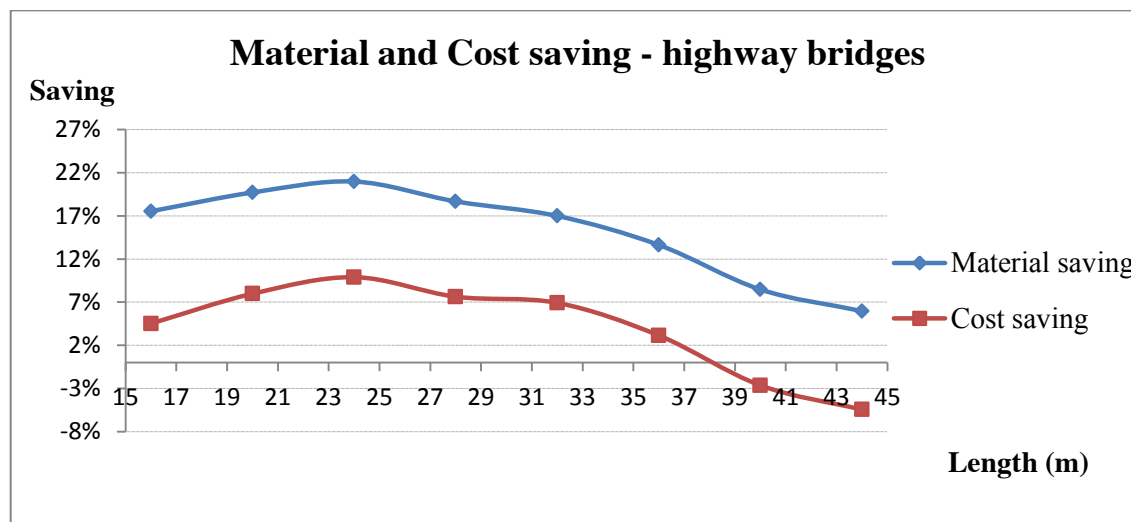


Figure 9.5 Material and cost saving achieved with the new design

It becomes obvious that the impact of the cost difference between S355 and S460 plays a dominant role. The section of the girders can be reduced by an amount close to those previously found for railway bridges. However, the material cost impact reduced the benefits of cost saving, shifting the cost curve downwards. In terms of cost saving, a peak is shown for spans between 22m and 26m.

A meaningful result is that for longer spans, in particular over 38m, the new design has no benefit. The material saving benefits are overcome by the higher price of S460.

In order to explain these results further, it is worth looking closer to the behaviour of the different bridges with regard to bending, deflection and fatigue. Figure 9.6 and Figure 9.7 show the variation of the respective utilization ratios with increasing span length.

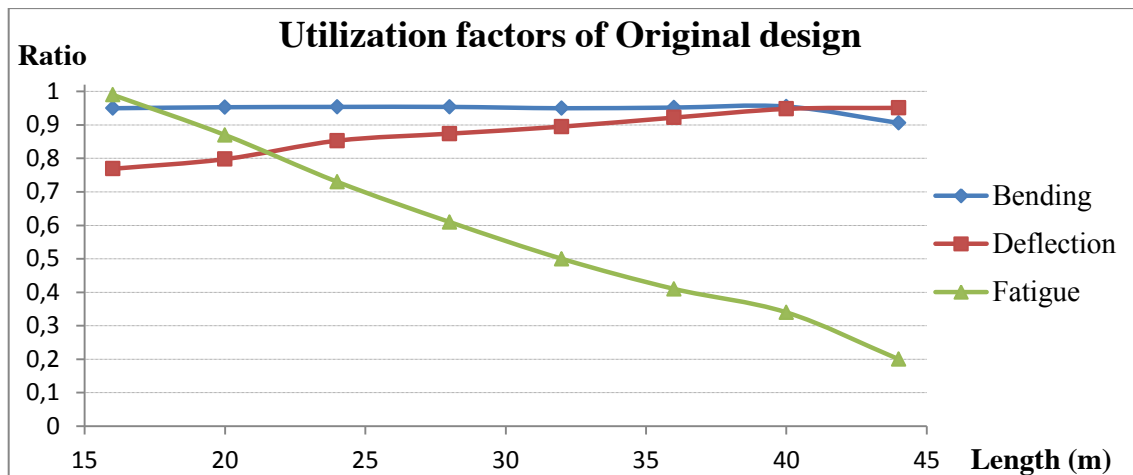


Figure 9.6 Utilization factors of Original design

The main conclusions about the original design that can be drawn from Figure 9.6 follow:

1. Only short spans are governed by fatigue. In the range studied, fatigue is never a problem.
2. Bending represents the design limit for most of the spans. The situation seems to change for spans longer than 40m. From that point on, deflection becomes critical.
3. The SLS utilization increases along with the increase of span length.

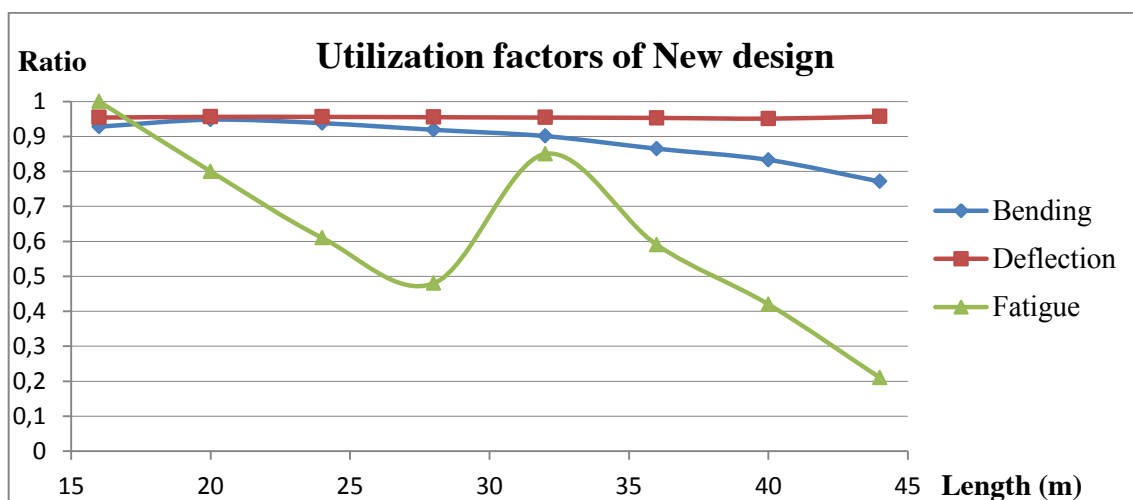


Figure 9.7 Utilization factors of New design with PWT

The main conclusions about the new design that can be drawn from Figure 9.7 follow:

1. Fatigue becomes critical since the section is reduced compared to the original design. This limitation can though be overcome by applying PWT.
2. For spans longer than 32m, no PWT is needed for the new design either.

3. The curve describing fatigue can be divided into two parts: in the first slope PWT is applied, while in the second no PWT is needed.
4. Deflection is the design limit for every span. This occurs since it is the only factor which is not affected by either PWT or steel quality.
5. The bending resistance cannot be utilized to its best since deflection governs the design for most of the spans.

9.5 Summary

In this chapter it has been shown that the use of HSS, combined with PWT where necessary, can result in benefits in terms of cost saving.

A case study has been performed on an existing bridge. The original design has shown to be limited by bending. In order to overcome this limitation a new design has been proposed, where the girders have been redesigned with steel quality S460. This new design showed that the reduction of the girders' cross section was large enough to overcome the higher price of the steel, leading to a saving in terms of total cost.

These positive results encouraged a parametric study to be performed. The main outcome highlighted that composite highway bridges with spans between 22m and 26m have the greatest benefits from the combination of higher strength steel and PWT (where needed). In the best case a cost saving of 10% was achieved.

10 Continuous highway bridges

The results obtained in Chapters 8 and 9 have shown that simply supported one-span bridges have great benefits from the use of PWT and HSS.

In this chapter the behaviour of continuous bridges is assessed, with the aim of investigating whether the same kind of benefits can be achieved. Two different case studies are assessed in detail. Both of them are presented below.

10.1 Original bridge designs

The hereby assessed bridges are both highway composite steel-concrete bridges, continuous over three spans. The geometry is similar but the size of span and cross section differs.

In the fatigue design of the girders, the design life of the bridge is given to be 80 years and the traffic details used are the ones defined in Section 7.3.

10.1.1 Geometry and loading

- Bridge A:

This bridge spans over Nissan over the lengths of 13,8m-11,3m-13,3m. It has a concrete in-situ cast deck supported by two steel girders, continuous over the piers.



Figure 10.1 Longitudinal view of the bridge over Nissan, Sweden

The concrete deck is 7,0m wide, excluding the concrete edge beams. The average depth of the concrete deck is assumed to be 270mm. Composite action between the concrete deck and the steel girders is achieved by means of two rows of shear studs welded to the top flange of each girder.

The dimensions of the steel cross-section are kept constant all along the length of the bridge as given in Figure 10.2.

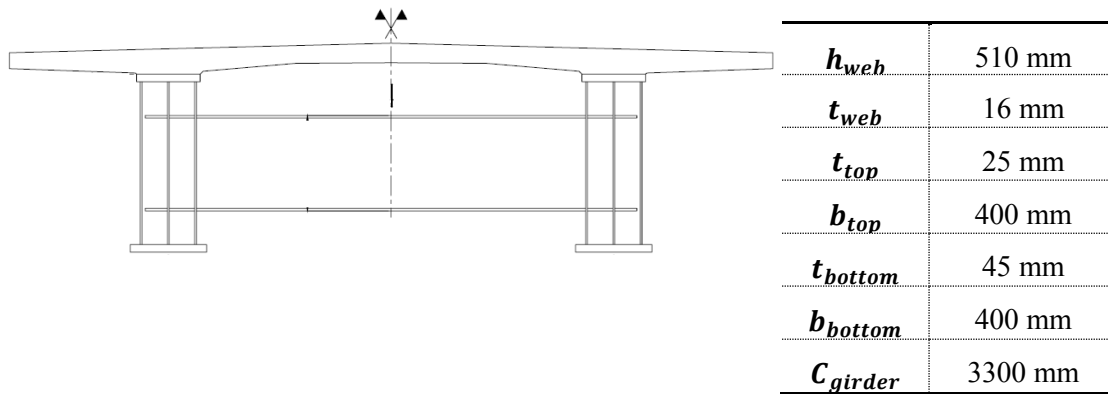


Figure 10.2 Bridge cross-section with dimensions

- Bridge B:

This bridge has the same layout and cross-section as bridge A, but the dimensions are quite different. It spans over the lengths of 60m-80m-60m. It has a concrete in-situ cast deck supported by two steel girders, continuous over the piers.

The concrete deck is 11,0m wide, excluding the concrete edge beams. The average depth of the concrete deck is assumed to be 307mm. Composite action between the concrete deck and the steel girders is achieved by means of two rows of shear studs welded to the top flange of each girder.

The dimensions of the steel cross-section vary along the length of the bridge to obtain the best usage of the material. In particular the design verification is performed considering two different sections, one for the span and one for the support. The data of each section is given in Table 10.1.

Table 10.1 Bridge cross-section dimensions

Span section		Support section	
h_{web}	2720 mm	h_{web}	2560 mm
t_{web}	18 mm	t_{web}	26 mm
t_{top}	40 mm	t_{top}	120 mm
b_{top}	1000 mm	b_{top}	1000 mm
t_{bottom}	40 mm	t_{bottom}	120 mm
b_{bottom}	1200 mm	b_{bottom}	1200 mm
C_{girder}	7000 mm	C_{girder}	7000 mm

The choice of span length was made in order to allow a holistic view over bridges of different sizes.

Both the original bridges are made of steel quality S355, which has a density of $\rho_{S355} = 7700 \frac{kg}{m^3}$ and tensile characteristics which vary depending on the specific thickness of each plate, as listed in Section 2.4.1.

The concrete deck is made of normal concrete C35/45 which has the following characteristics:

$$\begin{aligned}f_{ck} &= 35 \text{ MPa} \\f_{ctm} &= 3,2 \text{ MPa} \\E_{cm} &= 34,000 \text{ MPa}\end{aligned}$$

In this simplified analysis, the loads taken into account are the self-weight of the structural elements (including surfacing and parapets), wind load and traffic loads.

Load combinations are given in Eurocode EN 1990:2002: Basis of structural design.

- Self-weight

The different self-weights of the many components of the bridge are added to a cumulative self-weight, to be added to the self-weight of the structural elements.

- Wind

Analysis of the load-carrying capacity of the bridge in the ULS should also consider the effect of wind loads.

1. Wind acting on the bridge, $q_{w,bridge} = 6 \frac{kN}{m^2}$
2. Wind acting on the cars, $q_{w,car} = 1,4 \frac{kN}{m^2}$

- Train

The traffic loads are given in load model LM1 and LM2 according to Eurocode EN 1991-2, see Section 7.1.

For each bridge the traffic distribution is studied in detail in order to calculate the load distribution factor. This way it is possible to consider only one of the girders, given the symmetry of the section. The detailed calculations are found in Appendix A3.

10.1.2 Cross section verification

In this case study, only the dimensioning of the main girders is relevant. However, the contribution of the deck is taken into account. This is done through non-linear analysis of the sections, considering the sections as follows:

- *Support section*: the concrete is considered to be cracked, so only the contribution of the two layers of reinforcement is considered.
- *Span section*: the concrete is uncracked, so the whole concrete deck is considered through an equivalent section.

According to Eurocode EN 1090-2, the main girders should be verified in ULS, SLS and FLS. In this section the different checks are introduced, while the detailed assessment of the different bridges is found in Appendix A3.

- ULS verification:

The ULS verification includes bending and shear check. Both bridges are checked at the span and support locations, since the loads and the sectional stiffness change. In both cases the cross-section reduction due to instability phenomena is taken into account, as specified in EN 1993-1-1 Section 6.3.2.

- SLS verification:

The deflection verification includes the effects of both self-weight and traffic loads. This study is again performed through non-linear analysis in order to consider the different rotational capacity of the different supports.

All spans of each bridge are checked to assure that the deflection is kept below the limit along the whole length.

- Web breathing:

According to EN 1993-2 Section 7.4 we assure that such phenomenon is not an issue.

- Buckling during casting:

Since the concrete deck will be cast on site, there is a risk of buckling of the main girders, when they are not restrained by the deck itself. To ensure safe conditions the girders alone need to be capable to withstand the weight of the fresh concrete. This can be verified in accordance with the restrictions that EN 1993-1-1 Section 6.3.1 proposes for such kind of buckling.

- FLS verification:

The damage accumulation method is used in order to verify the fatigue resistance of the most critical welded detail along the span. At this stage, only one detail is considered.

<p>Detail 1 (C80) Vertical Stiffener</p> $x = \frac{L}{2} m$	<p>The global bending of the girder produces normal stresses in the bottom flange, which can cause a crack to start along the bottom weld of the vertical stiffener. These stresses are highest in the middle of the span. Since the influence line for the middle span creates the highest contribution, this detail is considered to be there, to assess the worst case scenario</p>
--	--

The FLS analysis is performed with bridgeFAT.

The following traffic loads were selected, in relation to the size of each bridge:

- Bridge A: “medium traffic load model” with $N_{\text{obs}}=500.000$ (see Section 7.3)
- Bridge B: “medium traffic load model” with $N_{\text{obs}}=500.000$ (see Section 7.3)

10.1.3 Results and remarks

The verification results for ULS, SLS and FLS are summarized in Table 10.2 and Table 10.3, for bridge A, and in Table 10.4 and Table 10.5, for bridge B. All the values are in terms of utilization ratios.

- Bridge A:

Table 10.2 Design verification in ULS and SLS

	Span	Support
ULS bending	0,76	0,87
ULS shear	0,72	0,91
SLS deflection	0,51	-

Table 10.3 Design verification in FLS

Detail	D_{L1}	D_{L2}	D_{L3}	D_{L4}	D_{L5}	D_{tot}
1 (C80)	0	0,10	0,08	0	0	0,18

- Bridge B:

Table 10.4 Design verification in ULS and SLS

	Span	Support
ULS bending	0,85	0,81
ULS shear	0,93	0,92
SLS deflection	0,75	-

Table 10.5 Design verification in FLS

Detail	D_{L1}	D_{L2}	D_{L3}	D_{L4}	D_{L5}	D_{tot}
1 (C80)	0	0	0,83	0,12	0,08	1,03

The results obtained from the analysis of the two bridges highlight quite different behaviours in terms of fatigue. The first bridge appears to be unaffected by fatigue, which instead represents a limit to the design for the second bridge.

This can be explained considering that the number of observations per year is higher for bridge B, along with the stress ranges.

10.2 New bridge designs

Both cases studied above showed to be limited in the design by the values for shear and bending.

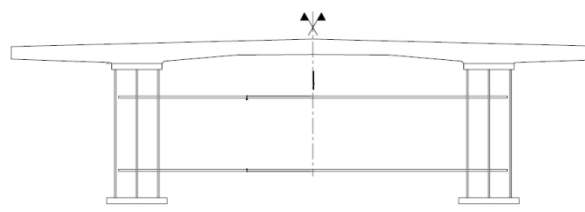
In this section, new and improved bridge designs are proposed and verified. A higher steel quality is adopted in order to improve the bending and shear resistance of the section, in order to achieve better utilization ratios in SLS and FLS.

In addition, PWT will be performed in the details which will become critical, as subjected to higher stress ranges.

10.2.1 Geometry and loading

The cross-section dimensions of the main girders are reduced. The new cross-section dimensions are listed in Figure 10.3, for bridge A, and in Table 10.6, for bridge B.

- Bridge A:



	Original	New
h_{web}	510 mm	465 mm
t_{web}	16 mm	11 mm
t_{top}	25 mm	20 mm
b_{top}	400 mm	400 mm
t_{bottom}	45 mm	35 mm
b_{bottom}	400 mm	400 mm
C_{girder}	3300 mm	3300 mm

Figure 10.3 New bridge cross-section with dimensions (kept constant for support and span)

- Bridge B:

Table 10.6 New bridge cross-section dimensions

Span section			Support section		
	Original	New		Original	New
h_{web}	2720 mm	2730 mm	h_{web}	2560 mm	2620 mm
t_{web}	18 mm	17 mm	t_{web}	26 mm	25 mm
t_{top}	40 mm	35 mm	t_{top}	120 mm	90 mm
b_{top}	1000 mm	1000 mm	b_{top}	1000 mm	1000 mm
t_{bottom}	40 mm	35 mm	t_{bottom}	120 mm	90 mm
b_{bottom}	1200 mm	1100 mm	b_{bottom}	1200 mm	1100 mm
C_{girder}	7000 mm	7000 mm	C_{girder}	7000 mm	7000 mm

The steel quality is increased to S460. This allows the reduction of cross section described in the previous paragraph.

The new steel has the same density but enhanced tensile characteristics which vary depending on the specific thickness of each plate, as listed in Section 2.4.1.

The concrete decks' characteristics are kept constant.

The reduction of the cross-section results into a decrease of the self-weight of the girders. All the other loads considered in the analysis remain unaffected.

10.2.2 Cross section verification

- ULS verification:

In this case, since the self-weight is slightly lowered, a small decrease of the actions acting on the girders is expected, i.e. M_{ULS} and V_{ULS} will decrease.

The resistance of the cross section is expected to stay on a constant level. The reduction of the cross-section is, in fact, compensated by the higher tensile characteristic of the steel.

The detailed assessment of the different bridges is found in Appendix A3.

- SLS verification:

As the cross-section is reduced, an increase of deflection is expected, since the loading remains basically unaffected, except for the self-weight.

- Web breathing:

This verification is affected by the reduction of the web thickness. It should be verified that such a reduction does not result in the development of the phenomenon.

- Buckling during casting:

This phenomenon is affected by the size of the top flange. Its dimensions have been reduced but still in accordance with the restrictions that EN 1993-1-1 Section 6.3.1 proposes for such kind of buckling.

- FLS verification:

The same analysis is performed as for the original design, taking into account the reduction of the cross-sectional properties. The stresses applied on each specific detail are higher compared to the former design, which results in an increase of damage.

10.2.3 Results and remarks

The verification results for ULS, SLS and FLS are summarized in Table 10.7 and Table 10.8, for bridge A, and in Table 10.9 and Table 10.10 for bridge B. All the values are in terms of utilization ratios.

- Bridge A:

Table 10.7 Design verification in ULS and SLS

	Span	Support
ULS bending	0,86	0,88
ULS shear	0,74	0,93
SLS deflection	0,75	-

Table 10.8 Design verification in FLS

Detail	D _{L1}	D _{L2}	D _{L3}	D _{L4}	D _{L5}	D _{tot}
1 (C80)	0,23	0,57	0,82	0,03	0,01	1,67
1 (C112)	0	0,11	0,09	0	0	0,20

- Bridge B:

Table 10.9 Design verification in ULS and SLS

	Span	Support
ULS bending	0,82	0,82
ULS shear	0,88	0,83
SLS deflection	0,87	-

Table 10.10 Design verification in FLS

Detail	D _{L1}	D _{L2}	D _{L3}	D _{L4}	D _{L5}	D _{tot}
1 (C80)	0	0,09	2,0	0,3	0,18	2,58
1 (C112)	0	0	0,37	0	0,03	0,40

In both cases the new bridge designs keep a more or less constant utilization ratio for bending and shear, which are still governing design.

The reduction of the cross section mostly affects SLS and FLS, since they do not gain any benefit from the higher steel quality. For this reason the utilization ratio for deflection is increased, as well as the ratios for fatigue.

It is to be remarked that both bridges need PWT since the values for fatigue damage are beyond the critical limits. The values shown in Table 10.8 are listed for both classes C80 and C112, e.g. before and after PWT. It is clearly shown that PWT benefits the FLS design lowering all the values.

10.3 Comparison between original and new bridge design

As stated at the beginning of the chapter, the main aim of this study is to quantify the decrease of the material costs. For these specific case studies, the results for both bridges are shown in Table 10.11 and Table 10.12.

- Bridge A:

Table 10.11 Cost analysis of original and new design

	Steel	A(m ²)	V(m ³)	Material cost(SEK)	PWT cost(SEK)	Total cost(SEK)
Original design	S355	0,072	2,76	149.000	0	149.000
New design	S460	0,054	2,07	125.300	1950	127.250

- Bridge B:

Table 10.12 Cost analysis of original and new design

	Steel	A(m ²)	V(m ³)	Material cost(SEK)	PWT cost(SEK)	Total cost(SEK)
Original design	S355	0,661	132,2	7.125.600	0	7.125.600
New design	S460	0,509	101,8	6.153.300	3700	6.157.000

As far as the cost analysis is concerned, in this case study PWT is needed for both bridge A and B.

The total cost reduction can thus be calculated:

- Bridge A: a total cost saving of 21.750 SEK can be achieved, which corresponds to 14%.
- Bridge B: a total cost saving of 968.600 SEK can be achieved, which corresponds to 13%.

10.4 Summary

In this chapter it has been shown that the use of HSS, combined with PWT where necessary, can result in benefits in terms of cost saving.

Two case studies have been performed on two different continuous three-span highway bridges. In both cases, the original designs have shown to be limited by bending and shear. In order to overcome these limitations, new designs have been proposed, where the girders have been redesigned with steel quality S460. These new designs showed that the reduction of the girders' cross section was large enough to overcome the higher price of the steel, leading to a saving in terms of total cost.

However, it is to be remarked that unlike bridge B, bridge A's new design with S460 is still not fully utilized in deflection, as shown in Table 10.7. In other words, the ULS ratios for both bending and shear can be further decreased if even higher steel quality is used. A brief summary of a further improved design with S690 is proposed and the results are, once again, assessed in terms of cost; see Table 10.13.

Table 10.13 Bridge A - Cost analysis of original and new designs with S460 and S690

	Steel	A(m ²)	V(m ³)	Material cost(SEK)	PWT cost(SEK)	Total cost(SEK)
Original design	S355	0,072	2,76	149.000	0	149.000
New design	S460	0,054	2,07	125.300	1950	127.250
New design	S690	0,042	1,61	131.600	1950	133.600

The use of higher strength steel results into a decrease of the utilization ratios of bending and shear but deflection becomes a limitation when the section is decreased in size. PWT is to be performed in this design as well and in particular its effects are shown in Table 10.14. The table highlights the role of PWT.

Table 10.14 Design verification in FLS for alternative with S690

Detail	D_{L1}	D_{L2}	D_{L3}	D_{L4}	D_{L5}	D_{tot}
1 (C80)	0,81	1,4	2,66	0,23	0,06	5,2
1 (C112)	0,08	0,38	0,54	0	0	1,0

In general terms, Table 10.13 clearly shows that the latest design with steel quality S690 can be beneficial in terms of material cost compared to the original design. In particular a total cost saving of 15.400 SEK can be achieved, which corresponds to 10%.

When considering the mere benefits with regard to total cost of the steel girders exclusively, the solution with steel quality S460 still represents the best alternative. However, the design with S690 may ensure secondary effects and gains in terms of total weight, environmental aspects related to the steel amount, reduced workmanship, use of smaller equipment (e.g. cranes) and cost for painting through the life cycle. All these aspects can be evaluated by the means of Life Cycle Cost and Life Cycle Assessment.

11 Long term benefits of the combination of HSS and PWT

In the previous Chapter different design alternatives for different kinds of bridges have been assessed. These case studies have taken into consideration the material cost of the steel girders and the cost of post weld treatment exclusively. However, these aspects affect only to the initial cost of a structure. In order to have a better overview of the benefits that can be achieved in terms of total cost over the life span of a specific structure, more aspects need to be included in the evaluation, among which cost for repainting. This can be performed through a Life Cycle Cost (LCC) analysis.

Along with the benefits concerning the mere price of the structure, environmental aspects play a crucial role in the choice of a design. Different designs have different environmental impacts, which can be evaluated thanks to a Life Cycle Assessment (LCA).

In this Chapter, bridge A, previously dimensioned with the use of three different kinds of steel, is further studied into detail. The purpose is to investigate the possible benefits that the new alternatives of design using HSS in combination with PWT can provide in the long term.

11.1 Life Cycle Cost analysis on Bridge A

Steel bridges have the need of being repainted during the life span of the structure. The frequency of such depends on the exposure conditions of the bridge. Other aspects such as the need for smaller cranes or the reduced need of workmanship are disregarded at this stage.

The structure has a life span of 80 years and need to be therefore painted and repainted three times, assuming intervals of thirty years.

The total cost of painting depends on the total surface to be treated and the actual cost of paint and workmanship. The relative area can be easily obtained when the cross-section is defined and the bridge length is known. It is then obvious that a reduction in cross-section results in a decreased cost for painting. The cost of paint and workmanship are tabled and given from Trafikverket (Swedish Transport Administration). The cost for repainting is given as $1700 \text{ SEK}/\text{m}^2$, which includes the price of old paint removal, workmanship and equipment needed to perform the job. Since these are not necessary during the first session, a price of $700 \text{ SEK}/\text{m}^2$ is assumed.

Further, the price of painting is affected through time since future costs will be affected by the discount rate. The discount rate takes inflation into account and is taken as 3,5% as recommended from Trafikverket.

Therefore the price of each specific painting session needs to be calculated individually (23). This can be performed through Equation 11.1.

$$C_{tot} = \sum_{n=0}^L \frac{C_n}{(1+r)^n} \quad \text{Equation 11.1}$$

Where:

C_{tot} = the life-cycle cost expressed as a present value

n = the year when the cost occurs

C_n = the initial cost

r = the discount rate

L = the service life-span

The total cost of the combined painting session can be calculated and the results are shown in Table 10.12.

Table 11.1 Partial and total repainting cost for Bridge A

	Original design	New design	New design
Steel quality	S355	S460	S690
Painting area (m^2)	178,8	170,3	164,2
Cost $t = 0$ years (SEK)	125.153	119.240	114.778
Cost $t = 30$ years (SEK)	108.289	103.172	99.311
Cost $t = 60$ years (SEK)	38.581	36.758	35.382
Total painting cost (SEK)	272.023	259.169	249.471

The conclusions are straight forward. The higher is the steel quality, the smaller is the area to be painted. Therefore the highest benefits in terms of painting cost are achieved with the S690 design.

In order to conclude the LCC analysis, these results are to be merged with the savings in terms of material cost assessed in Section 10.4. The results are shown in Table 11.2 and Figure 11.1.

Table 11.2 LCC analysis of Bridge A

	Original design	New design	New design
Steel quality	S355	S460	S690
Material cost (SEK)	149.000	125.300	133.600
Painting cost (SEK)	272.023	259.169	249.471
Total cost (SEK)	421.023	384.469	383.071

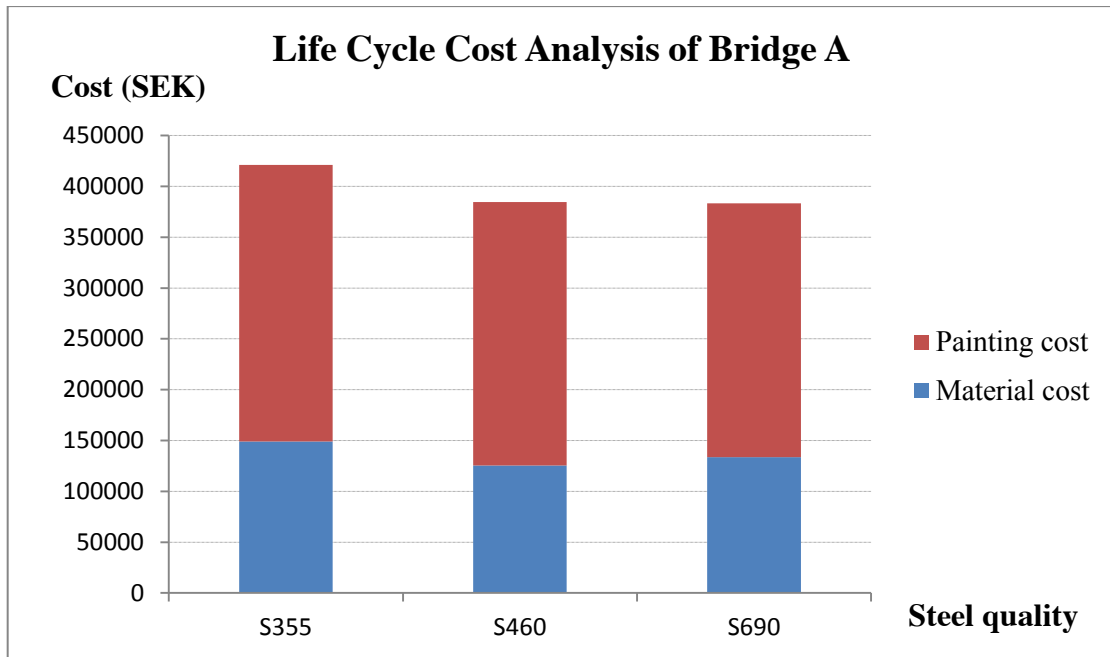


Figure 11.1 LCC analysis of Bridge A

The conclusions that can be made change the ones previously made when material cost was the only parameter. In fact, the design with steel grade S690 becomes now the most profitable solution in terms of life span costs. In particular a total cost saving of 37.600 SEK can be achieved, which corresponds to 9%.

As expected, the secondary effects of the use of HSS become now noticeable.

11.2 Life Cycle Assessment on Bridge A

Nowadays in Sweden, a big share of the state's energy consumption is attributed to the steel industry. The whole lifecycle of steel products, from production to final delivery, requires great amounts of energy with considerable emissions of CO₂ equivalents. Figure 11.2 shows the impact of steel industries, among all others, in Sweden.

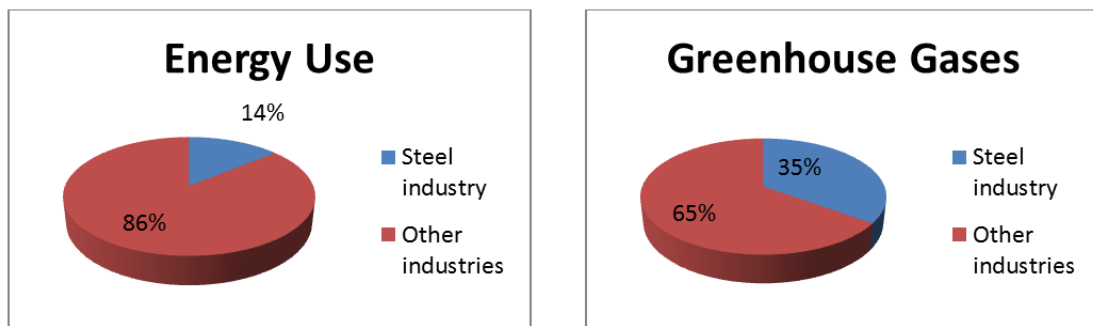


Figure 11.2 Energy use and greenhouse gases produced by the steel industry, compared to the rest of the industries in Sweden

The Life Cycle Assessment of a structure includes numerous effects and the environmental impact of a structure is determined on the basis of all these. Such a study can be very hard to be performed if some of the necessary information is missing. The required input is retrieved from Trafikverket's national database for bridge and tunnel management (BaTMan) and the analysis is performed with openLCA⁵.

In this thesis study, a simplified approach is described where only the steel girders are assessed. This includes all the side effects that develop around the production and the delivery of the steel girders, expressed in terms of equivalent CO₂ emissions.

The program calculates the effects that the steel girders produce on the environment in terms of an equivalent CO₂ amount. In particular a total of 1,61 kilos of CO₂ are produced for every kilo of steel.

Therefore, the total impact of each design proposed for Bridge A can be calculated when the amount of the steel used is known. Every design is assessed in detail and the results are summarized in Table 11.3.

Table 11.3 LCA of Bridge A

	Original design	New design	New design
Steel quality	S355	S460	S690
Weight (kg)	21.252	15.939	12.397
CO₂ emissions (kg)	34.215	25.661	19.959

The LCA analysis performed highlights all the benefits that the use of HSS has with regard to environmental impact of a structure. In this specific case study, a design using steel quality S690 allows the equivalent CO₂ emissions to be reduced up to 41%.

This can have great benefits towards a reduction of the overall CO₂ equivalents produced in Sweden by the steel industry.

11.3 LCC and LCA for Bridge B

The same sort of analysis has been performed for bridge B. The following tables summarize the results.

⁵ openLCA framework 1.3.0_rc1

Table 11.4 LCC analysis of Bridge B

	Original design	New design
Steel quality	S355	S460
Material cost (SEK)	7.125.600	6.157.000
Painting cost (SEK)	5.450.484	5.329.984
Total cost (SEK)	12.576.084	11.486.984

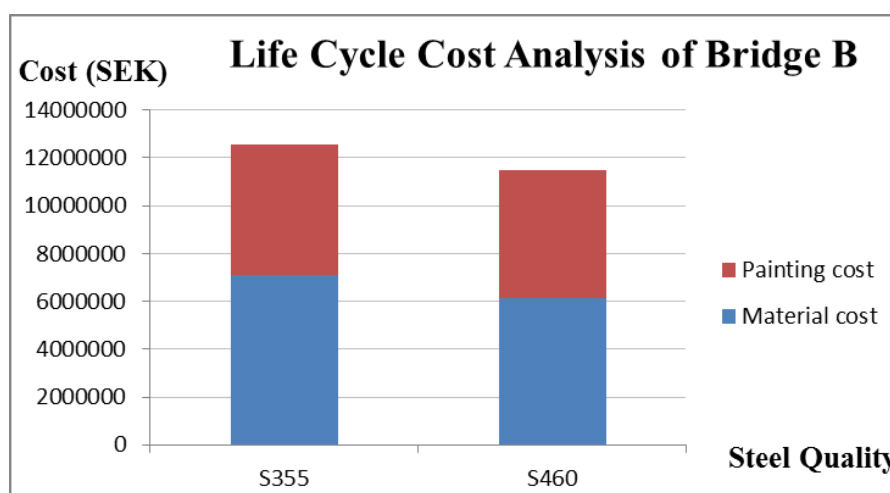


Figure 11.3 LCC analysis of Bridge B

The overall save in terms of total cost (painting and material) accounts to 1.089.000SEK, which corresponds to 8,6%.

Table 11.4 LCA analysis of Bridge B

	Original design	New design
Steel quality	S355	S460
Weight (kg)	1.017.940	783.860
CO₂ emissions (kg)	1.638.883	1.262.014

In this case as well, the results are straight forward. The less material used the less the emissions produced. Therefore the environmental impact could be cut by 23%.

12 Bibliography

1. *High Performance Steel Designers*. **US Federal Highway Safety Administration**. 2002, p. 1.
2. *High strength and high performance steels and their use in bridge structures*. **C.Miki, K.Homma, T.Tominaga**. 2002, Journal of Constructional Steel Research, pp. 3-20.
3. *High Performance Steel: Research Front—Historical Account of Research Activities*. **A.Azizinamini, K.Barth, R.Dexter, C.Rubeiz**. 3, s.l. : J. Bridge Eng, 2004, Vol. 9.
4. **Dan Dubina**. *Performance and benefits of using high strength steels*. s.l. : The Polithnica University of Timisoara, 2008.
5. **Chris Dolling**. *Material Selection*. 2006.
6. *High strength steel for steel constructions*. **R.Willms**. 2009.
7. *High-Strength Low-Alloy Steels*. **International, ASM**. 2001.
8. *High Performance Steel Designers' Guide*. **Federal Highway Administration**. 2, 2002.
9. *Steel bridges in Japan - current circumstances and future tasks*. **Dr Yozo Fujino**.
10. *Structural steel Metallurgical characteristics and properties*. **Metal Pass**. s.l. : e-biz.
11. **Eurocode EN 1993-3**. Design of steel structures. 2006.
12. **NDT resource center**. Fracture Toughness. *ndt-ed.org*. [Online]
13. **J.Billingham, J.V.Sharp, J.Spurrier, P.J.Kilgallon**. *Review of the performance of high strength steels used offshore*. s.l. : HSE books, 2003.
14. **H.Wendland**. *Hydrogen induced cold cracking*. s.l. : UTP Bad Krozingen.
15. **H.P.Gunther, C.Rasche, U.Kuhlmann**. *Strength and ductility of welded high strength steel connections in bridges*.
16. **A.Ilic, L.Ivanovic, D.Josifovic, V.Lazic**. *Advantages of high strength steels applications in mechanical constructions*. 2012.
17. **F.Schröter**. *High-strength heavy plates tor modern European medium and large span bridges*.
18. *Trends of using high strength steel for heavy steel structures*. **F.Schröter**.
19. **T.Dahlberg, A.Ekberg**. *Failure Fracture Fatigue: An Introduction*. s.l. : Studentlitteratur AB , 2002.
20. **T.R.Gurney**. *Fatigue of welded structures*. s.l. : Cambridge U.P., 1968.
21. **P.Paris, F.Erdogan** . *A Critical Analysis of Crack Propagation Laws*. s.l. : J. Fluids Eng., 1963.
22. **M.Aygul**. *Fatigue Analysis of Welded Structures Using the Finite Element Method*. s.l. : Chalmers University of Technology, 2012.

23. **M.Safi.** *Applications for Bridges and Integration with BMS.* s.l. : Royal Institute of Technology (KTH).
24. **O.Josat.** *Sustainable bridge constructions—elegant arches—filigree structures—cost effective design.* s.l. : V & M Deutschland Gmb.
25. **R. Satish Kumar, A.R. Santha Kumar.** *Design of steel structures.* s.l. : indian insitute of Technology Madras.
26. **M.M.Pedersen, O.Ø.Mouritsen et al.** *Comparison of Post Weld Treatment of High Strength Steel Welded Joints in Medium Cycle Fatigue.* s.l. : International Institute of Welding, 2009.
27. **Alliance, National Steel Bridge.** *Stringer bridges, making the tight choices. Steel bridge design handbook.*
28. *Composite highway bridge design: worked examples.* s.l. : The Steel Construction Institute, 2011.
29. *Simplified rules for use in student projects. Bridge Design to the Eurocodes.* s.l. : The steel construction institute, 2007.
30. *Weld detail fatigue life improvement techniques.* **K.J.Kirkhope, R.Bell, L.Caron, R.I.Basu, K.T.Ma.** s.l. : Elsevier, 1999.
31. *Fatigue of structures and materials.* **J.Schijve.** s.l. : Sprinder, 2009.
32. **P.J.Haagensen.** *Dominating factors for crack propagation - welded joints.* Trondheim : Norges teknisk-naturvitenskapelige universitet, 2011.
33. **J.Taylor.** *Successful welding of steel structures. An Engineer's Guide to Fabricating Steel Structures.* Vol. 2.
34. **M.Leitner, M.Stoschka.** *Influence of steel grade on the fatigue strength enhancement by high frequency peening technology on longitudinal fillet weld gusset.* s.l. : Journal of Engineering and Technology.
35. **M.Al-Emrani, R.Kliger.** *Fatigue prone details in steel bridges.* Göteborg, Sweden : Chalmers University of Technology, 2009.
36. **M.Al-Emrani, B.Åkesson.** *Steel structures.* Göteborg, Sweden : Chalmers University of Technology, 2012.
37. **G.B.Marquis, E.Mikkola, H.C.Yildirim, Z.Barsoum.** *Fatigue Strength Improvement of Steel Structures by HFMI: Proposed Fatigue Assessment Guidelines.* s.l. : International institute of welding.
38. *Eurocode for high strength steel and applications in construction.* **B.Johansson, P.Collin.**
39. *Brudges in high strength steel.* **B.Johansson, P.Collin.**

A.1 Railway Bridge over Östra Klarälven

A.1.1 Geometry

The detailed geometry and length is given in Chapter 7.

A.1.1.1 Bridge Geometry

$L := 23.8\text{m}$	Total span of the bridge
$C := 1510\text{mm}$	Distance between the girders
$h_{\text{rail}} := 220\text{mm}$	Assumed height of a rail
$c_{\text{rail}} := 1510\text{mm}$	Assumed distance between rails
$h_{\text{web}} := 1910\text{mm}$	Height of the web
$t_{\text{web}} := 20\text{mm}$	Thickness of the web
$b_{\text{top}} := 1200\text{mm}$	Half the width of the top plate
$t_{\text{top}} := 40\text{mm}$	Thickness of the top plate
$b_{\text{bottom}} := 500\text{mm}$	Width of the bottom flange
$t_{\text{bottom}} := 50\text{mm}$	Thickness of the bottom flange
$h_{\text{tot}} := t_{\text{top}} + h_{\text{web}} + t_{\text{bottom}} = 2\text{ m}$	Total height of the section
$b_{\text{inner}} := \frac{C}{2} = 0.755\text{ m}$	Top flange width of half section
$b_{\text{outer}} := b_{\text{top}} - \frac{C}{2} = 0.445\text{ m}$	Top flange width of half section
$A_{\text{half}} := b_{\text{top}} \cdot t_{\text{top}} + h_{\text{web}} \cdot t_{\text{web}} + b_{\text{bottom}} \cdot t_{\text{bottom}} = 0.111 \cdot \text{m}^2$	
$a := 5\text{mm}$	Weld thickness

A.1.1.2 Material Data

$E := 210\text{GPa}$	E modulus of the steel
$f_{\text{ytop}} := \begin{cases} 355\text{MPa} & \text{if } t_{\text{top}} < 16\text{mm} \\ 345\text{MPa} & \text{if } t_{\text{top}} \geq 16\text{mm} \end{cases}$	Yield strength of top flange

$$f_{yweb} := \begin{cases} 355\text{MPa} & \text{if } t_{web} < 16\text{mm} \\ 345\text{MPa} & \text{if } t_{web} \geq 16\text{mm} \end{cases}$$

Yield strength of web

$$f_{ybottom} := \begin{cases} 355\text{MPa} & \text{if } t_{bottom} < 16\text{mm} \\ 345\text{MPa} & \text{if } t_{bottom} \geq 16\text{mm} \end{cases}$$

Yield strength of bottom flange

$$\rho_{steel} := 7700 \frac{\text{kg}}{\text{m}^3}$$

Density of steel

A.1.1.3 Factors and Parameters

$$\alpha := 1.2$$

Amplification factor

$$h_{train} := 4000\text{mm}$$

Assumed height of a train

$$\gamma_{Mf} := 1.35$$

Partial factor for fatigue resistance

$$\gamma_{Ff} := 1.0$$

Partial factor for fatigue load

$$\gamma_{M0} := 1.0$$

Partial Factor for cross section resistance

$$\gamma_{M1} := 1.0$$

Partial Factor for instability

$$\nu := 0.3$$

Poisson's ratio

A.1.2 Loads

A.1.2.1 Self-weight

$$m_{\text{girder}} := 2A_{\text{half}} \cdot \rho_{\text{steel}} = 1.712 \times 10^3 \cdot \frac{\text{kg}}{\text{m}}$$

Selfweight of the girder

$$m_{\text{crossbeams}} := 10.5 \frac{\text{kg}}{\text{m}}$$

Selfweight of the cross-bracing

$$m_{\text{vstiff}} := 18.0 \frac{\text{kg}}{\text{m}}$$

Selfweight of the stiffeners

$$m_{\text{rails}} := 120 \frac{\text{kg}}{\text{m}}$$

Selfweight of the rails

$$m_{\text{screws}} := 66 \frac{\text{kg}}{\text{m}}$$

Selfweight of the fasteners

We consider only half of the section since the symmetry allows us to study only half the bridge.

$$q_{\text{selfweight}} := \frac{(m_{\text{crossbeams}} + m_{\text{vstiff}} + m_{\text{rails}} + m_{\text{screws}} + m_{\text{girder}})g}{2} = 9.449 \cdot \frac{\text{kN}}{\text{m}}$$

Maximum moment and shear force due to the self-weight

$$M_{\text{selfweight}} := q_{\text{selfweight}} \cdot \frac{L^2}{8} = 669.009 \cdot \text{kN} \cdot \text{m}$$

Moment due to selfweight

$$V_{\text{selfweight}} := q_{\text{selfweight}} \cdot \frac{L}{2} = 112.438 \cdot \text{kN}$$

Shear due to selfweight

A.1.2.2 Train loads

We assume the load combination as given in load model LM71

$$P := 250 \text{ kN}$$

Point load

$$Q := 80 \frac{\text{kN}}{\text{m}}$$

Distributed load

$$\phi_1 := \frac{1.44}{\sqrt{\left(\frac{L}{m}\right) - 0.2}} + 0.82 = 1.128$$

Dynamic amplification factor

$$\text{Display} := \begin{cases} \text{"OK"} & \text{if } 1.0 \leq \phi_1 \leq 1.67 \\ \text{"NOT OK"} & \text{otherwise} \end{cases}$$

Display = "OK"

A.1.2.3 Windload

$$q_{\text{windbridge}} := 6 \frac{\text{kN}}{\text{m}^2}$$

Wind pressure acting on the bridge

$$q_{\text{windtrain}} := 1.4 \frac{\text{kN}}{\text{m}^2}$$

Wind pressure acting on the train

$$M_{\text{wtrain}} := q_{\text{windtrain}} \cdot h_{\text{train}} \cdot L \cdot \frac{h_{\text{train}}}{2} = 266.56 \cdot \text{kN} \cdot \text{m}$$

Moment acting on the train

$$M_{\text{wbridge}} := q_{\text{windbridge}} \cdot h_{\text{tot}} \cdot L \cdot \frac{h_{\text{tot}}}{2} = 285.6 \cdot \text{kN} \cdot \text{m}$$

Moment acting on the bridge

$$\Delta M_{\text{wind}} := M_{\text{wtrain}} - M_{\text{wbridge}} = -19.04 \cdot \text{kN} \cdot \text{m}$$

Moment resultant

$$F_{\text{wind}} := \frac{\Delta M_{\text{wind}}}{C \cdot L} = -0.53 \cdot \frac{\text{kN}}{\text{m}}$$

Force resultant

$$M_{\text{wind}} := \frac{F_{\text{wind}} \cdot L^2}{8} = -37.513 \cdot \text{kN} \cdot \text{m}$$

Moment due to wind

$$V_{\text{wind}} := \frac{F_{\text{wind}} \cdot L}{2} = -6.305 \cdot \text{kN}$$

Shear due to wind

A.1.2.4 Train load location

The loads are positioned as described in Section 7.1.2.

$$P_d := \frac{P}{2} = 125 \cdot \text{kN}$$

Point load on one girder

$$Q_d := \frac{Q}{2} = 40 \cdot \frac{\text{kN}}{\text{m}}$$

Distributed load on one girder

$$L_{q1} := \frac{L - 6.4\text{m}}{2} = 8.7\text{ m}$$

Length of Q_d

$$V_{\text{train}} := \frac{4P_d + Q \cdot 2L_{q1}}{2} = 946 \cdot \text{kN}$$

Shear due to traffic

$$M_{\text{train}} := -Q \cdot L_{q1} \cdot \left(\frac{L_{q1}}{2} + 0.8\text{m} + 1.6\text{m} + 0.8\text{m} \right) \dots = 5.603 \times 10^3 \cdot \text{kN} \cdot \text{m} \quad \text{Moment due to traffic}$$

$$+ -P_d \cdot (1.6\text{m} + 0.8\text{m}) - P_d \cdot (0.8\text{m}) + V_{\text{train}} \cdot \frac{L}{2}$$

A.1.3 Load combinations

The load combinations are according to Section 7.1.4.

$$\gamma_g := 1.05 \quad \psi := 0.75$$

$$\gamma_D := 1.45 \quad \gamma_O := 1.5$$

Partial coefficients

A.1.3.1 Ultimate Limit State

$$M_{\text{ULS}} := \gamma_g \cdot M_{\text{selfweight}} + \gamma_D \cdot \alpha \cdot \phi_1 \cdot M_{\text{train}} + \psi \cdot \gamma_O \cdot M_{\text{wind}} = 11.655 \cdot \text{MN} \cdot \text{m}$$

$$V_{\text{ULS}} := \gamma_g \cdot V_{\text{selfweight}} + \gamma_D \cdot \alpha \cdot \phi_1 \cdot V_{\text{train}} + \psi \cdot \gamma_O \cdot V_{\text{wind}} = 1.967 \cdot \text{MN}$$

A.1.3.2 Servicability Limit State

$$M_{\text{SLS}} := M_{\text{selfweight}} + \alpha \cdot \phi_1 \cdot M_{\text{train}} + M_{\text{wind}} = 8.214 \cdot \text{MN} \cdot \text{m}$$

$$T_{\text{SLS}} := V_{\text{selfweight}} + \alpha \cdot \phi_1 \cdot V_{\text{train}} + V_{\text{wind}} = 1.386 \cdot \text{MN}$$

A.1.4 Bending resistance in ULS

A.1.4.1 Cross-sectional constants

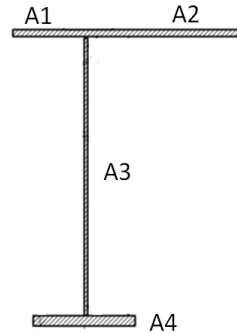
The cross sectional constants are calculated for one of the girders, given the symmetry.

$$A_1 := t_{\text{top}} \cdot \left(b_{\text{top}} - \frac{C}{2} \right) = 0.018 \text{ m}^2$$

$$A_2 := t_{\text{top}} \cdot \frac{C}{2} = 0.03 \text{ m}^2$$

$$A_3 := h_{\text{web}} \cdot t_{\text{web}} = 0.038 \text{ m}^2$$

$$A_4 := b_{\text{bottom}} \cdot t_{\text{bottom}} = 0.025 \text{ m}^2$$



Distance of each part from bottom to gravity center

$$z_1 := t_{\text{bottom}} + h_{\text{web}} + \frac{t_{\text{top}}}{2} = 1.98 \text{ m}$$

$$z_2 := t_{\text{bottom}} + h_{\text{web}} + \frac{t_{\text{top}}}{2} = 1.98 \text{ m}$$

$$z_3 := t_{\text{bottom}} + \frac{h_{\text{web}}}{2} = 1.005 \text{ m}$$

$$z_4 := \frac{t_{\text{bottom}}}{2} = 0.025 \text{ m}$$

Distance of gravity center from bottom of the bridge

$$y_{\text{gc}} := \frac{A_1 \cdot z_1 + A_2 \cdot z_2 + A_3 \cdot z_3 + A_4 \cdot z_4}{A_1 + A_2 + A_3 + A_4} = 1.206 \text{ m}$$

Distance from local and global gravity center

$$a_1 := y_{\text{gc}} - z_1 = -0.774 \text{ m}$$

$$a_2 := y_{\text{gc}} - z_2 = -0.774 \text{ m}$$

$$a_3 := y_{\text{gc}} - z_3 = 0.201 \text{ m}$$

$$a_4 := y_{\text{gc}} - z_4 = 1.181 \text{ m}$$

Moment of inertia

$$I_{\text{tot}} := \frac{b_{\text{outer}} \cdot t_{\text{top}}^3}{12} + A_1 \cdot a_1^2 + \frac{b_{\text{inner}} \cdot t_{\text{top}}^3}{12} + A_2 \cdot a_2^2 \dots = 0.077 \text{ m}^4$$

$$+ \frac{t_{\text{web}} \cdot h_{\text{web}}^3}{12} + A_3 \cdot a_3^2 + \frac{b_{\text{bottom}} \cdot t_{\text{bottom}}^3}{12} + A_4 \cdot a_4^2$$

A.1.4.2 Cross-sectional constants if top flange buckles

$$\text{weld} := \sqrt{2} \cdot a = 7.071 \text{ mm} \quad \text{Height of the weld}$$

$$\epsilon_{\text{top}} := \sqrt{\frac{235 \text{ MPa}}{f_{y\text{top}}}} = 0.825$$

Part 1 - Outer flange

$$c_{\text{outerflange}} := \frac{2b_{\text{top}} - C}{2} - \frac{t_{\text{web}}}{2} = 0.435 \text{ m} \quad \text{Width of the outer flange}$$

$$\text{outerflange} := \frac{c_{\text{outerflange}}}{t_{\text{top}}} = 10.875 \quad \text{c/t}$$

$$\text{Class}_{\text{outerflange}} := \begin{cases} 1 & \text{if } \text{outerflange} \leq 9\epsilon_{\text{top}} \\ 2 & \text{if } 9\epsilon_{\text{top}} < \text{outerflange} \leq 10\epsilon_{\text{top}} \\ 3 & \text{if } 10\epsilon_{\text{top}} < \text{outerflange} \leq 14\epsilon_{\text{top}} \\ 4 & \text{otherwise} \end{cases}$$

$$\text{Class}_{\text{outerflange}} = 3 \quad \text{Cross-sectional class}$$

$$k_{\sigma\text{outer}} := 0.43$$

$$\psi_{\text{outer}} := 1$$

$$\lambda_{\text{pouter}} := \frac{\frac{c_{\text{outerflange}}}{t_{\text{top}}}}{28.4\epsilon_{\text{top}} \cdot \sqrt{k_{\sigma\text{outer}}}} = 0.708$$

$$\rho_{\text{outer1}} := \begin{cases} 1 & \text{if } \lambda_{\text{pouter}} \leq 0.748 \\ \frac{\lambda_{\text{pouter}} - 0.188}{\lambda_{\text{pouter}}^2} & \text{if } \lambda_{\text{pouter}} > 0.748 \end{cases}$$

$$\rho_{\text{outer}} := \min(\rho_{\text{outer1}}, 1) = 1$$

$$b_{\text{outereff}} := \rho_{\text{outer}} \cdot c_{\text{outerflange}} = 0.435 \text{ m}$$

Effective width

Part 2 - Inner flange

$$c_{\text{innerflange}} := C - t_{\text{web}} = 1.49 \text{ m}$$

Width of the inner flange

$$\text{innerflange} := \frac{c_{\text{innerflange}}}{t_{\text{top}}} = 37.25$$

c/t

$$\text{Class}_{\text{innerflange}} := \begin{cases} 1 & \text{if } \text{innerflange} \leq 33\epsilon_{\text{top}} \\ 2 & \text{if } 33\epsilon_{\text{top}} < \text{innerflange} \leq 38\epsilon_{\text{top}} \\ 3 & \text{if } 38\epsilon_{\text{top}} < \text{innerflange} \leq 42\epsilon_{\text{top}} \\ 4 & \text{otherwise} \end{cases}$$

$$\text{Class}_{\text{innerflange}} = 4$$

Cross-sectional class

$$k_{\sigma\text{inner}} := 4$$

$$\psi_{\text{inner}} := 1$$

$$\lambda_{\text{pinner}} := \frac{\frac{c_{\text{innerflange}}}{t_{\text{top}}}}{28.4\epsilon_{\text{top}} \cdot \sqrt{k_{\sigma\text{inner}}}} = 0.795$$

$$\rho_{\text{inner1}} := \begin{cases} 1 & \text{if } \lambda_{\text{pinner}} \leq 0.673 \\ \frac{\lambda_{\text{pinner}} - 0.055 \cdot (3 + \psi_{\text{inner}})}{\lambda_{\text{pinner}}^2} & \text{if } \lambda_{\text{pinner}} > 0.673 \end{cases}$$

$$\rho_{\text{inner}} := \min(\rho_{\text{inner1}}, 1) = 0.91$$

$$b_{\text{innereff}} := \frac{\rho_{\text{inner}} \cdot c_{\text{innerflange}}}{2} = 0.678 \text{ m}$$

Effective width

The new cross sectional constants are calculated for one of the girders, given the symmetry.

$$A_{1\text{new}} := \begin{cases} \left(b_{\text{outereff}} + \frac{t_{\text{web}}}{2} \right) \cdot t_{\text{top}} & \text{if } \text{Class}_{\text{outerflange}} = 4 \\ A_1 & \text{otherwise} \end{cases}$$

$$A_{2\text{new}} := \begin{cases} \left(b_{\text{innereff}} + \frac{t_{\text{web}}}{2} \right) \cdot t_{\text{top}} & \text{if } \text{Class}_{\text{innerflange}} = 4 \\ A_2 & \text{otherwise} \end{cases}$$

New distance of gravity center from bottom of the bridge

$$y_{\text{gcnew}} := \frac{A_{1\text{new}} \cdot z_1 + A_{2\text{new}} \cdot z_2 + A_3 \cdot z_3 + A_4 \cdot z_4}{A_{1\text{new}} + A_{2\text{new}} + A_3 + A_4} = 1.186 \text{ m}$$

New distance from local and global gravity center

$$a_{1\text{new}} := y_{\text{gcnew}} - z_1 = -0.794 \text{ m}$$

$$a_{2\text{new}} := y_{\text{gcnew}} - z_2 = -0.794 \text{ m}$$

$$a_{3\text{new}} := y_{\text{gcnew}} - z_3 = 0.181 \text{ m}$$

$$a_{4\text{new}} := y_{\text{gcnew}} - z_4 = 1.161 \text{ m}$$

New moment of inertia

$$I_{\text{totnew1}} := \frac{b_{\text{outereff}} \cdot t_{\text{top}}^3}{12} + A_{1\text{new}} \cdot a_{1\text{new}}^2 + \frac{b_{\text{innereff}} \cdot t_{\text{top}}^3}{12} + A_{2\text{new}} \cdot a_{2\text{new}}^2 \dots = 0.075 \cdot \text{m}^4$$

$$+ \frac{t_{\text{web}} \cdot h_{\text{web}}^3}{12} + A_3 \cdot a_{3\text{new}}^2 + \frac{b_{\text{bottom}} \cdot t_{\text{bottom}}^3}{12} + A_4 \cdot a_{4\text{new}}^2$$

$$I_{\text{totnew2}} := \frac{b_{\text{outer}} \cdot t_{\text{top}}^3}{12} + A_{1\text{new}} \cdot a_{1\text{new}}^2 + \frac{b_{\text{innereff}} \cdot t_{\text{top}}^3}{12} + A_{2\text{new}} \cdot a_{2\text{new}}^2 \dots = 0.075 \cdot \text{m}^4$$

$$+ \frac{t_{\text{web}} \cdot h_{\text{web}}^3}{12} + A_3 \cdot a_{3\text{new}}^2 + \frac{b_{\text{bottom}} \cdot t_{\text{bottom}}^3}{12} + A_4 \cdot a_{4\text{new}}^2$$

$$I_{\text{totnew}} := \begin{cases} I_{\text{totnew1}} & \text{if } \text{Class}_{\text{outerflange}} = 4 \\ I_{\text{totnew2}} & \text{if } \text{Class}_{\text{outerflange}} \neq 4 \end{cases} \quad I_{\text{totnew}} = 0.075 \text{ m}^4$$

A.1.4.3 Cross-sectional constants if web buckles

Part 3 - web

$$\sigma_c := \frac{M_{ULS}}{I_{totnew}} \cdot (h_{tot} - y_{gcnew}) = 126.183 \cdot \text{MPa} \quad \text{Compressive stress in web}$$

$$\sigma_t := \frac{M_{ULS}}{I_{totnew}} \cdot (-y_{gcnew}) = -184.005 \cdot \text{MPa} \quad \text{Tensile stress in web}$$

$$\epsilon_{web} := \sqrt{\frac{235 \text{MPa}}{f_{yweb}}} = 0.825$$

$$\text{butt weld} := 5 \text{mm} \quad \text{Height of butt weld}$$

$$\text{web} := \frac{h_{web} - (\text{weld} + \text{butt weld})}{t_{web}} = 94.896 \quad \text{c/t}$$

$$\alpha_{gc} := \frac{h_{web} - y_{gcnew}}{h_{web}} = 0.379 \quad \psi_{gc} := \frac{\sigma_t}{\sigma_c} = -1.458$$

$$\text{Class}_{web1} := \begin{cases} 1 & \text{if } \text{web} \leq \frac{36\epsilon_{web}}{\alpha_{gc}} \\ 2 & \text{if } \frac{36\epsilon_{web}}{\alpha_{gc}} < \text{web} \leq \frac{41.5\epsilon_{web}}{\alpha_{gc}} \\ 3 & \text{if } \frac{41.5\epsilon_{web}}{\alpha_{gc}} < \text{web} \leq 62\epsilon_{web} \cdot (1 - \psi_{gc}) \cdot \sqrt{-\psi_{gc}} \\ 4 & \text{otherwise} \end{cases}$$

$$\text{Class}_{web2} := \begin{cases} 1 & \text{if } \text{web} \leq \frac{396\epsilon_{web}}{13\alpha_{gc} - 1} \\ 2 & \text{if } \frac{396\epsilon_{web}}{13\alpha_{gc} - 1} < \text{web} \leq \frac{456\epsilon_{web}}{13\alpha_{gc} - 1} \\ 3 & \text{if } \frac{456\epsilon_{web}}{13\alpha_{gc} - 1} < \text{web} \leq \frac{42\epsilon_{web}}{0.67 + 0.33 \cdot \psi_{gc}} \\ 4 & \text{otherwise} \end{cases}$$

$$\text{Class}_{web} := \begin{cases} \text{Class}_{web2} & \text{if } \alpha_{gc} > 0.5 \\ \text{Class}_{web1} & \text{if } \alpha_{gc} \leq 0.5 \end{cases} \quad \text{Class}_{web} = 3 \quad \text{Cross-sectional class}$$

$$k_{\sigma\text{web}} := \begin{cases} 7.81 - 6.29\psi_{\text{gc}} + 9.78\psi_{\text{gc}}^2 & \text{if } 0 > \psi_{\text{gc}} > -1 \\ 23.9 & \text{if } \psi_{\text{gc}} = -1 \\ 5.98 \cdot (1 - \psi_{\text{gc}})^2 & \text{if } -1 > \psi_{\text{gc}} > -3 \end{cases}$$

$$k_{\sigma\text{web}} = 36.137$$

$$\lambda_{\text{pweb}} := \frac{\frac{h_{\text{web}} - (\text{weld} + \text{butt weld})}{t_{\text{web}}}}{28.4 \epsilon_{\text{web}} \cdot \sqrt{k_{\sigma\text{web}}}} = 0.673$$

$$\rho_{\text{web1}} := \begin{cases} 1 & \text{if } \lambda_{\text{pweb}} \leq 0.673 \\ \frac{\lambda_{\text{pweb}} - 0.055 \cdot (3 + \psi_{\text{gc}})}{\lambda_{\text{pweb}}^2} & \text{if } \lambda_{\text{pweb}} > 0.673 \end{cases}$$

$$\rho_{\text{web}} := \min(\rho_{\text{web1}}, 1) = 1$$

$$b_{\text{webeff}} := \rho_{\text{web}} \cdot (h_{\text{tot}} - y_{\text{gcnew}} - t_{\text{top}} - \text{butt weld}) = 768.59 \cdot \text{mm}$$

$$b_{\text{web1}} := b_{\text{webeff}} \cdot 0.4 = 307.436 \cdot \text{mm}$$

$$b_{\text{web2}} := b_{\text{webeff}} \cdot 0.6 = 461.154 \cdot \text{mm}$$

$$b_{\text{webgap}} := h_{\text{tot}} - y_{\text{gcnew}} - t_{\text{top}} - \text{butt weld} - b_{\text{web1}} - b_{\text{web2}} = 0 \cdot \text{mm}$$

The final distance from bottom to gravity center

$$z_{31} := h_{\text{tot}} - t_{\text{top}} - \text{butt weld} - \frac{b_{\text{web1}}}{2} = 1.801 \text{ m}$$

$$z_{32} := y_{\text{gcnew}} + \frac{b_{\text{web2}}}{2} = 1.417 \text{ m}$$

$$z_{33} := y_{\text{gcnew}} - \left(\frac{y_{\text{gcnew}} - t_{\text{bottom}}}{2} \right) = 0.618 \text{ m}$$

$$z_{31\text{new}} := \begin{cases} z_{31} & \text{if } \text{Class}_{\text{web}} = 4 \\ 0 & \text{otherwise} \end{cases}$$

$$z_{32\text{new}} := \begin{cases} z_{32} & \text{if } \text{Class}_{\text{web}} = 4 \\ 0 & \text{otherwise} \end{cases}$$

$$z_{33\text{new}} := \begin{cases} z_{33} & \text{if } \text{Class}_{\text{web}} = 4 \\ \frac{h_{\text{web}}}{2} + t_{\text{bottom}} & \text{otherwise} \end{cases}$$

The final cross sectional constants are calculated for one of the girders, given the symmetry.

$$A_{31} := b_{web1} \cdot t_{web} = 6.149 \times 10^{-3} \text{ m}^2$$

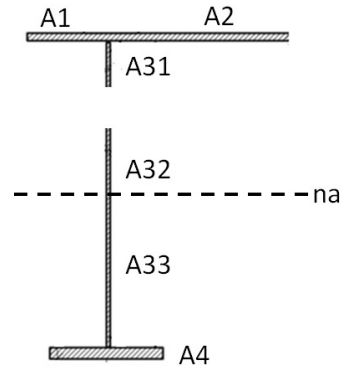
$$A_{32} := b_{web2} \cdot t_{web} = 9.223 \times 10^{-3} \text{ m}^2$$

$$A_{33} := (y_{gcnew} - t_{bottom}) \cdot t_{web} = 0.023 \text{ m}^2$$

$$A_{31new} := \begin{cases} A_{31} & \text{if } Class_{web} = 4 \\ 0 & \text{otherwise} \end{cases}$$

$$A_{32new} := \begin{cases} A_{32} & \text{if } Class_{web} = 4 \\ 0 & \text{otherwise} \end{cases}$$

$$A_{33new} := \begin{cases} A_{33} & \text{if } Class_{web} = 4 \\ h_{web} \cdot t_{web} & \text{otherwise} \end{cases}$$



Final distance of gravity center from bottom of the bridge

$$y_{gcfinal} := \frac{A_{1new} \cdot z_1 + A_{2new} \cdot z_2 + A_{31new} \cdot z_{31new} \dots + A_{32new} \cdot z_{32new} + A_{33new} \cdot z_{33new} + A_4 \cdot z_4}{A_{1new} + A_{2new} + A_{31new} + A_{32new} + A_{33new} + A_4} = 1.186 \text{ m}$$

Final moment of inertia

$$I_{totfinal1} := I_{totnew1} = 7.514 \times 10^{10} \cdot \text{mm}^4$$

$$I_{totfinal2} := I_{totnew2} = 7.514 \times 10^{10} \cdot \text{mm}^4$$

$$I_{totfinal3} := \frac{b_{outer} \cdot t_{top}^3}{12} + A_{1new} \cdot \left(h_{tot} - y_{gcfinal} - \frac{t_{top}}{2} \right)^2 \dots = 0.075 \cdot \text{m}^4$$

$$+ \frac{b_{innereff} \cdot t_{top}^3}{12} + A_{2new} \cdot \left(h_{tot} - y_{gcfinal} - \frac{t_{top}}{2} \right)^2 \dots$$

$$+ \frac{t_{web} \cdot b_{web1}^3}{12} + A_{31} \cdot \left(\frac{b_{web1}}{2} + b_{webgap} + b_{web2} \right)^2 \dots$$

$$+ \frac{t_{web} \cdot b_{web2}^3}{12} + A_{32} \cdot \left(\frac{b_{web2}}{2} \right)^2 \dots$$

$$+ \frac{t_{web} \cdot (y_{gcfinal} - t_{bottom})^3}{12} + A_{33} \cdot \left(\frac{y_{gcfinal} - t_{bottom}}{2} \right)^2 \dots$$

$$+ \frac{b_{bottom} \cdot t_{bottom}^3}{12} + A_4 \cdot \left(y_{gcfinal} - \frac{t_{bottom}}{2} \right)^2$$

$$\begin{aligned}
I_{\text{totfinal4}} := & \frac{b_{\text{outereff}} \cdot t_{\text{top}}^3}{12} + A_{1\text{new}} \left(h_{\text{tot}} - y_{\text{gcfinal}} - \frac{t_{\text{top}}}{2} \right)^2 \dots = 0.075 \cdot \text{m}^4 \\
& + \frac{b_{\text{innereff}} \cdot t_{\text{top}}^3}{12} + A_{2\text{new}} \left(h_{\text{tot}} - y_{\text{gcfinal}} - \frac{t_{\text{top}}}{2} \right)^2 \dots \\
& + \frac{t_{\text{web}} \cdot b_{\text{web1}}^3}{12} + A_{31} \cdot \left(\frac{b_{\text{web1}}}{2} + b_{\text{webgap}} + b_{\text{web2}} \right)^2 \dots \\
& + \frac{t_{\text{web}} \cdot b_{\text{web2}}^3}{12} + A_{32} \cdot \left(\frac{b_{\text{web2}}}{2} \right)^2 \dots \\
& + \frac{t_{\text{web}} \cdot (y_{\text{gcfinal}} - t_{\text{bottom}})^3}{12} + A_{33} \cdot \left(\frac{y_{\text{gcfinal}} - t_{\text{bottom}}}{2} \right)^2 \dots \\
& + \frac{b_{\text{bottom}} \cdot t_{\text{bottom}}^3}{12} + A_4 \cdot \left(y_{\text{gcfinal}} - \frac{t_{\text{bottom}}}{2} \right)^2
\end{aligned}$$

$$I_{\text{totfinal}} := \begin{cases} I_{\text{totfinal1}} & \text{if } \begin{cases} \text{Class}_{\text{outerflange}} \neq 4 \\ \text{Class}_{\text{web}} \neq 4 \end{cases} \\ I_{\text{totfinal2}} & \text{if } \begin{cases} \text{Class}_{\text{outerflange}} = 4 \\ \text{Class}_{\text{web}} \neq 4 \end{cases} \\ I_{\text{totfinal3}} & \text{if } \begin{cases} \text{Class}_{\text{outerflange}} \neq 4 \\ \text{Class}_{\text{web}} = 4 \end{cases} \\ I_{\text{totfinal4}} & \text{if } \begin{cases} \text{Class}_{\text{outerflange}} = 4 \\ \text{Class}_{\text{web}} = 4 \end{cases} \end{cases}$$

$$I_{\text{totfinal}} = 7.514 \times 10^{10} \cdot \text{mm}^4$$

A.1.4.4 Bending verification in ULS

$$y_c := h_{\text{tot}} - y_{\text{gcfinal}} = 0.814 \text{ m}$$

Distance to most compressed fibre

$$W_{\text{effc}} := \frac{I_{\text{totfinal}}}{y_c} = 9.236 \times 10^7 \cdot \text{mm}^3$$

Sectional modulus of compressed area

$$W_{\text{efft}} := \frac{I_{\text{totfinal}}}{y_{\text{gcfinal}}} = 6.334 \times 10^7 \cdot \text{mm}^3$$

Sectional modulus of tensile area

$$M_{Rdt} := W_{efft} \cdot \frac{f_{ybottom}}{1.0} = 21.852 \cdot MN \cdot m$$

Moment resistance in tension

$$M_{Rdc} := W_{effc} \cdot \frac{f_{ytop}}{1.0} = 31.865 \cdot MN \cdot m$$

Moment resistance in compression

$$M_{Rd} := \min(M_{Rdt}, M_{Rdc}) = 21.852 \cdot MN \cdot m$$

Moment resistance of the weakest part

$$\mu_1 := \frac{M_{ULS}}{M_{Rd}} = 0.533$$

Utilization factor in bending

A.1.5 Shear resistance in ULS

A.1.5.1 Web only

Control if shear buckling needs to be considered

$$\eta := \begin{cases} 1.2 & \text{if } f_{yweb} \leq 460 \text{MPa} \\ 1.0 & \text{otherwise} \end{cases}$$

Factor due to material

$$a_{stiff} := 5 \text{m}$$

Distance between vertical stiffeners

$$\kappa_T := \begin{cases} 5.34 + 4 \left(\frac{h_{web}}{a_{stiff}} \right)^2 & \text{if } \frac{a_{stiff}}{h_{web}} \geq 1 \\ 4 + 5.34 \left(\frac{h_{web}}{a_{stiff}} \right)^2 & \text{if } \frac{a_{stiff}}{h_{web}} < 1 \end{cases}$$

$$\kappa_T = 5.924$$

$$\text{Checkshear} := \begin{cases} \text{"yes"} & \text{if } \frac{h_{web}}{t_{web}} > \left(\frac{31}{\eta} \cdot \epsilon_{web} \cdot \sqrt{\kappa_T} \right) \\ \text{"no"} & \text{otherwise} \end{cases}$$

$$\text{Checkshear} = \text{"yes"}$$

$$\tau_{cr} := \kappa_T \cdot \frac{\pi^2 \cdot E \cdot t_{web}^2}{12(1 - \nu^2) \cdot (h_{web})^2} = 123.277 \cdot \text{MPa}$$

Critical stress

$$\lambda_w := 0.76 \cdot \sqrt{\frac{f_{yweb}}{\tau_{cr}}} = 1.271$$

Slenderness

$$\chi_w := \begin{cases} \eta & \text{if } \lambda_w < \frac{0.83}{\eta} \\ \frac{0.83}{\lambda_w} & \text{if } \frac{0.83}{\eta} \leq \lambda_w < 1.08 \\ \frac{1.37}{(0.7 + \lambda_w)} & \text{otherwise} \end{cases}$$

Rigid end post

$$\chi_w = 0.695$$

Shear force capacity considering web only

$$V_{bwRd} := \chi_w \cdot \frac{f_{yweb} \cdot (h_{web}) \cdot t_{web}}{\sqrt{3} \cdot \gamma_{M1}} = 5.288 \cdot \text{MN}$$

$$\mu_2 := \frac{V_{ULS}}{V_{bwRd}} = 0.372$$

Utilization factor of the web only in bending

A.1.5.2 Contribution from the flanges

Since the contribution is based on the flange which provides the least resistance, we need to check the capacities of each one.

$$R_{top} := t_{top} \cdot b_{top} \cdot f_{ytop} = 16.56 \cdot \text{MN}$$

Resistance of top flange

$$R_{bottom} := t_{bottom} \cdot b_{bottom} \cdot f_{ybottom} = 8.625 \cdot \text{MN}$$

Resistance of bottom flange

$$\epsilon_{bottom} := \sqrt{\frac{235 \text{MPa}}{f_{ybottom}}} = 0.825$$

Geometrical limitations of the flanges

$$b_{fmaxtop} := 15 \cdot t_{top} \cdot \epsilon_{top} = 0.495 \text{ m}$$

$$b_{ftop} := \min(b_{fmaxtop}, c_{outerflange}) = 0.435 \text{ m}$$

$$b_{fmaxbottom} := 15 \cdot t_{bottom} \cdot \epsilon_{bottom} = 0.619 \text{ m}$$

$$b_{fbottom} := \min\left(b_{fmaxbottom}, \frac{b_{bottom}}{2}\right) = 0.25 \text{ m}$$

$$b_{topshear} := \begin{cases} (b_{fmaxtop} + c_{outerflange}) & \text{if } b_{fmaxtop} > c_{outerflange} \\ (2b_{fmaxtop}) & \text{if } b_{fmaxtop} \leq c_{outerflange} \end{cases}$$

The contribution from the flanges can be taken into account only if they are not fully utilized in bending. So it needs to be checked that their utilization is below 1.

$$b_{topshear} = 0.93 \text{ m}$$

$$b_{bottomshear} := 2 \cdot b_{fbottom} = 0.5 \text{ m}$$

$$b_f := \begin{cases} b_{\text{topshear}} & \text{if } R_{\text{top}} < R_{\text{bottom}} \\ b_{\text{bottomshear}} & \text{otherwise} \end{cases} \quad b_f = 500 \cdot \text{mm}$$

$$t_f := \begin{cases} t_{\text{top}} & \text{if } R_{\text{top}} < R_{\text{bottom}} \\ t_{\text{bottom}} & \text{otherwise} \end{cases} \quad t_f = 50 \cdot \text{mm}$$

$$f_{\text{yshear}} := \begin{cases} f_{y\text{top}} & \text{if } R_{\text{top}} < R_{\text{bottom}} \\ f_{y\text{bottom}} & \text{otherwise} \end{cases} \quad f_{\text{yshear}} = 345 \cdot \text{MPa}$$

$$M_{fRd} := \frac{f_{y\text{top}} \cdot b_{\text{topshear}} \cdot t_{\text{top}} \cdot \left(h_{\text{tot}} - \frac{t_{\text{top}}}{2} - y_{\text{gcfinal}} \right)}{\gamma_{M0}} \dots = 20.204 \cdot \text{MN} \cdot \text{m}$$

$$+ \frac{f_{y\text{bottom}} \cdot 2b_{\text{bottomshear}} \cdot t_{\text{bottom}} \cdot \left(y_{\text{gcfinal}} - \frac{t_{\text{bottom}}}{2} \right)}{\gamma_{M0}}$$

$$\mu_3 := \frac{M_{\text{ULS}}}{M_{fRd}} = 0.577 \quad \text{Utilization factor of the flanges only in bending}$$

Shear capacity contribution from the flanges

$$c_c := a_{\text{stiff}} \cdot \left[0.25 + \frac{1.6b_f \cdot t_f^2 \cdot f_{\text{yshear}}}{t_{\text{web}} \cdot (h_{\text{web}})^2 \cdot f_{y\text{web}}} \right] = 1.387 \text{ m}$$

$$V_{bfRd} := \frac{b_f \cdot t_f^2 \cdot f_{\text{yshear}}}{c_c \cdot \gamma_{M1}} \cdot \left[1 - \left(\frac{M_{\text{ULS}}}{M_{fRd}} \right)^2 \right] = 0.207 \cdot \text{MN}$$

A.1.5.3 Total shear capacity

$$V_{bRd} := \begin{cases} (V_{bwRd} + V_{bfRd}) & \text{if } \mu_3 < 1 \\ V_{bwRd} & \text{otherwise} \end{cases} \quad \text{Shear capacity of web and flanges (if not fully utilized in bending)}$$

$$V_{bRd} = 5.495 \cdot \text{MN}$$

$$\mu_4 := \frac{V_{\text{ULS}}}{V_{bRd}} = 0.358 \quad \text{Utilization factor in shear}$$

A.1.6 Combined shear and bending

$$\eta_3 := \frac{V_{ULS}}{V_{bwRd}}$$

Parameter

$$\text{Checkcombined} := \begin{cases} \text{"yes"} & \text{if } \eta_3 > 0.5 \\ \text{"no"} & \text{otherwise} \end{cases}$$

$$\text{Checkcombined} = \text{"no"}$$

Plastic moment resistance

$$\begin{aligned} M_{plRd} := & t_{top} \cdot b_{top} \cdot \left| h_{tot} - y_{gcfinal} - \frac{t_{top}}{2} \right| \cdot f_{ytop} \dots & = 25.616 \cdot \text{MN} \cdot \text{m} \\ & + h_{web} \cdot t_{web} \cdot \left| \frac{h_{tot}}{2} - y_{gcfinal} \right| \cdot f_{yweb} \dots \\ & + t_{bottom} \cdot b_{bottom} \cdot \left| y_{gcfinal} - \frac{t_{bottom}}{2} \right| \cdot f_{ybottom} \end{aligned}$$

$$\mu_5 := \frac{M_{ULS}}{M_{plRd}} + \left(1 - \frac{M_{fRd}}{M_{plRd}} \right) \cdot (2 \cdot \eta_3 - 1)^2 = 0.469$$

Utilization factor in shear and bending

A.1.7 Check for deflection in SLS

The maximum deflection is calculated at the center of the bridge.

Deflection due to traffic

$x := 0\text{m}, 0.01\text{m}.. L$

$$\text{dispP1}(x) := \left[\begin{array}{l} \left[\frac{P \cdot \left(\frac{L - 6.4\text{m}}{2} + 5.6\text{m} \right) \cdot x \left[L^2 - \left(\frac{L - 6.4\text{m}}{2} + 5.6\text{m} \right)^2 - x^2 \right]}{6E \cdot 2I_{\text{tot}} \cdot L} \right] \text{ if } 0 \leq x < \frac{L - 6.4\text{m}}{2} + 0.8\text{m} \\ \left. \begin{array}{l} \frac{P \cdot \left(\frac{L - 6.4\text{m}}{2} + 5.6\text{m} \right)}{6E \cdot 2I_{\text{tot}} \cdot L} \left[\frac{L}{\frac{L - 6.4\text{m}}{2} + 5.6\text{m}} \cdot \left(x - \frac{L - 6.4\text{m}}{2} + 0.8\text{m} \right)^3 \dots \right] \text{ otherwise} \\ + \left[L^2 - \left(\frac{L - 6.4\text{m}}{2} + 5.6\text{m} \right)^2 \right] \cdot x - x^3 \end{array} \right] \end{array} \right.$$

$$\text{dispP2}(x) := \left[\begin{array}{l} \left[\frac{P \cdot \left(\frac{L - 6.4\text{m}}{2} + 4\text{m} \right) \cdot x \left[L^2 - \left(\frac{L - 6.4\text{m}}{2} + 4\text{m} \right)^2 - x^2 \right]}{6E \cdot 2I_{\text{tot}} \cdot L} \right] \text{ if } 0 \leq x < \frac{L - 6.4\text{m}}{2} + 2.4\text{m} \\ \left. \begin{array}{l} \frac{P \cdot \left(\frac{L - 6.4\text{m}}{2} + 4\text{m} \right)}{6E \cdot 2I_{\text{tot}} \cdot L} \left[\frac{L}{\frac{L - 6.4\text{m}}{2} + 4\text{m}} \cdot \left(x - \frac{L - 6.4\text{m}}{2} + 2.4\text{m} \right)^3 \dots \right] \text{ otherwise} \\ + \left[L^2 - \left(\frac{L - 6.4\text{m}}{2} + 4\text{m} \right)^2 \right] \cdot x - x^3 \end{array} \right] \end{array} \right.$$

$$\text{dispP3}(x) := \left[\begin{array}{l} \left[\frac{P \cdot \left(\frac{L - 6.4\text{m}}{2} + 2.4\text{m} \right) \cdot x \left[L^2 - \left(\frac{L - 6.4\text{m}}{2} + 2.4\text{m} \right)^2 - x^2 \right]}{6E \cdot 2I_{\text{tot}} \cdot L} \right] \text{ if } 0 \leq x < \frac{L - 6.4\text{m}}{2} + 4\text{m} \\ \left. \begin{array}{l} \frac{P \cdot \left(\frac{L - 6.4\text{m}}{2} + 2.4\text{m} \right)}{6E \cdot 2I_{\text{tot}} \cdot L} \left[\frac{L}{\frac{L - 6.4\text{m}}{2} + 2.4\text{m}} \cdot \left(x - \frac{L - 6.4\text{m}}{2} + 4\text{m} \right)^3 \dots \right] \text{ otherwise} \\ + \left[L^2 - \left(\frac{L - 6.4\text{m}}{2} + 2.4\text{m} \right)^2 \right] \cdot x - x^3 \end{array} \right] \end{array} \right.$$

$$\text{dispP4}(x) := \begin{cases} \left[\frac{P \cdot \left(\frac{L - 6.4\text{m}}{2} + 0.8\text{m} \right) \cdot x \left[L^2 - \left(\frac{L - 6.4\text{m}}{2} + 0.8\text{m} \right)^2 - x^2 \right]}{6E \cdot 2I_{\text{tot}} \cdot L} \right] & \text{if } 0 \leq x < \frac{L - 6.4\text{m}}{2} + 5.6\text{m} \\ \left[\frac{P \cdot \left(\frac{L - 6.4\text{m}}{2} + 0.8\text{m} \right)}{6E \cdot 2I_{\text{tot}} \cdot L} \left[\frac{L}{\frac{L - 6.4\text{m}}{2} + 0.8\text{m}} \cdot \left(x - \frac{L - 6.4\text{m}}{2} + 5.6\text{m} \right)^3 \dots \right. \right. \\ \left. \left. + \left[L^2 - \left(\frac{L - 6.4\text{m}}{2} + 0.8\text{m} \right)^2 \right] \cdot x - x^3 \right] \right] & \text{otherwise} \end{cases}$$

$$\text{dispTot}(x) := \text{dispP1}(x) + \text{dispP2}(x) + \text{dispP3}(x) + \text{dispP4}(x)$$

Deflection due to selfweight

$$\text{dispW}_{\text{self}}(x) := \frac{2q_{\text{selfweight}} \cdot x}{24E \cdot 2I_{\text{tot}}} (L^3 - 2L \cdot x^2 + x^3)$$

Total deflection

$$\delta_{\text{TOTSLS}} := \text{dispTot} \left(\frac{L}{2} \right) + 2 \cdot \frac{5Q \cdot L^4}{768 \cdot E \cdot 2I_{\text{tot}}} + \text{dispW}_{\text{self}} \left(\frac{L}{2} \right) = 21.533 \cdot \text{mm}$$

$$\mu_6 := \frac{\delta_{\text{TOTSLS}}}{\frac{L}{600}} = 0.543$$

Utilization ratio for deflection

A.1.8 Web breathing

According to Eurocode, we make sure that the limits for web breathing are met.

$$\text{Webbreathing} := \begin{cases} \text{"OK"} & \text{if } \frac{h_{\text{web}} + t_{\text{bottom}} - y_{\text{gc}}}{t_{\text{web}}} \leq 55 + 3.3 \cdot \frac{L}{m} \\ \text{"NOT OK"} & \text{otherwise} \end{cases}$$

Webbreathing = "OK"

A.1.9 Verification Summary

$$\mu_1 = 0.533$$

Bending resistance

$$\mu_4 = 0.358$$

Shear resistance from either web only or web and flanges

$$\mu_5 = 0.469$$

Combined bending and shear

$$\mu_6 = 0.543$$

Deflection in SLS

Webbreathing = "OK"

A.2 Highway Bridge over E4 in Skulnäs

A.2.1 Geometry

The detailed geometry and length are given in Chapter 8

A.2.1.1 Bridge geometry

$L := 32\text{m}$	Total span of the bridge
$C := 3000\text{mm}$	Distance between the girders
$h_{\text{web}} := 1410\text{mm}$	Height of the web
$t_{\text{web}} := 11\text{mm}$	Thickness of the web
$b_{\text{top}} := 400\text{mm}$	Half the width of the top plate
$t_{\text{top}} := 25\text{mm}$	Thickness of the top plate
$b_{\text{bottom}} := 450\text{mm}$	Width of the bottom flange
$t_{\text{bottom}} := 35\text{mm}$	Thickness of the bottom flange
$h_{\text{tot}} := t_{\text{top}} + h_{\text{web}} + t_{\text{bottom}} = 1.47\text{m}$	Total height of the section
$h_{\text{deck}} := 265\text{mm}$	Height of the deck
$b_{\text{deck}} := 2500\text{mm}$	Width of the deck
$b_{\text{foot}} := 0\text{m}$	Width of the footpath
$b_{\text{parapet}} := 0\text{mm}$	Width of the parapet
$a := 5\text{mm}$	Weld thickness
$a_{\text{stiff}} := 8\text{m}$	Distance between stiffeners
$A_{\text{halfsteel}} := b_{\text{top}} \cdot t_{\text{top}} + h_{\text{web}} \cdot t_{\text{web}} + b_{\text{bottom}} \cdot t_{\text{bottom}} = 0.041 \cdot \text{m}^2$	
$A_{\text{halfdeck}} := b_{\text{deck}} \cdot h_{\text{deck}} = 0.663 \text{m}^2$	

A.2.1.2 Material Data

$f_{y\text{top}} := \begin{cases} 460\text{MPa} & \text{if } t_{\text{top}} < 16\text{mm} \\ 440\text{MPa} & \text{if } 16\text{mm} < t_{\text{top}} \leq 25\text{mm} \\ 420\text{MPa} & \text{otherwise} \end{cases}$	Yield strength of top flange
--	------------------------------

$f_{yweb} := \begin{cases} 460\text{MPa} & \text{if } t_{web} < 16\text{mm} \\ 440\text{MPa} & \text{if } 16\text{mm} < t_{web} \leq 25\text{mm} \\ 420\text{MPa} & \text{otherwise} \end{cases}$	Yield strength of web
$f_{ybottom} := \begin{cases} 460\text{MPa} & \text{if } t_{bottom} < 16\text{mm} \\ 440\text{MPa} & \text{if } 16\text{mm} < t_{bottom} \leq 25\text{mm} \\ 420\text{MPa} & \text{otherwise} \end{cases}$	Yield strength of bottom flange
$f_{ycon} := 345\text{MPa}$	
$\rho_{concrete} := 2500 \frac{\text{kg}}{\text{m}^3}$	Density of concrete
$\rho_{steel} := 7700 \frac{\text{kg}}{\text{m}^3}$	Density of steel
$E_c := 34\text{GPa}$	E modulus of concrete
$E_s := 210\text{GPa}$	E modulus of the steel
$n := \frac{E_s}{E_c} = 6.176$	E modulus ratio

A.2.1.3 Factors and Parameters

$\gamma_{Mf} := 1.35$	Partial factor for fatigue resistance
$\gamma_{Ff} := 1.0$	Partial factor for fatigue load
$\gamma_{M0} := 1.0$	Partial Factor for cross section resistance
$\gamma_{M1} := 1.0$	Partial Factor for instability
$\nu := 0.3$	Poisson's ratio
$h_{car} := 2000\text{mm}$	Assumed height of a car

A.2.2 Loads

A.2.2.1 Self-weight

$$\begin{aligned}m_{\text{girder}} &:= 2A_{\text{halfsteel}} \cdot \rho_{\text{steel}} \cdot g = 6.231 \cdot \frac{\text{kN}}{\text{m}} && \text{Selfweight of the girder} \\m_{\text{deck}} &:= 2A_{\text{halfdeck}} \cdot \rho_{\text{concrete}} \cdot g = 32.485 \cdot \frac{\text{kN}}{\text{m}} && \text{Selfweight of the concrete deck} \\m_{\text{surfacing}} &:= 6.15 \frac{\text{kN}}{\text{m}} && \text{Selfweight of the surfacing} \\m_{\text{footway}} &:= 4.8 \frac{\text{kN}}{\text{m}^2} \cdot (2 \cdot b_{\text{foot}}) = 0 \cdot \frac{\text{kN}}{\text{m}} && \text{Selfweight of the footway} \\m_{\text{parapets}} &:= 4 \frac{\text{kN}}{\text{m}} && \text{Selfweight of the parapets}\end{aligned}$$

We consider only half of the section since the symmetry allows us to study only half the bridge.

$$q_{\text{selfweight}} := \frac{m_{\text{girder}} + m_{\text{deck}} + m_{\text{surfacing}} + m_{\text{footway}} + m_{\text{parapets}}}{2} = 24.433 \cdot \frac{\text{kN}}{\text{m}}$$

Maximum moment and shear force due to the self-weight

$$\begin{aligned}M_{\text{selfweight}} &:= q_{\text{selfweight}} \cdot \frac{L^2}{8} = 3.127 \times 10^3 \cdot \text{kN} \cdot \text{m} && \text{Moment due to selfweight} \\V_{\text{selfweight}} &:= q_{\text{selfweight}} \cdot \frac{L}{2} = 390.926 \cdot \text{kN} && \text{Shear due to selfweight}\end{aligned}$$

A.2.2.2 Traffic loads

We assume the load combinations as given in models LM1 and LM2.

LM1:

$$\text{LDF1} := 0.5 + \frac{1000}{3000} = 0.833 \quad \text{Load Distribution Factor}$$

$$Q_1 := 300\text{kN}$$

Point load

$$q_1 := 9 \frac{\text{kN}}{\text{m}^2}$$

Distributed load

$$q_{1\text{rem}} := 2.5 \frac{\text{kN}}{\text{m}^2}$$

Load on other lanes

$$\alpha_Q := 0.9$$

Partial factor for Q

$$\alpha_q := 0.7$$

Partial factor for q

$$L_1 := \frac{L - 2\text{m}}{2} = 15\text{m}$$

$$V_{\text{LM1}} := \alpha_Q \cdot Q_1 + \frac{L - 2\text{m}}{L} \cdot \alpha_Q \cdot Q_1 + \frac{\alpha_q \cdot q_1 \cdot 3\text{m} \cdot L}{2} = 0.826 \cdot \text{MN}$$

Shear due to traffic

$$M_{\text{LM1}} := \alpha_Q \cdot Q_1 \cdot \frac{L}{2} - \alpha_Q \cdot Q_1 \cdot \frac{2\text{m}}{2} + \frac{\alpha_q \cdot q_1 \cdot 3\text{m} \cdot L^2}{8} = 6.469 \cdot \text{MN} \cdot \text{m}$$

Moment due to traffic

LM2:

$$\text{LDF2} := 0.5 + \frac{1200}{3000} = 0.9$$

Load Distribution Factor

$$Q_2 := 400\text{kN}$$

Point load

$$V_{\text{LM2}} := \alpha_Q \cdot Q_2 = 0.36 \cdot \text{MN}$$

Shear due to traffic

$$M_{\text{LM2}} := \alpha_Q \cdot Q_2 \cdot \frac{L}{4} = 2.88 \cdot \text{MN} \cdot \text{m}$$

Moment due to traffic

A.2.2.3 Windload

$$q_{\text{windbridge}} := 6 \frac{\text{kN}}{\text{m}^2}$$

Wind pressure acting on the bridge

$$q_{\text{windcar}} := 1.4 \frac{\text{kN}}{\text{m}^2}$$

Wind pressure acting on the car

$$M_{\text{wcar}} := q_{\text{windcar}} \cdot h_{\text{car}} \cdot L \cdot \frac{h_{\text{car}}}{2} = 89.6 \cdot \text{kN} \cdot \text{m}$$

Moment acting on the car

$$M_{w\text{bridge}} := q_{w\text{indbridge}} \cdot h_{\text{tot}} \cdot L \cdot \frac{h_{\text{tot}}}{2} = 207.446 \cdot \text{kN} \cdot \text{m}$$

Moment acting on the bridge

$$\Delta M_{w\text{ind}} := M_{w\text{car}} - M_{w\text{bridge}} = -117.846 \cdot \text{kN} \cdot \text{m}$$

Moment resultant

$$F_{w\text{ind}} := -\frac{\Delta M_{w\text{ind}}}{C \cdot L} = 1.228 \cdot \frac{\text{kN}}{\text{m}}$$

Force resultant

$$M_{w\text{ind}} := \frac{F_{w\text{ind}} \cdot L^2}{8} = 157.129 \cdot \text{kN} \cdot \text{m}$$

Moment due to wind

$$V_{w\text{ind}} := \frac{F_{w\text{ind}} \cdot L}{2} = 19.641 \cdot \text{kN}$$

Shear due to wind

A.2.3 Load combinations

The load combinations are according to Section 8.1.2.

$$\begin{array}{ll} \gamma_g := 1.2 & \psi := 0.75 \\ \gamma_D := 1.5 & \gamma_O := 1.5 \end{array} \quad \text{Partial coefficients}$$

A.2.3.1 Ultimate Limit State

$$M_{ULS1} := \gamma_g \cdot M_{\text{selfweight}} + \gamma_D \cdot LDF1 \cdot M_{LM1} + \psi \cdot \gamma_O \cdot M_{\text{wind}} = 12.016 \cdot \text{MN} \cdot \text{m}$$

$$V_{ULS1} := \gamma_g \cdot V_{\text{selfweight}} + \gamma_D \cdot LDF1 \cdot V_{LM1} + \psi \cdot \gamma_O \cdot V_{\text{wind}} = 1.523 \cdot \text{MN}$$

$$M_{ULS2} := \gamma_g \cdot M_{\text{selfweight}} + \gamma_D \cdot LDF2 \cdot M_{LM2} + \psi \cdot \gamma_O \cdot M_{\text{wind}} = 7.818 \cdot \text{MN} \cdot \text{m}$$

$$V_{ULS2} := \gamma_g \cdot V_{\text{selfweight}} + \gamma_D \cdot LDF1 \cdot V_{LM2} + \psi \cdot \gamma_O \cdot V_{\text{wind}} = 0.941 \cdot \text{MN}$$

$$M_{ULS} := \max(M_{ULS1}, M_{ULS2}) = 12.016 \cdot \text{MN} \cdot \text{m}$$

$$V_{ULS} := \max(V_{ULS1}, V_{ULS2}) = 1.523 \cdot \text{MN}$$

A.2.3.2 Servicability Limit State

$$M_{SLS1} := M_{\text{selfweight}} + M_{LM1} + \psi \cdot M_{\text{wind}} = 9.714 \cdot \text{MN} \cdot \text{m}$$

$$V_{SLS1} := V_{\text{selfweight}} + V_{LM1} + \psi \cdot V_{\text{wind}} = 1.231 \cdot \text{MN}$$

$$M_{SLS2} := M_{\text{selfweight}} + M_{LM2} + \psi \cdot M_{\text{wind}} = 6.125 \cdot \text{MN} \cdot \text{m}$$

$$V_{SLS2} := V_{\text{selfweight}} + V_{LM2} + \psi \cdot V_{\text{wind}} = 0.766 \cdot \text{MN}$$

$$M_{SLS} := \max(M_{SLS1}, M_{SLS2}) = 9.714 \cdot \text{MN} \cdot \text{m}$$

$$V_{SLS} := \max(V_{SLS1}, V_{SLS2}) = 1.231 \cdot \text{MN}$$

A.2.3.3 Ultimate Limit State LT

$$M_{ULSLT} := \gamma_g \cdot \left(q_{\text{selfweight}} \cdot \frac{L^2}{8} \right) = 3.753 \cdot \text{MN} \cdot \text{m}$$

A.2.4 Bending resistance in ULS

A.2.4.1 Cross-sectional constants

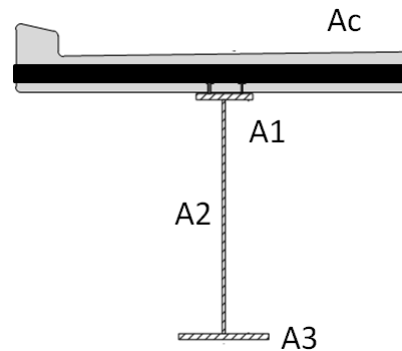
The cross sectional constants are calculated for one of the girders, given the symmetry. The concrete deck is taken into account through its equivalent steel section.

$$A_1 := t_{\text{top}} \cdot b_{\text{top}} = 0.01 \text{ m}^2$$

$$A_2 := h_{\text{web}} \cdot t_{\text{web}} = 0.016 \text{ m}^2$$

$$A_3 := b_{\text{bottom}} \cdot t_{\text{bottom}} = 0.016 \text{ m}^2$$

$$A_c := \frac{b_{\text{deck}} \cdot h_{\text{deck}}}{n} = 0.107 \text{ m}^2$$



Distance of each part from bottom to gravity center

$$z_1 := t_{\text{bottom}} + h_{\text{web}} + \frac{t_{\text{top}}}{2} = 1.457 \text{ m}$$

$$z_2 := t_{\text{bottom}} + \frac{h_{\text{web}}}{2} = 0.74 \text{ m}$$

$$z_3 := \frac{t_{\text{bottom}}}{2} = 0.018 \text{ m}$$

$$z_c := h_{\text{tot}} + 107 \text{ mm} = 1.577 \text{ m}$$

Gravity of center from bottom of the bridge

$$y_{\text{gcfinal}} := \frac{A_1 \cdot z_1 + A_2 \cdot z_2 + A_3 \cdot z_3 + A_c \cdot z_c}{A_1 + A_2 + A_3 + A_c} = 1.316 \text{ m}$$

Distance from local and global gravity center

$$a_1 := y_{\text{gcfinal}} - z_1 = -0.141 \text{ m}$$

$$a_2 := y_{\text{gcfinal}} - z_2 = 0.576 \text{ m}$$

$$a_3 := y_{\text{gcfinal}} - z_3 = 1.299 \text{ m}$$

$$a_c := y_{\text{gcfinal}} - z_c = -0.261 \text{ m}$$

Moment of inertia

$$I_{\text{totfinal}} := \frac{b_{\text{top}} \cdot t_{\text{top}}^3}{12} + A_1 \cdot a_1^2 + \frac{t_{\text{web}} \cdot h_{\text{web}}^3}{12} + A_2 \cdot a_2^2 \dots = 0.042 \cdot \text{m}^4$$

$$+ \frac{b_{\text{bottom}} \cdot t_{\text{bottom}}^3}{12} + A_3 \cdot a_3^2 + \frac{b_{\text{deck}} \cdot \left(\frac{h_{\text{deck}}}{n}\right)^3}{12} + A_c \cdot a_c^2$$

In this case, no parts of the steel section can buckle:

top flange: it is restrained by the concrete deck (see EN 1994 section 6.6.5.5)

web: the part of the web in compression is always minimal. For this reason a reduction will not be needed. Anyway, the moment of inertia is barely affected.

A.2.4.2 Bending verification in ULS

$$\sigma_c := \frac{M_{\text{ULS}}}{I_{\text{totfinal}}} \cdot (h_{\text{tot}} - y_{\text{gcfinal}}) = 44.224 \cdot \text{MPa} \quad \text{Maximum compressive stress}$$

$$\sigma_t := \frac{M_{\text{ULS}}}{I_{\text{totfinal}}} \cdot (-y_{\text{gcfinal}}) = -378.382 \cdot \text{MPa} \quad \text{Maximum tensile stress}$$

$$\varepsilon_{\text{web}} := \sqrt{\frac{235 \text{MPa}}{f_{y\text{web}}}} = 0.715$$

$$W_{\text{efft}} := \frac{I_{\text{totfinal}}}{y_{\text{gcfinal}}} = 3.176 \times 10^7 \cdot \text{mm}^3 \quad \text{Sectional modulus of tensile area}$$

$$M_{\text{Rd}} := W_{\text{efft}} \cdot \frac{f_{y\text{bottom}}}{1.0} = 13.338 \cdot \text{MN} \cdot \text{m} \quad \text{Moment resistance in tension}$$

$$\mu_1 := \frac{M_{\text{ULS}}}{M_{\text{Rd}}} = 0.901 \quad \text{Utilization ratio in bending}$$

A.2.5 Shear resistance in ULS

A.2.5.1 Web only

Control if shear buckling needs to be considered

$$\eta := \begin{cases} 1.2 & \text{if } f_{yweb} \leq 460 \text{ MPa} \\ 1.0 & \text{otherwise} \end{cases}$$

$$\kappa_T := \begin{cases} 5.34 + 4 \left(\frac{h_{web}}{a_{stiff}} \right)^2 & \text{if } \frac{a_{stiff}}{h_{web}} \geq 1 \\ 4 + 5.34 \left(\frac{h_{web}}{a_{stiff}} \right)^2 & \text{if } \frac{a_{stiff}}{h_{web}} < 1 \end{cases}$$

$$\kappa_T = 5.464$$

$$\text{Checkshear} := \begin{cases} \text{"yes"} & \text{if } \frac{h_{web}}{t_{web}} > \left(\frac{31}{\eta} \cdot \epsilon_{web} \cdot \sqrt{\kappa_T} \right) \\ \text{"no"} & \text{otherwise} \end{cases} \quad \text{Checkshear} = \text{"yes"}$$

$$\tau_{cr} := \kappa_T \cdot \frac{\pi^2 \cdot E_s \cdot t_{web}^2}{12(1 - \nu^2) \cdot (h_{web})^2} = 63.121 \cdot \text{MPa} \quad \text{Critical stress}$$

$$\lambda_w := 0.76 \cdot \sqrt{\frac{f_{yweb}}{\tau_{cr}}} = 2.052 \quad \text{Slenderness}$$

$$\chi_w := \begin{cases} \eta & \text{if } \lambda_w < \frac{0.83}{\eta} \\ \frac{0.83}{\lambda_w} & \text{if } \frac{0.83}{\eta} \leq \lambda_w < 1.08 \\ \frac{1.37}{(0.7 + \lambda_w)} & \text{otherwise} \end{cases} \quad \text{Rigid end post}$$

$$\chi_w = 0.498$$

Shear force capacity considering web only

$$V_{bwRd} := \chi_w \cdot \frac{f_{yweb} \cdot (h_{web}) \cdot t_{web}}{\sqrt{3} \cdot \gamma_{M1}} = 2.051 \cdot \text{MN}$$

$$\mu_2 := \frac{V_{ULS}}{V_{bwRd}} = 0.743$$

A.2.5.2 Contribution from the flanges

Since the top flange is restrained by the concrete, the bottom flange will provide the least resistance

$$R_{\text{bottom}} := t_{\text{bottom}} \cdot b_{\text{bottom}} \cdot f_{y\text{bottom}} = 6.615 \cdot \text{MN} \quad \text{Resistance of bottom flange}$$

Geometrical limitations of the flanges

$$\epsilon_{\text{bottom}} := \sqrt{\frac{235 \text{MPa}}{f_{y\text{bottom}}}} = 0.748$$

$$b_{\text{fmaxbottom}} := 15 \cdot t_{\text{bottom}} \cdot \epsilon_{\text{bottom}} = 0.393 \text{ m}$$

$$b_{\text{fbottom}} := \min\left(b_{\text{fmaxbottom}}, \frac{b_{\text{bottom}}}{2}\right) = 0.225 \text{ m}$$

$$b_{\text{bottomshear}} := 2 \cdot b_{\text{fbottom}} = 0.45 \text{ m}$$

The contribution from the flanges can be taken into account only if they are not fully utilized in bending. So it needs to be checked that their utilization is below 1.

$$M_{\text{fRd}} := \frac{(f_{y\text{top}} \cdot b_{\text{top}} \cdot t_{\text{top}}) \cdot \left(h_{\text{tot}} + \frac{t_{\text{top}}}{2} - y_{\text{gcfinal}}\right)}{\gamma_{\text{M0}}} \dots = 9.323 \cdot \text{MN} \cdot \text{m}$$

$$+ \frac{f_{y\text{bottom}} \cdot 2b_{\text{fbottom}} \cdot t_{\text{bottom}} \cdot \left(y_{\text{gcfinal}} - \frac{t_{\text{bottom}}}{2}\right)}{\gamma_{\text{M0}}}$$

$$\mu_3 := \frac{M_{\text{ULS}}}{M_{\text{fRd}}} = 1.289 \quad \text{Utilization ratio of the flanges only in bending}$$

Shear capacity contribution from the flanges

$$c_c := a_{\text{stiff}} \cdot \left[0.25 + \frac{1.6b_{\text{fbottom}} \cdot t_{\text{bottom}}^2 \cdot f_{y\text{bottom}}}{t_{\text{web}} \cdot (h_{\text{web}})^2 \cdot f_{y\text{web}}} \right] = 2.147 \text{ m}$$

$$V_{\text{bfRd}} := \frac{b_{\text{fbottom}} \cdot t_{\text{bottom}}^2 \cdot f_{y\text{bottom}}}{c_c \cdot \gamma_{\text{M1}}} \cdot \left[1 - \left(\frac{M_{\text{ULS}}}{M_{\text{fRd}}} \right)^2 \right] = -0.036 \cdot \text{MN}$$

A.2.5.3 Total shear capacity

$$V_{bRd} := \begin{cases} (V_{bwRd} + V_{bfRd}) & \text{if } \mu_3 < 1 \\ V_{bwRd} & \text{otherwise} \end{cases}$$

Shear capacity of web and flanges (if not fully utilized in bending)

$$V_{bRd} = 2.051 \cdot MN$$

$$\mu_4 := \frac{V_{ULS}}{V_{bRd}} = 0.743$$

Utilization ratio in shear

A.2.6 Check for deflection in SLS

The maximum deflection is calculated at the center of the bridge.

Deflection due to traffic

$x := 0\text{m}, 0.01\text{m}.. L$

$$\text{dispP1}(x) := \begin{cases} \left[\frac{\alpha_Q \cdot Q_1 \cdot \left(\frac{L-2m}{2} + 2m \right) \cdot x \left[L^2 - \left(\frac{L-2m}{2} + 2m \right)^2 - x^2 \right]}{6E_S \cdot 2I_{\text{totfinal}} \cdot L} \right] & \text{if } 0 \leq x < \frac{L-2m}{2} \\ \frac{\alpha_Q \cdot Q_1 \cdot \left(\frac{L-2m}{2} + 2m \right)}{6E_S \cdot 2I_{\text{totfinal}} \cdot L} \left[\frac{L}{\frac{L-2m}{2} + 2m} \cdot \left(x - \frac{L-2m}{2} \right)^3 \dots \right. & \text{otherwise} \\ \left. + \left[L^2 - \left(\frac{L-2m}{2} + 2m \right)^2 \right] \cdot x - x^3 \right] & \end{cases}$$

$$\text{dispP2}(x) := \begin{cases} \left[\frac{\alpha_Q \cdot Q_1 \cdot \left(\frac{L-2m}{2} \right) \cdot x \left[L^2 - \left(\frac{L-2m}{2} \right)^2 - x^2 \right]}{6E_S \cdot 2I_{\text{totfinal}} \cdot L} \right] & \text{if } 0 \leq x < \frac{L-2m}{2} + 2m \\ \frac{\alpha_Q \cdot Q_1 \cdot \left(\frac{L-2m}{2} \right)}{6E_S \cdot 2I_{\text{totfinal}} \cdot L} \left[\frac{L}{\frac{L-2m}{2}} \cdot \left(x - \frac{L-2m}{2} + 2m \right)^3 + \left[L^2 - \left(\frac{L-2m}{2} \right)^2 \right] \cdot x - x^3 \right] & \text{otherwise} \end{cases}$$

$$\text{dispTot}(x) := \text{dispP1}(x) + \text{dispP2}(x)$$

Deflection due to selfweight

$$\text{dispW}_{\text{self}}(x) := \frac{2q_{\text{selfweight}} \cdot x}{24E_S \cdot 2I_{\text{totfinal}}} (L^3 - 2L \cdot x^2 + x^3)$$

Total deflection

$$\delta_{\text{TOTSLS}} := \text{dispTot} \left(\frac{L}{2} \right) + \frac{5(\alpha_q \cdot q_1 \cdot 3m + \alpha_q \cdot q_{1\text{rem}} \cdot 2m) \cdot L^4}{384 \cdot E_S \cdot 2I_{\text{totfinal}}} + \text{dispW}_{\text{self}} \left(\frac{L}{2} \right) = 76.306 \cdot \text{mm}$$

$$\mu_5 := \frac{\delta_{\text{TOTSLS}}}{\frac{L}{400}} = 0.954$$

Utilization ratio for deflection

A.2.7 Web breathing

According to Eurocode, we make sure that the limits for web breathing are met

$$\text{Webbreathing} := \begin{cases} \text{"OK"} & \text{if } \frac{h_{\text{web}} + t_{\text{bottom}} - y_{\text{gcfinal}}}{t_{\text{web}}} \leq 30 + 4 \cdot \frac{L}{m} \\ \text{"NOT OK"} & \text{otherwise} \end{cases}$$

Webbreathing = "OK"

A.2.8 Buckling top flange during casting

We here consider that the top flange could buckle during casting since it will not be restrained by the concrete deck. We assume a load combination with only the weight of the concrete acting and we recalculated the properties of the cross section.

Gravity center from bottom of the bridge

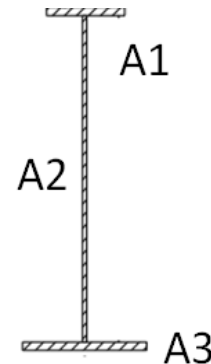
$$y_{gcLT} := \frac{A_1 \cdot z_1 + A_2 \cdot z_2 + A_3 \cdot z_3}{A_1 + A_2 + A_3} = 0.638 \text{ m}$$

Distance from local and global gravity center

$$a_{1LT} := y_{gcLT} - z_1 = -0.819 \text{ m}$$

$$a_{2LT} := y_{gcLT} - z_2 = -0.102 \text{ m}$$

$$a_{3LT} := y_{gcLT} - z_3 = 0.621 \text{ m}$$



Moment of inertia

$$I_{totLT} := \frac{b_{top} \cdot t_{top}^3}{12} + A_1 \cdot a_{1LT}^2 + \frac{t_{web} \cdot h_{web}^3}{12} \dots = 1.551 \times 10^{10} \cdot \text{mm}^4$$

$$+ A_2 \cdot a_{2LT}^2 + \frac{b_{bottom} \cdot t_{bottom}^3}{12} + A_3 \cdot a_{3LT}^2$$

A.2.8.1 Cross-sectional constants if top flange buckles

$$\text{weld} := \sqrt{2} \cdot a = 7.071 \cdot \text{mm}$$

Height of a fillet weld

$$\text{butt weld} := 5 \text{ mm}$$

Height of a butt weld

$$\epsilon_{top} := \sqrt{\frac{235 \text{ MPa}}{f_{ytop}}} = 0.731$$

$$c_{top} := \frac{b_{top} - t_{web}}{2} = 0.195 \text{ m}$$

Width of the top flange

$$\text{topflange} := \frac{c_{top}}{t_{top}} = 7.78$$

c/t

$$\text{Class}_{\text{topflangeLT}} := \begin{cases} 1 & \text{if } \text{topflange} \leq 9\epsilon_{\text{top}} \\ 2 & \text{if } 9\epsilon_{\text{top}} < \text{topflange} \leq 10\epsilon_{\text{top}} \\ 3 & \text{if } 10\epsilon_{\text{top}} < \text{topflange} \leq 14\epsilon_{\text{top}} \\ 4 & \text{otherwise} \end{cases}$$

$$\text{Class}_{\text{topflangeLT}} = 3$$

Cross sectional class

$$k_{\sigma\text{top}} := 0.43$$

$$\psi_{\text{top}} := 1$$

$$\lambda_{\text{ptop}} := \frac{\text{topflange}}{28.4\epsilon_{\text{top}} \cdot \sqrt{k_{\sigma\text{top}}}} = 0.572$$

$$\rho_{\text{top1}} := \begin{cases} 1 & \text{if } \lambda_{\text{ptop}} \leq 0.748 \\ \frac{\lambda_{\text{ptop}} - 0.188}{\lambda_{\text{ptop}}^2} & \text{if } \lambda_{\text{ptop}} > 0.748 \end{cases}$$

$$\rho_{\text{top}} := \min(\rho_{\text{top1}}, 1) = 1$$

$$b_{\text{topLTeff}} := 2\rho_{\text{top}} \cdot c_{\text{top}} + t_{\text{web}} = 0.4 \text{ m}$$

Effective width

The new cross sectional constants are calculated for one of the girders, given the symmetry.

$$A_{1\text{newLT}} := \begin{cases} b_{\text{topLTeff}} \cdot t_{\text{top}} & \text{if } \text{Class}_{\text{topflangeLT}} = 4 \\ A_1 & \text{otherwise} \end{cases}$$

New distance of gravity center from bottom of the bridge

$$y_{\text{gnewLT}} := \frac{A_{1\text{newLT}} \cdot z_1 + A_2 \cdot z_2 + A_3 \cdot z_3}{A_{1\text{newLT}} + A_2 + A_3} = 0.638 \text{ m}$$

New distance from local and global gravity center

$$a_{1\text{newLT}} := y_{\text{gnewLT}} - z_1 = -0.819 \text{ m}$$

$$a_{2\text{newLT}} := y_{\text{gnewLT}} - z_2 = -0.102 \text{ m}$$

$$a_{3\text{newLT}} := y_{\text{gnewLT}} - z_3 = 0.621 \text{ m}$$

$$a_{\text{cnewLT}} := y_{\text{gnewLT}} - z_c = -0.939 \text{ m}$$

New moment of inertia

$$I_{\text{totnew1LT}} := \frac{b_{\text{topLTeff}} \cdot t_{\text{top}}^3}{12} + A_{1\text{newLT}} \cdot a_{1\text{newLT}}^2 + \frac{t_{\text{web}} \cdot h_{\text{web}}^3}{12} \dots = 1.551 \times 10^{10} \cdot \text{mm}^4$$

$$+ A_2 \cdot a_{2\text{newLT}}^2 + \frac{b_{\text{bottom}} \cdot t_{\text{bottom}}^3}{12} + A_3 \cdot a_{3\text{newLT}}^2$$

$$I_{\text{totnew2LT}} := \frac{b_{\text{top}} \cdot t_{\text{top}}^3}{12} + A_{1\text{newLT}} \cdot a_{1\text{newLT}}^2 + \frac{t_{\text{web}} \cdot h_{\text{web}}^3}{12} \dots = 1.551 \times 10^{10} \cdot \text{mm}^4$$

$$+ A_2 \cdot a_{2\text{newLT}}^2 + \frac{b_{\text{bottom}} \cdot t_{\text{bottom}}^3}{12} + A_3 \cdot a_{3\text{newLT}}^2$$

$$I_{\text{totnewLT}} := \begin{cases} I_{\text{totnew1LT}} & \text{if } \text{Class}_{\text{topflangeLT}} = 4 \\ I_{\text{totnew2LT}} & \text{if } \text{Class}_{\text{topflangeLT}} \neq 4 \end{cases}$$

$$I_{\text{totfinal}} = 0.042 \text{ m}^4$$

A.2.8.2 Cross-sectional constants if web buckles

Part 3 - web

$$\sigma_{\text{cLTweb}} := \frac{M_{\text{ULSLT}}}{I_{\text{totnewLT}}} \cdot (h_{\text{tot}} - y_{\text{gcnewLT}}) = 201.252 \cdot \text{MPa} \quad \text{Compressive stress in the web}$$

$$\sigma_{\text{tLTweb}} := \frac{M_{\text{ULSLT}}}{I_{\text{totnewLT}}} \cdot (-y_{\text{gcnewLT}}) = -154.369 \cdot \text{MPa} \quad \text{Tensile stress in the web}$$

$$\text{web} := \frac{h_{\text{web}} - (\text{weld} + \text{butt weld})}{t_{\text{web}}} = 127.084 \quad \text{c/t}$$

$$\alpha_{\text{gcLT}} := \frac{h_{\text{web}} - y_{\text{gcnewLT}}}{h_{\text{web}}} = 0.547 \quad \psi_{\text{gcLT}} := \frac{\sigma_{\text{tLTweb}}}{\sigma_{\text{cLTweb}}} = -0.767$$

$$\text{Class}_{\text{webLT1}} := \begin{cases} 1 & \text{if } \text{web} \leq \frac{36\epsilon_{\text{web}}}{\alpha_{\text{gcLT}}} \\ 2 & \text{if } \frac{36\epsilon_{\text{web}}}{\alpha_{\text{gcLT}}} < \text{web} \leq \frac{41.5\epsilon_{\text{web}}}{\alpha_{\text{gcLT}}} \\ 3 & \text{if } \frac{41.5\epsilon_{\text{web}}}{\alpha_{\text{gcLT}}} < \text{web} \leq 62\epsilon_{\text{web}} \cdot (1 - \psi_{\text{gcLT}}) \cdot \sqrt{-\psi_{\text{gcLT}}} \\ 4 & \text{otherwise} \end{cases}$$

$$\text{Class}_{\text{webLT2}} := \begin{cases} 1 & \text{if } \text{web} \leq \frac{396\epsilon_{\text{web}}}{13\alpha_{\text{gcLT}} - 1} \\ 2 & \text{if } \frac{396\epsilon_{\text{web}}}{13\alpha_{\text{gcLT}} - 1} < \text{web} \leq \frac{456\epsilon_{\text{web}}}{13\alpha_{\text{gcLT}} - 1} \\ 3 & \text{if } \frac{456\epsilon_{\text{web}}}{13\alpha_{\text{gcLT}} - 1} < \text{web} \leq \frac{42\epsilon_{\text{web}}}{0.67 + 0.33 \cdot \psi_{\text{gcLT}}} \\ 4 & \text{otherwise} \end{cases}$$

$$\text{Class}_{\text{webLT}} := \begin{cases} \text{Class}_{\text{webLT2}} & \text{if } \alpha_{\text{gcLT}} > 0.5 \\ \text{Class}_{\text{webLT1}} & \text{if } \alpha_{\text{gcLT}} \leq 0.5 \end{cases}$$

$$\text{Class}_{\text{webLT}} = 4$$

Cross sectional class

$$k_{\sigma\text{webLT}} := \begin{cases} 7.81 - 6.29\psi_{\text{gcLT}} + 9.78\psi_{\text{gcLT}}^2 & \text{if } 0 > \psi_{\text{gcLT}} > -1 \\ 23.9 & \text{if } \psi_{\text{gcLT}} = -1 \\ 5.98 \cdot (1 - \psi_{\text{gcLT}})^2 & \text{if } -1 > \psi_{\text{gcLT}} > -3 \end{cases}$$

$$k_{\sigma\text{webLT}} = 18.389$$

$$\lambda_{\text{pwebLT}} := \frac{\frac{h_{\text{web}} - (\text{weld} + \text{butt weld})}{t_{\text{web}}}}{28.4\epsilon_{\text{web}} \cdot \sqrt{k_{\sigma\text{webLT}}}} = 1.46$$

$$\rho_{\text{webLT1}} := \begin{cases} 1 & \text{if } \lambda_{\text{pwebLT}} \leq 0.673 \\ \frac{\lambda_{\text{pwebLT}} - 0.055 \cdot (3 + \psi_{\text{gcLT}})}{\lambda_{\text{pwebLT}}^2} & \text{if } \lambda_{\text{pwebLT}} > 0.673 \end{cases}$$

$$\rho_{\text{webLT}} := \min(\rho_{\text{webLT1}}, 1) = 0.627$$

$$b_{\text{webeffLT}} := \rho_{\text{webLT}} (h_{\text{tot}} - y_{\text{gcnewLT}} - t_{\text{top}} - \text{butt weld}) = 503.055 \cdot \text{mm}$$

$$b_{\text{webLT1}} := b_{\text{webeffLT}} \cdot 0.4 = 201.222 \cdot \text{mm}$$

$$b_{\text{webLT2}} := b_{\text{webeffLT}} \cdot 0.6 = 301.833 \cdot \text{mm}$$

$$b_{\text{webgapLT}} := h_{\text{tot}} - y_{\text{gcnewLT}} - t_{\text{top}} - \text{butt weld} - b_{\text{webLT1}} - b_{\text{webLT2}} = 298.844 \cdot \text{mm}$$

The final distance from bottom to gravity center.

$$z_{21} := h_{\text{tot}} - t_{\text{top}} - \text{butt weld} - \frac{b_{\text{webLT1}}}{2} = 1.339 \text{ m} \quad z_{21\text{new}} := \begin{cases} z_{21} & \text{if Class}_{\text{webLT}} = 4 \\ 0 & \text{otherwise} \end{cases}$$

$$z_{22} := y_{\text{gcnewLT}} + \frac{b_{\text{webLT2}}}{2} = 0.789 \text{ m} \quad z_{22\text{new}} := \begin{cases} z_{22} & \text{if Class}_{\text{webLT}} = 4 \\ 0 & \text{otherwise} \end{cases}$$

$$z_{23} := y_{\text{gcnewLT}} - \left(\frac{y_{\text{gcnewLT}} - t_{\text{bottom}}}{2} \right) = 0.337 \text{ m} \quad z_{23\text{new}} := \begin{cases} z_{23} & \text{if Class}_{\text{webLT}} = 4 \\ \frac{h_{\text{web}}}{2} + t_{\text{bottom}} & \text{otherwise} \end{cases}$$

The final cross sectional constants are calculated for one of the girders, given the symmetry.

$$A_{21} := b_{\text{webLT1}} \cdot t_{\text{web}} = 2.213 \times 10^{-3} \text{ m}^2$$

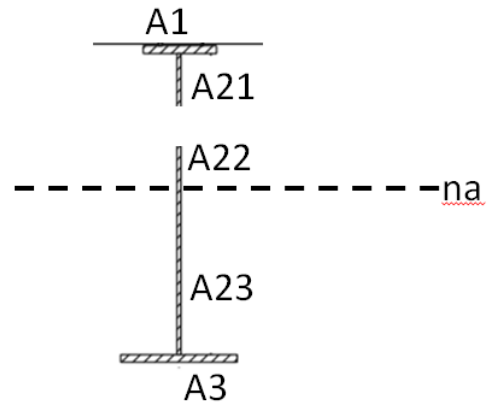
$$A_{22} := b_{\text{webLT2}} \cdot t_{\text{web}} = 3.32 \times 10^{-3} \text{ m}^2$$

$$A_{23} := (y_{\text{gcnewLT}} - t_{\text{bottom}}) \cdot t_{\text{web}} = 6.634 \times 10^{-3} \text{ m}^2$$

$$A_{21\text{new}} := \begin{cases} A_{21} & \text{if Class}_{\text{webLT}} = 4 \\ 0 & \text{otherwise} \end{cases}$$

$$A_{22\text{new}} := \begin{cases} A_{22} & \text{if Class}_{\text{webLT}} = 4 \\ 0 & \text{otherwise} \end{cases}$$

$$A_{23\text{new}} := \begin{cases} A_{23} & \text{if Class}_{\text{webLT}} = 4 \\ h_{\text{web}} \cdot t_{\text{web}} & \text{otherwise} \end{cases}$$



The final gravity center from bottom of the bridge

$$y_{\text{gcfinalLT}} := \frac{A_{1\text{newLT}} \cdot z_1 + A_{21\text{new}} \cdot z_{21\text{new}} + A_{22\text{new}} \cdot z_{22\text{new}} + A_{23\text{new}} \cdot z_{23\text{new}} + A_3 \cdot z_3}{A_{1\text{newLT}} + A_{21\text{new}} + A_{22\text{new}} + A_{23\text{new}} + A_3} = 0.598 \text{ m}$$

The final moment of inertia

$$I_{\text{totfinalLT1}} := I_{\text{totnew1LT}} = 1.551 \times 10^{10} \cdot \text{mm}^4$$

$$I_{\text{totfinalLT2}} := I_{\text{totnew2LT}} = 1.551 \times 10^{10} \cdot \text{mm}^4$$

$$I_{\text{totfinalLT3}} := \frac{b_{\text{top}} \cdot t_{\text{top}}^3}{12} + A_{1\text{newLT}} \cdot \left(h_{\text{tot}} - y_{\text{gcfinalLT}} - \frac{t_{\text{top}}}{2} \right)^2 \dots = 0.015 \cdot \text{m}^4$$

$$+ \frac{t_{\text{web}} \cdot b_{\text{webLT1}}^3}{12} + A_{21\text{new}} \cdot \left(\frac{b_{\text{webLT1}}}{2} + b_{\text{webgapLT}} + b_{\text{webLT2}} \right)^2 \dots$$

$$+ \frac{t_{\text{web}} \cdot b_{\text{webLT2}}^3}{12} + A_{22\text{new}} \cdot \left(\frac{b_{\text{webLT2}}}{2} \right)^2 \dots$$

$$+ \frac{t_{\text{web}} \cdot (y_{\text{gcfinalLT}} - t_{\text{bottom}})^3}{12} + A_{23\text{new}} \cdot \left(\frac{y_{\text{gcfinalLT}} - t_{\text{bottom}}}{2} \right)^2 \dots$$

$$+ \frac{b_{\text{bottom}} \cdot t_{\text{bottom}}^3}{12} + A_3 \cdot \left(y_{\text{gcfinalLT}} - \frac{t_{\text{bottom}}}{2} \right)^2$$

$$I_{\text{totfinalLT4}} := \frac{b_{\text{topLEff}} \cdot t_{\text{top}}^3}{12} + A_{1\text{newLT}} \cdot \left(h_{\text{tot}} - y_{\text{gcfinalLT}} - \frac{t_{\text{top}}}{2} \right)^2 \dots = 0.015 \cdot \text{m}^4$$

$$+ \frac{t_{\text{web}} \cdot b_{\text{webLT1}}^3}{12} + A_{21\text{new}} \cdot \left(\frac{b_{\text{webLT1}}}{2} + b_{\text{webgapLT}} + b_{\text{webLT2}} \right)^2 \dots$$

$$+ \frac{t_{\text{web}} \cdot b_{\text{webLT2}}^3}{12} + A_{22\text{new}} \cdot \left(\frac{b_{\text{webLT2}}}{2} \right)^2 \dots$$

$$+ \frac{t_{\text{web}} \cdot (y_{\text{gcfinalLT}} - t_{\text{bottom}})^3}{12} + A_{23\text{new}} \cdot \left(\frac{y_{\text{gcfinalLT}} - t_{\text{bottom}}}{2} \right)^2 \dots$$

$$+ \frac{b_{\text{bottom}} \cdot t_{\text{bottom}}^3}{12} + A_3 \cdot \left(y_{\text{gcfinalLT}} - \frac{t_{\text{bottom}}}{2} \right)^2$$

$$I_{\text{totfinalLT}} := \begin{cases} I_{\text{totfinalLT1}} & \text{if } \begin{cases} \text{Class}_{\text{topflangeLT}} \neq 4 \\ \text{Class}_{\text{webLT}} \neq 4 \end{cases} \\ I_{\text{totfinalLT2}} & \text{if } \begin{cases} \text{Class}_{\text{topflangeLT}} = 4 \\ \text{Class}_{\text{webLT}} \neq 4 \end{cases} \\ I_{\text{totfinalLT3}} & \text{if } \begin{cases} \text{Class}_{\text{topflangeLT}} \neq 4 \\ \text{Class}_{\text{webLT}} = 4 \end{cases} \\ I_{\text{totfinalLT4}} & \text{if } \begin{cases} \text{Class}_{\text{topflangeLT}} = 4 \\ \text{Class}_{\text{webLT}} = 4 \end{cases} \end{cases}$$

$$I_{\text{totfinalLT}} = 1.458 \times 10^{10} \cdot \text{mm}^4$$

A.2.8.3 Buckling during casting verification

The verification is done considering a fictitious compressed column.

$$\sigma_{\text{cLT}} := \frac{M_{\text{ULSLT}}}{I_{\text{totfinalLT}}} \cdot (h_{\text{tot}} - y_{\text{gcfinalLT}}) = 224.464 \cdot \text{MPa} \quad \text{Maximum compressive stress}$$

$$l_{\text{cr}} := a_{\text{stiff}} = 8 \text{ m} \quad \text{Length of column}$$

$$A_{\text{top}} := b_{\text{top}} \cdot t_{\text{top}} = 0.01 \text{ m}^2 \quad \text{Area of top flange}$$

$$N_{\text{Ed}} := A_{\text{top}} \cdot \sigma_{\text{cLT}} = 2.245 \times 10^3 \cdot \text{kN} \quad \text{Compressive force}$$

$$I_{\text{top}} := \frac{b_{\text{top}}^3 \cdot t_{\text{top}}}{12} = 1.333 \times 10^{-4} \text{ m}^4 \quad \text{Moment of inertia of top flange}$$

$$N_{\text{cr}} := \frac{\pi^2 \cdot E_s \cdot I_{\text{top}}}{l_{\text{cr}}^2} = 4.318 \times 10^3 \cdot \text{kN} \quad \text{Critical buckling force}$$

$$\lambda_{\text{top}} := \sqrt{\frac{A_{\text{top}} \cdot f_{\text{ytop}}}{N_{\text{cr}}}} = 1.009 \quad \text{Slenderness}$$

$$\alpha_{\text{LT}} := \begin{cases} 0.49 & \text{if } t_{\text{top}} \leq 40 \text{ mm} \\ 0.76 & \text{otherwise} \end{cases}$$

$$\alpha_{\text{LT}} = 0.49$$

$$\Phi_{\text{LT}} := 0.5 \cdot \left[1 + \alpha_{\text{LT}} \cdot (\lambda_{\text{top}} - 0.2) + \lambda_{\text{top}}^2 \right] = 1.208$$

$$\chi_{\text{LT}} := \frac{1}{\Phi_{\text{LT}} + \left(\Phi_{\text{LT}}^2 - \lambda_{\text{top}}^2 \right)^{0.5}} = 0.534$$

$$N_{\text{Rd}} := \chi_{\text{LT}} \cdot A_{\text{top}} \cdot \frac{f_{\text{ytop}}}{\gamma_{\text{M1}}} = 2.352 \times 10^3 \cdot \text{kN} \quad \text{Compressive resistance}$$

$$\mu_6 := \frac{N_{\text{Ed}}}{N_{\text{Rd}}} = 0.954 \quad \text{Utilization ratio in buckling during castin}$$

A.2.9 Verification Summary

$\mu_1 = 0.901$ **Bending resistance**

$\mu_4 = 0.743$ **Shear resistance from either web only or web and flanges**

$\mu_5 = 0.954$ **Deflection in SLS**

$\mu_6 = 0.954$ **Buckling during casting**

Webbreathing = "OK"

A.3 Continuous Highway Bridge B

A.3.1 Geometry

The detailed geometry and length are given in Chapter 10

A.3.1.1 Bridge geometry

$L_a := 60\text{m}$	Length of span 1
$L_b := 80\text{m}$	Length of span 2
$L_c := 60\text{m}$	Length of span 3
$C := 7000\text{mm}$	Distance between the girders
$h_{\text{car}} := 2000\text{mm}$	Assumed height of a car
$h_{\text{tot}} := 2800\text{mm}$	Height of the main girder
$b_{\text{top}} := 1000\text{mm}$	Half the width of the top plate
$b_{\text{bottom}} := 1200\text{mm}$	Width of the bottom flange

Support: the support section is referred to as 1

$t_{\text{top1}} := 120\text{mm}$	Thickness of the top plate
$t_{\text{bottom1}} := 120\text{mm}$	Thickness of the bottom flange
$h_{\text{web1}} := h_{\text{tot}} - t_{\text{bottom1}} - t_{\text{top1}} = 2.56 \cdot \text{m}$	Height of the web
$t_{\text{web1}} := 26\text{mm}$	Thickness of the web

Span: the span section is referred to as 2

$t_{\text{top2}} := 40\text{mm}$	Thickness of the top plate
$t_{\text{bottom2}} := 40\text{mm}$	Thickness of the bottom flange
$h_{\text{web2}} := h_{\text{tot}} - t_{\text{bottom2}} - t_{\text{top2}} = 2.72 \cdot \text{m}$	Height of the web
$t_{\text{web2}} := 18\text{mm}$	Thickness of the web

Deck:

$h_{\text{deck}} := 307.5\text{mm}$	Height of the deck
$b_{\text{deck}} := 6000\text{mm}$	Width of the deck
$b_{\text{foot}} := 0\text{m}$	Width of the footpath
$b_{\text{parapet}} := 0\text{mm}$	Width of the parapet

The top layer of reinforcement of the concrete deck is made of 45 $\Phi 20$ while the bottom is $\Phi 16$

$$A_{\text{steel}} := h_{\text{web1}} \cdot t_{\text{web1}} + t_{\text{top1}} \cdot b_{\text{top}} + t_{\text{bottom1}} \cdot b_{\text{bottom}} = 0.331 \text{ m}^2$$

A.3.1.2 Material Data

Yield strength of top flange

$f_{y\text{top1}} :=$	$\left\{ \begin{array}{l} 355\text{MPa} \text{ if } t_{\text{top1}} < 16\text{mm} \\ 345\text{MPa} \text{ if } 16\text{mm} < t_{\text{top1}} \leq 40\text{mm} \\ 335\text{MPa} \text{ if } 40\text{mm} < t_{\text{top1}} \leq 63\text{mm} \\ 325\text{MPa} \text{ if } 63\text{mm} < t_{\text{top1}} \leq 80\text{mm} \\ 315\text{MPa} \text{ if } 80\text{mm} < t_{\text{top1}} \leq 100\text{mm} \\ 295\text{MPa} \text{ otherwise} \end{array} \right.$	$f_{y\text{top2}} :=$	$\left\{ \begin{array}{l} 355\text{MPa} \text{ if } t_{\text{top2}} < 16\text{mm} \\ 345\text{MPa} \text{ if } 16\text{mm} < t_{\text{top2}} \leq 40\text{mm} \\ 335\text{MPa} \text{ if } 40\text{mm} < t_{\text{top2}} \leq 63\text{mm} \\ 325\text{MPa} \text{ if } 63\text{mm} < t_{\text{top2}} \leq 80\text{mm} \\ 315\text{MPa} \text{ if } 80\text{mm} < t_{\text{top2}} \leq 100\text{mm} \\ 295\text{MPa} \text{ otherwise} \end{array} \right.$
-----------------------	--	-----------------------	--

Yield strength of web

$f_{y\text{web2}} :=$	$\left\{ \begin{array}{l} 355\text{MPa} \text{ if } t_{\text{web2}} < 16\text{mm} \\ 345\text{MPa} \text{ if } 16\text{mm} < t_{\text{web2}} \leq 40\text{mm} \\ 335\text{MPa} \text{ if } 40\text{mm} < t_{\text{web2}} \leq 63\text{mm} \\ 325\text{MPa} \text{ if } 63\text{mm} < t_{\text{web2}} \leq 80\text{mm} \\ 315\text{MPa} \text{ if } 80\text{mm} < t_{\text{web2}} \leq 100\text{mm} \\ 295\text{MPa} \text{ otherwise} \end{array} \right.$	$f_{y\text{web1}} :=$	$\left\{ \begin{array}{l} 355\text{MPa} \text{ if } t_{\text{web1}} < 16\text{mm} \\ 345\text{MPa} \text{ if } 16\text{mm} < t_{\text{web1}} \leq 40\text{mm} \\ 335\text{MPa} \text{ if } 40\text{mm} < t_{\text{web1}} \leq 63\text{mm} \\ 325\text{MPa} \text{ if } 63\text{mm} < t_{\text{web1}} \leq 80\text{mm} \\ 315\text{MPa} \text{ if } 80\text{mm} < t_{\text{web1}} \leq 100\text{mm} \\ 295\text{MPa} \text{ otherwise} \end{array} \right.$
-----------------------	--	-----------------------	--

Yield strength of bottom flange

$$f_{y\text{bottom1}} := \begin{cases} 355\text{MPa} & \text{if } t_{\text{bottom1}} < 16\text{mm} \\ 345\text{MPa} & \text{if } 16\text{mm} < t_{\text{bottom1}} \leq 40\text{mm} \\ 335\text{MPa} & \text{if } 40\text{mm} < t_{\text{bottom1}} \leq 63\text{mm} \\ 325\text{MPa} & \text{if } 63\text{mm} < t_{\text{bottom1}} \leq 80\text{mm} \\ 315\text{MPa} & \text{if } 80\text{mm} < t_{\text{bottom1}} \leq 100\text{mm} \\ 295\text{MPa} & \text{otherwise} \end{cases}$$

$$f_{y\text{bottom2}} := \begin{cases} 355\text{MPa} & \text{if } t_{\text{bottom2}} < 16\text{mm} \\ 345\text{MPa} & \text{if } 16\text{mm} < t_{\text{bottom2}} \leq 40\text{mm} \\ 335\text{MPa} & \text{if } 40\text{mm} < t_{\text{bottom2}} \leq 63\text{mm} \\ 325\text{MPa} & \text{if } 63\text{mm} < t_{\text{bottom2}} \leq 80\text{mm} \\ 315\text{MPa} & \text{if } 80\text{mm} < t_{\text{bottom2}} \leq 100\text{mm} \\ 295\text{MPa} & \text{otherwise} \end{cases}$$

$$f_{y\text{con}} := 345\text{MPa}$$

$$f_{y\text{r}} := 500\text{MPa}$$

Yield strength of reinforcement

$$\rho_{\text{concrete}} := 2500 \frac{\text{kg}}{\text{m}^3} \quad \rho_{\text{steel}} := 7700 \frac{\text{kg}}{\text{m}^3}$$

Density of concrete and steel

$$E_{\text{c}} := 34\text{GPa} \quad E_{\text{s}} := 210\text{GPa}$$

E modulus of concrete and steel

$$n := \frac{E_{\text{s}}}{E_{\text{c}}} = 6.176$$

E modulus ratio

A.2.1.3 Factors and Parameters

$$\gamma_{\text{Mf}} := 1.35$$

Partial factor for fatigue resistance

$$\gamma_{\text{FF}} := 1.0$$

Partial factor for fatigue load

$$\gamma_{\text{M0}} := 1.0$$

Partial factor for cross section resistance

$$\gamma_{\text{M1}} := 1.1$$

Partial factor for instability

$$\gamma_{\text{S}} := 1.15$$

$$\nu := 0.3$$

Poisson's ratio

A.3.2 Loads

A.3.2.1 Self-weight

$$q_{\text{stiffener}} := 1.5 \frac{\text{kN}}{\text{m}}$$

Selfweight of the stiffeners

$$q_{\text{max}} := 23.82 \frac{\text{kN}}{\text{m}}$$

Selfweight of the elements

A.3.2.2 Traffic loads

We assume the load combinations as given in models LM1 and LM2.

LM1:

$$Q_1 := 300\text{kN} \quad Q_2 := 200\text{kN} \quad Q_3 := 100\text{kN}$$

Point loads

$$\alpha_{Q1} := 0.9 \quad \alpha_{Q2} := 0.8 \quad \alpha_{Q3} := 0.8$$

Partial factors

$$R_{1c} := 409.3\text{kN}$$

Resultant on most loaded girder

$$R_{2c} := 100.7\text{kN}$$

Resultant on least loaded girder

$$q_1 := 9 \frac{\text{kN}}{\text{m}} \quad q_2 := 2.5 \frac{\text{kN}}{\text{m}} \quad q_3 := 2.5 \frac{\text{kN}}{\text{m}}$$

Distributed loads

$$\alpha_{q1} := 0.7 \quad \alpha_{q2} := 1 \quad \alpha_{q3} := 1$$

Partial factors

$$R_{1d} := 26.7 \frac{\text{kN}}{\text{m}}$$

Resultant on most loaded girder

$$R_{2d} := 7.2 \frac{\text{kN}}{\text{m}}$$

Resultant on least loaded girder

$$\text{LDF} := \frac{R_{1c}}{R_{1c} + R_{2c}} = 0.803$$

Load Distribution Factor

A.3.2.3 Windload

$$q_{\text{windbridge}} := 6 \frac{\text{kN}}{\text{m}^2} \quad \text{Wind pressure acting on the bridge}$$

$$q_{\text{windcar}} := 1.4 \frac{\text{kN}}{\text{m}^2} \quad \text{Wind pressure acting on the car}$$

$$M_{\text{wcar}} := q_{\text{windcar}} \cdot h_{\text{car}} \cdot L_{\text{b}} \cdot \frac{h_{\text{car}}}{2} = 224 \cdot \text{kN} \cdot \text{m} \quad \text{Moment acting on the car}$$

$$M_{\text{wbridge}} := q_{\text{windbridge}} \cdot (h_{\text{tot}} + h_{\text{deck}}) \cdot L_{\text{b}} \cdot \frac{(h_{\text{tot}} + h_{\text{deck}})}{2} = 2.318 \times 10^3 \cdot \text{kN} \cdot \text{m} \quad \text{Moment acting on the bridge}$$

$$\Delta M_{\text{wind}} := M_{\text{wcar}} - M_{\text{wbridge}} = -2.094 \times 10^3 \cdot \text{kN} \cdot \text{m} \quad \text{Moment resultant}$$

$$F_{\text{wind}} := -\frac{\Delta M_{\text{wind}}}{C \cdot L_{\text{b}}} = 3.739 \cdot \frac{\text{kN}}{\text{m}} \quad \text{Force resultant}$$

A.3.3 Load combinations

The load combinations are according to Section 8.1.2.

A.3.3.1 Ultimate Limit State

$$\text{UDL}_{\text{ULS}} := 1.35 \cdot (h_{\text{deck}} \cdot b_{\text{deck}} \cdot \rho_{\text{concrete}} \cdot g + q_{\text{max}} + A_{\text{steel}} \cdot \rho_{\text{steel}} \cdot g) \dots = 190.895 \cdot \frac{\text{kN}}{\text{m}} \\ + 1.5 \cdot (F_{\text{wind}} \cdot 0.7 + R_{1d}) + 20 \frac{\text{kN}}{\text{m}}$$

Once the load is calculated, the resultants have been found through hand calculations. Linear elastic analysis has been performed.

$M_{\text{ULS1}} := 96.56 \text{MN} \cdot \text{m}$	Maximum moment in support section
$V_{\text{ULS1}} := 7.64 \text{MN}$	Maximum shear in support section
$M_{\text{ULS2}} := 56.24 \text{MN} \cdot \text{m}$	Maximum moment in span section
$V_{\text{ULS2}} := 4.12 \text{MN}$	Maximum shear in span section

A.3.3.2 Serviciability Limit State

$$\text{UDL}_{\text{SLS}} := 0.4 \cdot 1 \cdot (h_{\text{deck}} \cdot b_{\text{deck}} \cdot \rho_{\text{concrete}} \cdot g + q_{\text{max}} + A_{\text{steel}} \cdot \rho_{\text{steel}} \cdot g) = 37.606 \cdot \frac{\text{kN}}{\text{m}}$$

A.3.3.3 Ultimate Limit State LT

$$\text{UDL}_{\text{ULSLT}} := 1.35 \cdot (h_{\text{deck}} \cdot b_{\text{deck}} \cdot \rho_{\text{concrete}} \cdot g) = 61.065 \cdot \frac{\text{kN}}{\text{m}}$$

$M_{\text{ULSLT1}} := 30.84 \text{MN} \cdot \text{m}$	Maximum moment in support section
$M_{\text{ULSLT2}} := 17.96 \text{MN} \cdot \text{m}$	Maximum moment in span section

A.3.4 Bending resistance in ULS: support

A.3.4.1 Cross-sectional constants for the support

The cross sectional constants are calculated for one of the girders, given the symmetry. The concrete deck is taken into account through the reinforcement only, since the concrete is assumed to be cracked,..

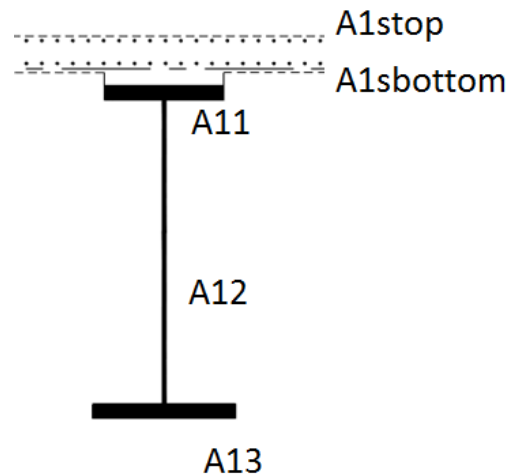
$$A_{11} := t_{\text{top1}} \cdot b_{\text{top}} = 0.12 \text{ m}^2$$

$$A_{12} := h_{\text{web1}} \cdot t_{\text{web1}} = 0.067 \text{ m}^2$$

$$A_{13} := b_{\text{bottom}} \cdot t_{\text{bottom1}} = 0.144 \text{ m}^2$$

$$A_{1\text{stop}} := 45 \cdot \pi \cdot (10\text{mm})^2 = 0.014 \text{ m}^2$$

$$A_{1\text{sbottom}} := 45 \cdot \pi \cdot (8\text{mm})^2 = 9.048 \times 10^{-3} \text{ m}^2$$



Distance of each part from bottom to gravity center

$$z_{11} := t_{\text{bottom1}} + h_{\text{web1}} + \frac{t_{\text{top1}}}{2} = 2.74 \text{ m}$$

$$z_{12} := t_{\text{bottom1}} + \frac{h_{\text{web1}}}{2} = 1.4 \text{ m}$$

$$z_{13} := \frac{t_{\text{bottom1}}}{2} = 0.06 \text{ m}$$

$$z_{1\text{stop}} := h_{\text{tot}} + h_{\text{deck}} + 109\text{mm} - 73\text{mm} = 3.144 \text{ m}$$

$$z_{1\text{sbottom}} := h_{\text{tot}} + 109\text{mm} + 46\text{mm} = 2.955 \text{ m}$$

Gravity of center from bottom of the bridge

$$y_{\text{gc1}} := \frac{A_{11} \cdot z_{11} + A_{12} \cdot z_{12} + A_{13} \cdot z_{13} + A_{1\text{stop}} \cdot z_{1\text{stop}} + A_{1\text{sbottom}} \cdot z_{1\text{sbottom}}}{A_{11} + A_{12} + A_{13} + A_{1\text{stop}} + A_{1\text{sbottom}}} = 1.419 \text{ m}$$

Moment of inertia

$$\begin{aligned}
 I_{\text{tot1}} := & \frac{b_{\text{top}} \cdot t_{\text{top1}}^3}{12} + A_{11} \cdot \left(h_{\text{tot}} - y_{\text{gc1}} - \frac{t_{\text{top1}}}{2} \right)^2 \dots & = 0.575 \text{ m}^4 \\
 & + \frac{t_{\text{web1}} \cdot h_{\text{web1}}^3}{12} + A_{12} \cdot \left(y_{\text{gc1}} - \frac{h_{\text{web1}}}{2} - t_{\text{bottom1}} \right)^2 \dots \\
 & + \frac{b_{\text{bottom}} \cdot t_{\text{bottom1}}^3}{12} + A_{13} \cdot \left(y_{\text{gc1}} - \frac{t_{\text{bottom1}}}{2} \right)^2 \dots \\
 & + \frac{\pi \cdot (10\text{mm})^4}{4} \cdot 45 + A_{1\text{stop}} \cdot (h_{\text{tot}} - y_{\text{gc1}} + h_{\text{deck}} - 73\text{mm} + 109\text{mm})^2 \dots \\
 & + \frac{\pi \cdot (8\text{mm})^4}{4} \cdot 45 + A_{1\text{sbottom}} \cdot (h_{\text{tot}} - y_{\text{gc1}} + 46\text{mm} + 109\text{mm})^2
 \end{aligned}$$

A.3.4.2 Cross-sectional constants if top flange buckles

weld := 5mm Height of a fillet weld

butt weld := 5mm Height of a butt weld

$$\epsilon_{\text{bottom1}} := \sqrt{\frac{235\text{MPa}}{f_{y\text{bottom1}}}} = 0.893 \qquad \epsilon_{\text{top1}} := \sqrt{\frac{235\text{MPa}}{f_{y\text{top1}}}} = 0.893$$

Part 3 - Bottom flange

$c_{\text{bottom1}} := \frac{b_{\text{bottom}} - t_{\text{web1}}}{2} = 0.587 \text{ m}$ Width of the bottom flange

$\text{bottomflange1} := \frac{c_{\text{bottom1}}}{t_{\text{bottom1}}} = 4.892$ c/t

$$\text{Class}_{\text{bottomflange1}} := \begin{cases} 1 & \text{if } \text{bottomflange1} \leq 9\epsilon_{\text{bottom1}} \\ 2 & \text{if } 9\epsilon_{\text{bottom1}} < \text{bottomflange1} \leq 10\epsilon_{\text{bottom1}} \\ 3 & \text{if } 10\epsilon_{\text{bottom1}} < \text{bottomflange1} \leq 14\epsilon_{\text{bottom1}} \\ 4 & \text{otherwise} \end{cases}$$

$\text{Class}_{\text{bottomflange1}} = 1$ Cross sectional class

$k_{\sigma\text{bottom1}} := 0.43$

$$\psi_{\text{bottom1}} := 1$$

$$\lambda_{\text{pbottom1}} := \frac{\text{bottomflange1}}{28.4 \epsilon_{\text{bottom1}} \sqrt{k_{\sigma \text{bottom1}}}} = 0.294$$

$$\rho_{\text{bottom11}} := \begin{cases} 1 & \text{if } \lambda_{\text{pbottom1}} \leq 0.748 \\ \frac{\lambda_{\text{pbottom1}} - 0.188}{\lambda_{\text{pbottom1}}^2} & \text{if } \lambda_{\text{pbottom1}} > 0.748 \end{cases}$$

$$\rho_{\text{bottom1}} := \min(\rho_{\text{bottom11}}, 1) = 1$$

$$b_{\text{bottom1eff}} := t_{\text{web1}} + 2\rho_{\text{bottom1}} \cdot c_{\text{bottom1}} = 1.2 \text{ m} \quad \text{Effective width}$$

The new cross sectional constants are calculated for one of the girders, given the symmetry.

$$A_{13\text{new}} := \begin{cases} b_{\text{bottom1eff}} \cdot t_{\text{bottom1}} & \text{if } \text{Class}_{\text{bottomflange1}} = 4 \\ A_{13} & \text{otherwise} \end{cases}$$

New distance of gravity center from bottom of the bridge

$$y_{\text{gc1new}} := \frac{A_{11} \cdot z_{11} + A_{12} \cdot z_{12} + A_{13\text{new}} \cdot z_{13} + A_{1\text{stop}} \cdot z_{1\text{stop}} + A_{1\text{sbottom}} \cdot z_{1\text{sbottom}}}{A_{11} + A_{12} + A_{13\text{new}} + A_{1\text{stop}} + A_{1\text{sbottom}}} = 1.419 \text{ m}$$

New moment of inertia

$$\begin{aligned} I_{\text{tot1new1}} := & \frac{b_{\text{top}} \cdot t_{\text{top1}}^3}{12} + A_{11} \cdot \left(h_{\text{tot}} - y_{\text{gc1new}} - \frac{t_{\text{top1}}}{2} \right)^2 \dots & = 5.754 \times 10^{11} \cdot \text{mm}^4 \\ & + \frac{t_{\text{web1}} \cdot h_{\text{web1}}^3}{12} + A_{12} \cdot \left(y_{\text{gc1new}} - \frac{h_{\text{web1}}}{2} - t_{\text{bottom1}} \right)^2 \dots \\ & + \frac{b_{\text{bottom}} \cdot t_{\text{bottom1}}^3}{12} + A_{13\text{new}} \cdot \left(y_{\text{gc1new}} - \frac{t_{\text{bottom1}}}{2} \right)^2 \dots \\ & + \frac{\pi \cdot (10\text{mm})^4}{4} \cdot 45 \dots \\ & + A_{1\text{stop}} \cdot (h_{\text{tot}} - y_{\text{gc1new}} + 109\text{mm} + h_{\text{deck}} - 73\text{mm})^2 \dots \\ & + \frac{\pi \cdot (8\text{mm})^4}{4} \cdot 45 + A_{1\text{sbottom}} \cdot (h_{\text{tot}} - y_{\text{gc1new}} + 109\text{mm} + 46\text{mm})^2 \end{aligned}$$

$$\begin{aligned}
I_{\text{tot1new2}} := & \frac{b_{\text{top1}} \cdot t_{\text{top1}}^3}{12} + A_{11} \cdot \left(h_{\text{tot}} - y_{\text{gc1new}} - \frac{t_{\text{top1}}}{2} \right)^2 \dots & = 5.754 \times 10^{11} \cdot \text{mm}^4 \\
& + \frac{t_{\text{web1}} \cdot h_{\text{web1}}^3}{12} + A_{12} \cdot \left(y_{\text{gc1new}} - \frac{h_{\text{web1}}}{2} - t_{\text{bottom1}} \right)^2 \dots \\
& + \frac{b_{\text{bottom1eff}} \cdot t_{\text{bottom1}}^3}{12} + A_{13\text{new}} \cdot \left(y_{\text{gc1new}} - \frac{t_{\text{bottom1}}}{2} \right)^2 \dots \\
& + \frac{\pi \cdot (10\text{mm})^4}{4} \cdot 45 \dots \\
& + A_{1\text{stop}} \cdot (h_{\text{tot}} - y_{\text{gc1new}} + 109\text{mm} + h_{\text{deck}} - 73\text{mm})^2 \dots \\
& + \frac{\pi \cdot (8\text{mm})^4}{4} \cdot 45 + A_{1\text{sbottom}} \cdot (h_{\text{tot}} - y_{\text{gc1new}} + 109\text{mm} + 46\text{mm})^2
\end{aligned}$$

$$I_{\text{tot1new}} := \begin{cases} I_{\text{tot1new1}} & \text{if } \text{Class}_{\text{bottomflange1}} \neq 4 \\ I_{\text{tot1new2}} & \text{if } \text{Class}_{\text{bottomflange1}} = 4 \end{cases} \quad I_{\text{tot1new}} = 0.575 \text{m}^4$$

A.3.4.3 Cross-sectional constants if web buckles

Part 2 - web

$$\sigma_t := \frac{-M_{\text{ULS1}}}{I_{\text{tot1new}}} \cdot (h_{\text{tot}} - y_{\text{gc1new}} - t_{\text{top1}}) = -211.677 \cdot \text{MPa} \quad \text{Compressive stress in web}$$

$$\sigma_c := \frac{M_{\text{ULS1}}}{I_{\text{tot1new}}} \cdot (y_{\text{gc1new}} - t_{\text{bottom1}}) = 217.898 \cdot \text{MPa} \quad \text{Tensile stress in web}$$

$$\varepsilon_{\text{web1}} := \sqrt{\frac{235\text{MPa}}{f_{y\text{web1}}}} = 0.825$$

$$\text{web1} := \frac{h_{\text{web1}} - (\text{weld} + \text{butt weld})}{t_{\text{web1}}} = 98.077 \quad \text{c/t}$$

$$\alpha_{\text{gc1}} := \frac{y_{\text{gc1new}} - t_{\text{bottom1}}}{h_{\text{web1}}} = 0.507 \quad \psi_{\text{gc1}} := \frac{\sigma_t}{\sigma_c} = -0.971$$

$$\text{Class}_{\text{web1a}} := \begin{cases} 1 & \text{if } \text{web1} \leq \frac{36\epsilon_{\text{web1}}}{\alpha_{\text{gc1}}} \\ 2 & \text{if } \frac{36\epsilon_{\text{web1}}}{\alpha_{\text{gc1}}} < \text{web1} \leq \frac{41.5\epsilon_{\text{web1}}}{\alpha_{\text{gc1}}} \\ 3 & \text{if } \frac{41.5\epsilon_{\text{web1}}}{\alpha_{\text{gc1}}} < \text{web1} \leq 62\epsilon_{\text{web1}} \cdot (1 - \psi_{\text{gc1}}) \cdot \sqrt{-\psi_{\text{gc1}}} \\ 4 & \text{otherwise} \end{cases}$$

$$\text{Class}_{\text{web1b}} := \begin{cases} 1 & \text{if } \text{web1} \leq \frac{396\epsilon_{\text{web1}}}{13\alpha_{\text{gc1}} - 1} \\ 2 & \text{if } \frac{396\epsilon_{\text{web1}}}{13\alpha_{\text{gc1}} - 1} < \text{web1} \leq \frac{456\epsilon_{\text{web1}}}{13\alpha_{\text{gc1}} - 1} \\ 3 & \text{if } \frac{456\epsilon_{\text{web1}}}{13\alpha_{\text{gc1}} - 1} < \text{web1} \leq \frac{42\epsilon_{\text{web1}}}{0.67 + 0.33 \cdot \psi_{\text{gc1}}} \\ 4 & \text{otherwise} \end{cases}$$

$$\text{Class}_{\text{web1}} := \begin{cases} \text{Class}_{\text{web1b}} & \text{if } \alpha_{\text{gc1}} > 0.5 \\ \text{Class}_{\text{web1a}} & \text{if } \alpha_{\text{gc1}} \leq 0.5 \end{cases} \quad \text{Class}_{\text{web1}} = 3 \quad \text{Cross-sectional class}$$

$$k_{\sigma\text{web1}} := \begin{cases} 7.81 - 6.29\psi_{\text{gc1}} + 9.78\psi_{\text{gc1}}^2 & \text{if } 0 > \psi_{\text{gc1}} > -1 \\ 23.9 & \text{if } \psi_{\text{gc1}} = -1 \\ 5.98 \cdot (1 - \psi_{\text{gc1}})^2 & \text{if } -1 > \psi_{\text{gc1}} > -3 \end{cases}$$

$$k_{\sigma\text{web1}} = 23.15$$

$$\lambda_{\text{pweb1}} := \frac{\text{web1}}{28.4\epsilon_{\text{web1}} \cdot \sqrt{k_{\sigma\text{web1}}}} = 0.87$$

$$\rho_{\text{web11}} := \begin{cases} 1 & \text{if } \lambda_{\text{pweb1}} \leq 0.673 \\ \frac{\lambda_{\text{pweb1}} - 0.055 \cdot (3 + \psi_{\text{gc1}})}{\lambda_{\text{pweb1}}^2} & \text{if } \lambda_{\text{pweb1}} > 0.673 \end{cases}$$

$$\rho_{\text{web1}} := \min(\rho_{\text{web11}}, 1) = 1$$

$$b_{\text{web1eff}} := \rho_{\text{web1}} \cdot (y_{\text{gc1new}} - t_{\text{bottom1}}) = 1.299 \times 10^3 \cdot \text{mm}$$

$$b_{web1a} := b_{web1eff} \cdot 0.4 = 519.415 \cdot \text{mm}$$

$$b_{web1b} := b_{web1eff} \cdot 0.6 = 779.122 \cdot \text{mm}$$

$$b_{web1gap} := y_{gc1new} - t_{bottom1} - b_{web1a} - b_{web1b} = 0 \cdot \text{mm}$$

The final cross sectional constants are calculated for one of the girders, given the symmetry.

$$A_{12a} := b_{web1a} \cdot t_{web1} = 0.014 \text{ m}^2$$

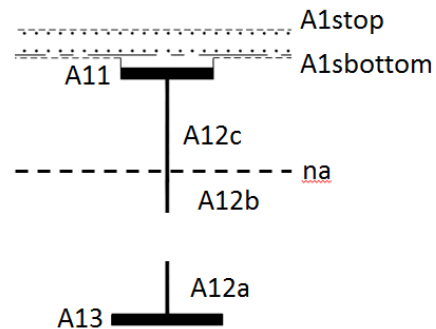
$$A_{12b} := b_{web1b} \cdot t_{web1} = 0.02 \text{ m}^2$$

$$A_{12c} := (h_{web1} - y_{gc1new} + t_{bottom1}) \cdot t_{web1} = 0.033 \text{ m}^2$$

$$A_{12anew} := \begin{cases} A_{12a} & \text{if } \text{Class}_{web1} = 4 \\ 0 & \text{otherwise} \end{cases}$$

$$A_{12bnew} := \begin{cases} A_{12b} & \text{if } \text{Class}_{web1} = 4 \\ 0 & \text{otherwise} \end{cases}$$

$$A_{12cnew} := \begin{cases} A_{12c} & \text{if } \text{Class}_{web1} = 4 \\ h_{web1} \cdot t_{web1} & \text{otherwise} \end{cases}$$



The final distance from bottom to gravity center

$$z_{12a} := t_{bottom1} + \frac{b_{web1a}}{2} = 0.38 \text{ m}$$

$$z_{12b} := t_{bottom1} + b_{web1a} + b_{web1gap} + \frac{b_{web1b}}{2} = 1.029 \text{ m}$$

$$z_{12c} := y_{gc1} + \frac{h_{web1} - y_{gc1new} + t_{bottom1}}{2} = 2.049 \text{ m}$$

$$z_{12anew} := \begin{cases} z_{12a} & \text{if } \text{Class}_{web1} = 4 \\ 0 & \text{otherwise} \end{cases}$$

$$z_{12bnew} := \begin{cases} z_{12b} & \text{if } \text{Class}_{web1} = 4 \\ 0 & \text{otherwise} \end{cases}$$

$$z_{12cnew} := \begin{cases} z_{12c} & \text{if } \text{Class}_{web1} = 4 \\ \frac{h_{web1}}{2} + t_{bottom1} & \text{otherwise} \end{cases}$$

Final distance of gravity center from bottom of the bridge

$$y_{gc1final} := \frac{A_{11} \cdot z_{11} + A_{12anew} \cdot z_{12anew} + A_{12bnew} \cdot z_{12bnew} + A_{12cnew} \cdot z_{12cnew} \dots + A_{13new} \cdot z_{13} + A_{1stop} \cdot z_{1stop} + A_{1sbottom} \cdot z_{1sbottom}}{A_{11} + A_{12anew} + A_{12bnew} + A_{12cnew} + A_{13new} + A_{1stop} + A_{1sbottom}} = 1.419 \text{ m}$$

Final moment of inertia

$$I_{tot1final1} := I_{tot1new1} = 5.754 \times 10^{11} \cdot \text{mm}^4$$

$$I_{tot1final2} := I_{tot1new2} = 5.754 \times 10^{11} \cdot \text{mm}^4$$

$$I_{tot1final3} := \frac{b_{top} \cdot t_{top1}^3}{12} + A_{11} \cdot \left(h_{tot} - y_{gc1final} - \frac{t_{top1}}{2} \right)^2 \dots = 5.754 \times 10^{11} \cdot \text{mm}^4$$

$$+ \frac{t_{web1} \cdot b_{web1a}^3}{12} + A_{12a} \cdot \left(\frac{b_{web1a}}{2} + b_{web1gap} + b_{web1b} \right)^2 \dots$$

$$+ \frac{t_{web1} \cdot b_{web1b}^3}{12} + A_{12b} \cdot \left(\frac{b_{web1b}}{2} \right)^2 \dots$$

$$+ \frac{t_{web1} \cdot (h_{web1} - b_{web1eff})^3}{12} + A_{12c} \cdot \left(\frac{h_{tot} - t_{top1} - y_{gc1final}}{2} \right)^2 \dots$$

$$+ \frac{b_{bottom} \cdot t_{bottom1}^3}{12} + A_{13new} \cdot \left(y_{gc1final} - \frac{t_{bottom1}}{2} \right)^2 \dots$$

$$+ \frac{\pi \cdot (10\text{mm})^4}{4} \cdot 45 \dots$$

$$+ A_{1stop} \cdot (h_{tot} - y_{gc1final} + 109\text{mm} + h_{deck} - 73\text{mm})^2 \dots$$

$$+ \frac{\pi \cdot (8\text{mm})^4}{4} \cdot 45 + A_{1sbottom} \cdot (h_{tot} - y_{gc1final} + 109\text{mm} + 46\text{mm})^2$$

$$\begin{aligned}
I_{\text{tot1final4}} := & \frac{b_{\text{top}} \cdot t_{\text{top1}}^3}{12} + A_{11} \cdot \left(h_{\text{tot}} - y_{\text{gc1final}} - \frac{t_{\text{top1}}}{2} \right)^2 \dots & = 5.754 \times 10^{11} \cdot \text{mm}^4 \\
& + \frac{t_{\text{web1}} \cdot b_{\text{web1a}}^3}{12} + A_{12a} \cdot \left(\frac{b_{\text{web1a}}}{2} + b_{\text{web1gap}} + b_{\text{web1b}} \right)^2 \dots \\
& + \frac{t_{\text{web1}} \cdot b_{\text{web1b}}^3}{12} + A_{12b} \cdot \left(\frac{b_{\text{web1b}}}{2} \right)^2 \dots \\
& + \frac{t_{\text{web1}} \cdot (h_{\text{web1}} - b_{\text{web1eff}})^3}{12} + A_{12c} \cdot \left(\frac{h_{\text{tot}} - t_{\text{top1}} - y_{\text{gc1final}}}{2} \right)^2 \dots \\
& + \frac{b_{\text{bottom1eff}} \cdot t_{\text{bottom1}}^3}{12} + A_{13\text{new}} \cdot \left(y_{\text{gc1final}} - \frac{t_{\text{bottom1}}}{2} \right)^2 \dots \\
& + \frac{\pi \cdot (10\text{mm})^4}{4} \cdot 45 \dots \\
& + A_{1\text{stop}} \cdot (h_{\text{tot}} - y_{\text{gc1final}} + 109\text{mm} + h_{\text{deck}} - 73\text{mm})^2 \dots \\
& + \frac{\pi \cdot (8\text{mm})^4}{4} \cdot 45 + A_{1\text{sbottom}} \cdot (h_{\text{tot}} - y_{\text{gc1final}} + 109\text{mm} + 46\text{mm})^2
\end{aligned}$$

$$I_{\text{tot1final}} := \begin{cases} I_{\text{tot1final1}} & \text{if } \begin{cases} \text{Class}_{\text{bottomflange1}} \neq 4 \\ \text{Class}_{\text{web1}} \neq 4 \end{cases} \\ I_{\text{tot1final2}} & \text{if } \begin{cases} \text{Class}_{\text{bottomflange1}} = 4 \\ \text{Class}_{\text{web1}} \neq 4 \end{cases} \\ I_{\text{tot1final3}} & \text{if } \begin{cases} \text{Class}_{\text{bottomflange1}} \neq 4 \\ \text{Class}_{\text{web1}} = 4 \end{cases} \\ I_{\text{tot1final4}} & \text{if } \begin{cases} \text{Class}_{\text{bottomflange1}} = 4 \\ \text{Class}_{\text{web1}} = 4 \end{cases} \end{cases}$$

$$I_{\text{tot1final}} = 5.754 \times 10^{11} \cdot \text{mm}^4$$

A.3.4.4 Bending verification in ULS

$$W_{\text{effc1}} := \frac{I_{\text{tot1final}}}{y_{\text{gc1final}}} = 4.057 \times 10^8 \cdot \text{mm}^3 \quad \text{Sectional modulus of compressed area}$$

$$W_{\text{efft1}} := \frac{I_{\text{tot1final}}}{(h_{\text{tot}} - y_{\text{gc1final}})} = 4.165 \times 10^8 \cdot \text{mm}^3 \quad \text{Sectional modulus of tensile area}$$

$$M_{Rdt1} := W_{efft1} \cdot \frac{f_{ytop1}}{1.0} = 122.88 \cdot \text{MN} \cdot \text{m}$$

Moment resistance in tension

$$M_{Rdc1} := W_{effc1} \cdot \frac{f_{ybottom1}}{1.0} = 119.668 \cdot \text{MN} \cdot \text{m}$$

Moment resistance in compression

$$M_{Rd1} := \min(M_{Rdt1}, M_{Rdc1}) = 119.668 \cdot \text{MN} \cdot \text{m}$$

Moment resistance of the weakest part

$$\mu_{11} := \frac{M_{ULS1}}{M_{Rd1}} = 0.807$$

Utilization factor in bending

A.3.5 Shear resistance in ULS: support

A.3.5.1 Web only

Control if shear buckling needs to be considered

$$\eta_1 := \begin{cases} 1.2 & \text{if } f_{yweb1} \leq 460 \text{ MPa} \\ 1.0 & \text{otherwise} \end{cases}$$

Factor due to material

$$a_{stiff} := 8 \text{ m}$$

Distance between vertical stiffeners

$$\kappa_{\tau 1} := \begin{cases} 5.34 + 4 \left(\frac{h_{web1}}{a_{stiff}} \right)^2 & \text{if } \frac{a_{stiff}}{h_{web1}} \geq 1 \\ 4 + 5.34 \left(\frac{h_{web1}}{a_{stiff}} \right)^2 & \text{if } \frac{a_{stiff}}{h_{web1}} < 1 \end{cases}$$

$$\kappa_{\tau 1} = 5.75$$

$$\text{Checkshear}_1 := \begin{cases} \text{"yes"} & \text{if } \frac{h_{web1}}{t_{web1}} > \left(\frac{31}{\eta_1} \cdot \epsilon_{web1} \cdot \sqrt{\kappa_{\tau 1}} \right) \\ \text{"no"} & \text{otherwise} \end{cases}$$

$$\text{Checkshear}_1 = \text{"yes"}$$

$$\tau_{cr1} := \kappa_{\tau 1} \cdot \frac{\pi^2 \cdot E_s \cdot t_{web1}^2}{12(1 - \nu^2) \cdot (h_{web1})^2} = 112.564 \cdot \text{MPa}$$

$$\lambda_{w1} := 0.76 \cdot \sqrt{\frac{f_{yweb1}}{\tau_{cr1}}} = 1.331$$

$$\chi_{w1} := \begin{cases} \eta_1 & \text{if } \lambda_{w1} < \frac{0.83}{\eta_1} \\ \frac{0.83}{\lambda_{w1}} & \text{if } \frac{0.83}{\eta_1} \leq \lambda_{w1} < 1.08 \\ \frac{1.37}{(0.7 + \lambda_{w1})} & \text{otherwise} \end{cases}$$

$$\chi_{w1} = 0.675$$

Shear force capacity considering web only

$$V_{bwRd1} := \chi_{w1} \cdot \frac{f_{yweb1} \cdot (h_{web1}) \cdot t_{web1}}{\sqrt{3} \cdot \gamma_{M1}} = 8.132 \cdot \text{MN}$$

$$\mu_{12} := \frac{V_{ULS1}}{V_{bwRd1}} = 0.94 \quad \text{Utilization factor of the web only in shear}$$

A.3.5.2 Contribution from the flanges

Since the contribution is based on the flange which provides the least resistance, we need to check the capacities of each one.

$$R_{bottom1} := t_{bottom1} \cdot b_{bottom1} \cdot f_{ybottom1} = 42.48 \cdot \text{MN} \quad \text{Resistance of top flange}$$

$$R_{top1} := t_{top1} \cdot b_{top1} \cdot f_{ytop1} = 35.4 \cdot \text{MN} \quad \text{Resistance of bottom flange}$$

Geometrical limitations of the flanges

$$b_{fmaxbottom1} := 15 \cdot t_{bottom1} \cdot \epsilon_{bottom1} = 1.607 \text{ m}$$

$$b_{fbottom1} := \min\left(b_{fmaxbottom1}, \frac{b_{bottom1}}{2}\right) = 0.6 \text{ m}$$

$$b_{fmaxtop1} := 15 \cdot t_{top1} \cdot \epsilon_{top1} = 1.607 \text{ m}$$

$$b_{ftop1} := \min\left(b_{fmaxtop1}, \frac{b_{top1}}{2}\right) = 0.5 \text{ m}$$

The contribution from the flanges can be taken into account only if they are not fully utilized in bending. So it needs to be checked that their utilization is below 1.

$$b_{bottomshear1} := 2 \cdot b_{fbottom1} = 1.2 \text{ m} \quad b_{topshear1} := 2 \cdot b_{ftop1} = 1 \text{ m}$$

$$M_{fRd1} := \frac{(f_{ytop1} \cdot 2 \cdot b_{ftop1} \cdot t_{top1}) \cdot \left(h_{tot} - \frac{t_{top1}}{2} - y_{gc1final}\right)}{\gamma_{M0}} \dots = 104.49 \cdot \text{MN} \cdot \text{m}$$

$$+ \frac{f_{ybottom1} \cdot 2 \cdot b_{fbottom1} \cdot t_{bottom1} \cdot \left(y_{gc1final} - \frac{t_{bottom1}}{2}\right)}{\gamma_{M0}}$$

$$\mu_{13} := \frac{M_{ULS1}}{M_{fRd1}} = 0.924 \quad \text{Utilization factor of the flanges only in bending}$$

Shear capacity contribution from the flanges

$$b_{f1} := \begin{cases} b_{bottomshear1} & \text{if } R_{bottom1} < R_{top1} \\ b_{topshear1} & \text{otherwise} \end{cases}$$

$$t_{f1} := \begin{cases} t_{bottom1} & \text{if } R_{bottom1} < R_{top1} \\ t_{top1} & \text{otherwise} \end{cases}$$

$$f_{yf1} := \begin{cases} f_{ybottom1} & \text{if } R_{bottom1} < R_{top1} \\ f_{ytop1} & \text{otherwise} \end{cases}$$

$$c_{c1} := a_{stiff} \cdot \left[0.25 + \frac{1.6b_{f1} \cdot t_{f1}^2 \cdot f_{yf1}}{t_{web1} \cdot (h_{web1})^2 \cdot f_{yweb1}} \right] = 2.925 \text{ m}$$

$$V_{bfRd1} := \frac{b_{f1} \cdot t_{f1}^2 \cdot f_{yf1}}{c_{c1} \cdot \gamma_{M1}} \cdot \left[1 - \left(\frac{M_{ULS1}}{M_{fRd1}} \right)^2 \right] = 0.193 \cdot \text{MN}$$

A.3.5.3 Total shear capacity

$$V_{bRd1} := \begin{cases} (V_{bwRd1} + V_{bfRd1}) & \text{if } \mu_{13} < 1 \\ V_{bwRd1} & \text{otherwise} \end{cases} \quad \text{Shear capacity of web and flanges (if not fully utilized in bending)}$$

$$V_{bRd1} = 8.325 \cdot \text{MN}$$

$$\mu_{14} := \frac{V_{ULS1}}{V_{bRd1}} = 0.918 \quad \text{Utilization factor in shear}$$

A.3.6 Bending resistance in ULS: span

A.3.6.1 Cross-sectional constants for the span

The cross sectional constants are calculated for one of the girders, given the symmetry. The concrete deck is taken into account through an equivalent cross section and the layers of reinforcement.

$$A_{21} := t_{\text{top}2} \cdot b_{\text{top}} = 0.04 \text{ m}^2$$

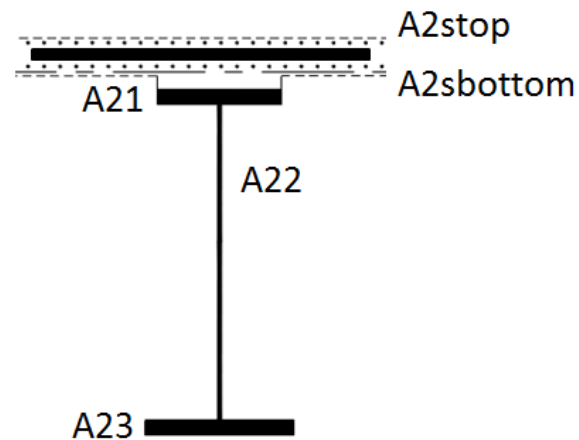
$$A_{22} := h_{\text{web}2} \cdot t_{\text{web}2} = 0.049 \text{ m}^2$$

$$A_{23} := b_{\text{bottom}2} \cdot t_{\text{bottom}2} = 0.048 \text{ m}^2$$

$$A_{2c} := \frac{b_{\text{deck}} \cdot h_{\text{deck}}}{n} = 0.299 \text{ m}^2$$

$$A_{2\text{stop}} := 45 \cdot \pi \cdot (10\text{mm})^2 = 0.014 \text{ m}^2$$

$$A_{2\text{sbottom}} := 45 \cdot \pi \cdot (8\text{mm})^2 = 9.048 \times 10^{-3} \text{ m}^2$$



Distance of each part from bottom to gravity center

$$z_{21} := t_{\text{bottom}2} + h_{\text{web}2} + \frac{t_{\text{top}2}}{2} = 2.78 \text{ m}$$

$$z_{22} := t_{\text{bottom}2} + \frac{h_{\text{web}2}}{2} = 1.4 \text{ m}$$

$$z_{23} := \frac{t_{\text{bottom}2}}{2} = 0.02 \text{ m}$$

$$z_{2c} := h_{\text{tot}} + 109\text{mm} + \frac{h_{\text{deck}}}{2} = 3.063 \text{ m}$$

$$z_{2\text{stop}} := h_{\text{tot}} + h_{\text{deck}} + 109\text{mm} - 73\text{mm} = 3.144 \text{ m}$$

$$z_{2\text{sbottom}} := h_{\text{tot}} + 109\text{mm} + 46\text{mm} = 2.955 \text{ m}$$

Gravity of center from bottom of the bridge

$$y_{gc2final} := \frac{A_{21} \cdot z_{21} + A_{22} \cdot z_{22} + A_{23} \cdot z_{23} + A_{2c} \cdot z_{2c} \dots + A_{2stop} \cdot z_{2stop} + A_{2sbottom} \cdot z_{2sbottom}}{A_{21} + A_{22} + A_{23} + A_{2c} + A_{2stop} + A_{2sbottom}} = 2.543 \text{ m}$$

Distance from local and global gravity center

$$a_{21} := y_{gc2final} - z_{21} = -0.237 \text{ m}$$

$$a_{22} := y_{gc2final} - z_{22} = 1.143 \text{ m}$$

$$a_{23} := y_{gc2final} - z_{23} = 2.523 \text{ m}$$

$$a_{2c} := y_{gc2final} - z_{2c} = -0.52 \text{ m}$$

Moment of inertia

$$I_{tot2final} := \frac{b_{top} \cdot t_{top2}^3}{12} + A_{21} \cdot a_{21}^2 \dots = 0.489 \cdot \text{m}^4$$

$$+ \frac{t_{web2} \cdot h_{web2}^3}{12} + A_{22} \cdot a_{22}^2 \dots$$

$$+ \frac{b_{bottom} \cdot t_{bottom2}^3}{12} + A_{23} \cdot a_{23}^2 \dots$$

$$+ \frac{b_{deck} \cdot \left(\frac{h_{deck}}{n}\right)^3}{12} + A_{2c} \cdot a_{2c}^2 \dots$$

$$+ \frac{\pi \cdot (10\text{mm})^4}{4} \cdot 45 \dots$$

$$+ A_{2stop} \cdot (h_{tot} - y_{gc2final} + h_{deck} - 73\text{mm} + 109\text{mm})^2 \dots$$

$$+ \frac{\pi \cdot (8\text{mm})^4}{4} \cdot 45 + A_{2sbottom} \cdot (h_{tot} - y_{gc2final} + 46\text{mm} + 109\text{mm})^2$$

In this case, no parts of the steel section can buckle:

top flange: it is restrained by the concrete deck (see EN 1994 section 6.6.5.5)

web: the part of the web in compression is always minimal. For this reason a reduction will not be needed. Anyway, the moment of inertia is barely affected.

A.3.6.2 Bending verification in ULS

$$\sigma_{c2} := \frac{M_{\text{ULS}2}}{I_{\text{tot}2\text{final}}} \cdot (h_{\text{tot}} - y_{\text{gc}2\text{final}}) = 29.565 \cdot \text{MPa}$$

Maximum compressive stress

$$\sigma_{t2} := \frac{M_{\text{ULS}2}}{I_{\text{tot}2\text{final}}} \cdot (-y_{\text{gc}2\text{final}}) = -292.238 \cdot \text{MPa}$$

Maximum tensile stress

$$W_{\text{eff}2} := \frac{I_{\text{tot}2\text{final}}}{y_{\text{gc}2\text{final}}} = 1.924 \times 10^8 \cdot \text{mm}^3$$

Sectional modulus of tensile area

$$M_{\text{Rd}2} := W_{\text{eff}2} \cdot \frac{f_{y\text{bottom}2}}{1.0} = 66.394 \cdot \text{MN} \cdot \text{m}$$

Moment resistance in tension

$$\mu_{21} := \frac{M_{\text{ULS}2}}{M_{\text{Rd}2}} = 0.847$$

Utilization ratio in bending

A.3.7 Shear resistance in ULS: span

A.3.7.1 Web only

Control if shear buckling needs to be considered

$$\eta_2 := \begin{cases} 1.2 & \text{if } f_{yweb2} \leq 460 \text{MPa} \\ 1.0 & \text{otherwise} \end{cases} \quad \text{Factor due to material}$$

$$\kappa_{\tau 2} := \begin{cases} 5.34 + 4 \left(\frac{h_{web2}}{a_{stiff}} \right)^2 & \text{if } \frac{a_{stiff}}{h_{web2}} \geq 1 \\ 4 + 5.34 \left(\frac{h_{web2}}{a_{stiff}} \right)^2 & \text{if } \frac{a_{stiff}}{h_{web2}} < 1 \end{cases}$$

$$\kappa_{\tau 2} = 5.802$$

$$\varepsilon_{web2} := \sqrt{\frac{235 \text{MPa}}{f_{yweb2}}} = 0.825$$

$$\text{Checkshear}_2 := \begin{cases} \text{"yes"} & \text{if } \frac{h_{web2}}{t_{web2}} > \left(\frac{31}{\eta_2} \cdot \varepsilon_{web2} \cdot \sqrt{\kappa_{\tau 2}} \right) \\ \text{"no"} & \text{otherwise} \end{cases}$$

$$\text{Checkshear}_2 = \text{"yes"}$$

$$\tau_{cr2} := \kappa_{\tau 2} \cdot \frac{\pi^2 \cdot E_s \cdot t_{web2}^2}{12(1 - \nu^2) \cdot (h_{web2})^2} = 48.229 \cdot \text{MPa}$$

$$\lambda_{w2} := 0.76 \cdot \sqrt{\frac{f_{yweb2}}{\tau_{cr2}}} = 2.033$$

$$\chi_{w2} := \begin{cases} \eta_2 & \text{if } \lambda_{w2} < \frac{0.83}{\eta_2} \\ \frac{0.83}{\lambda_{w2}} & \text{if } \frac{0.83}{\eta_2} \leq \lambda_{w2} < 1.08 \\ \frac{1.37}{(0.7 + \lambda_{w2})} & \text{otherwise} \end{cases}$$

$$\chi_{w2} = 0.501$$

Shear force capacity considering web only

$$V_{bwRd2} := \chi_{w2} \cdot \frac{f_{yweb2} \cdot (h_{web2}) \cdot t_{web2}}{\sqrt{3} \cdot \gamma_{M1}} = 4.445 \cdot \text{MN}$$

$$\mu_{22} := \frac{V_{ULS2}}{V_{bwRd2}} = 0.927 \quad \text{Utilization factor of the web only in shear}$$

A.3.7.2 Contribution from the flanges

Since the top flange is restrained by the concrete, the bottom flange will provide the least resistance

$$R_{bottom2} := t_{bottom2} \cdot b_{bottom2} \cdot f_{ybottom2} = 16.56 \cdot \text{MN} \quad \text{Resistance of bottom flange}$$

Geometrical limitations of the flanges

$$\epsilon_{bottom2} := \sqrt{\frac{235 \text{MPa}}{f_{ybottom2}}} = 0.825$$

$$b_{fmaxbottom2} := 15 \cdot t_{bottom2} \cdot \epsilon_{bottom2} = 0.495 \text{ m}$$

$$b_{fbottom2} := \min\left(b_{fmaxbottom2}, \frac{b_{bottom2}}{2}\right) = 0.495 \text{ m}$$

$$b_{bottomshear2} := 2 \cdot b_{fbottom2} = 0.99 \text{ m}$$

$$M_{fRd2} := \frac{(f_{ytop2} \cdot b_{top2} \cdot t_{top2}) \cdot \left(h_{tot} - \frac{t_{top2}}{2} - y_{gc2final}\right)}{\gamma_{M0}} \dots = 37.753 \cdot \text{MN} \cdot \text{m}$$

$$+ \frac{f_{ybottom2} \cdot b_{bottomshear2} \cdot t_{bottom2} \cdot \left(y_{gc2final} - \frac{t_{bottom2}}{2}\right)}{\gamma_{M0}}$$

$$\mu_{23} := \frac{M_{ULS2}}{M_{fRd2}} = 1.49 \quad \text{Utilization factor of the flanges only in bending}$$

Shear capacity contribution from the flanges

$$c_{c2} := a_{\text{stiff}} \cdot \left[0.25 + \frac{1.6 b_{\text{fbottom2}} \cdot t_{\text{bottom2}}^2 \cdot f_{y\text{bottom2}}}{t_{\text{web2}} \cdot (h_{\text{web2}})^2 \cdot f_{y\text{web2}}} \right] = 2.076 \text{ m}$$

$$V_{\text{bfRd2}} := \frac{b_{\text{fbottom2}} \cdot t_{\text{bottom2}}^2 \cdot f_{y\text{bottom2}}}{c_{c2} \cdot \gamma_{\text{M1}}} \cdot \left[1 - \left(\frac{M_{\text{ULS2}}}{M_{\text{fRd2}}} \right)^2 \right] = -0.146 \cdot \text{MN}$$

A.3.7.3 Total shear capacity

$$V_{\text{bRd2}} := \begin{cases} (V_{\text{bwRd2}} + V_{\text{bfRd2}}) & \text{if } \mu_{23} < 1 \\ V_{\text{bwRd2}} & \text{otherwise} \end{cases} \quad \begin{array}{l} \text{Shear capacity of web and flanges (if not fully} \\ \text{utilized in bending)} \end{array}$$

$$V_{\text{bRd2}} = 4.445 \cdot \text{MN}$$

$$\mu_{24} := \frac{V_{\text{ULS2}}}{V_{\text{bRd2}}} = 0.927 \quad \text{Utilization factor in shear}$$

A.3.8 Check for deflection in SLS

A.3.8.1 Deflection in the side span

Side span: the axel loads are located in the center of the span while the distributed loads create a maximum deflection offcentered from the middle. Anyway this displacement can be neglected and the deflection is calculated in the center of the span.

The actions deriving from the axel loads in the middle of the span are as follows:

$$F := R_{1c} \cdot 0.75 = 306.975 \cdot \text{kN}$$

$$M_1 := 7.35 \text{MN} \cdot \text{m} \quad M_2 := 3.22 \text{MN} \cdot \text{m}$$

$$EI_{\text{span}} := E_s \cdot I_{\text{tot2final}} = 1.028 \times 10^{11} \frac{\text{m}^3 \cdot \text{kg}}{\text{s}^2}$$

$$l_0 := 29 \text{m} \cdot \frac{M_1}{M_1 + M_2} = 20.166 \text{m}$$

$$EI_{\text{support}} := E_s \cdot I_{\text{tot1final}} = 1.208 \times 10^{11} \frac{\text{m}^3 \cdot \text{kg}}{\text{s}^2}$$

$$\Theta_{B1\text{conc}} := \frac{\frac{1}{2} \cdot \frac{M_1}{EI_{\text{span}}} \cdot 29 \text{m} \cdot \frac{2 \cdot 29 \text{m}}{3} + \frac{M_1}{EI_{\text{span}}} \cdot 2 \text{m} \cdot 30 \text{m} \dots}{L_a} + \frac{1}{2} \cdot \frac{M_1}{EI_{\text{span}}} \cdot l_0 \cdot \left(31 \text{m} + \frac{l_0}{3} \right) \dots + \frac{1}{2} \cdot \frac{M_2}{EI_{\text{support}}} \cdot (29 \text{m} - l_0) \cdot \left(60 \text{m} - \frac{29 \text{m} - l_0}{3} \right) = 7.472 \times 10^{-4}$$

The actions deriving from the distributed traffic load are as follows:

$$q := R_{1d} \cdot 0.75 = 20.025 \cdot \frac{\text{kN}}{\text{m}}$$

$$M_1 := 4.65 \text{MN} \cdot \text{m} \quad M_2 := 10.11 \text{MN} \cdot \text{m} \quad R_A := 431 \text{kN}$$

$$l_0 := \frac{2 \cdot R_A}{q} = 43.046 \text{m}$$

$$l_b := L_a - l_0 = 16.954 \text{ m}$$

$$z_c := l_b \cdot \frac{\frac{l_0}{3} + \frac{l_b}{4}}{\frac{l_0}{2} + \frac{l_b}{3}} = 11.596 \text{ m}$$

$$\Theta_{B1dist} := \frac{\frac{2}{3} \cdot \frac{M_1}{EI_{span}} \cdot l_0 \cdot \frac{l_0}{2} + \frac{q}{2EI_{support}} \cdot \left(l_0 \cdot \frac{l_b^2}{2} + \frac{l_b^3}{3} \right) (l_0 + z_c)}{L_a} = 1.055 \times 10^{-3}$$

The actions deriving from the distributed selfweight in the middle of the span are as follows, regardless of the variation due to the dimensions of the girders. Such variation is small and can be neglected.

$$M_1 := 8.75 \text{ MN} \cdot \text{m} \quad M_2 := 19 \text{ MN} \cdot \text{m} \quad R_A := 811 \text{ kN}$$

$$l_0 := \frac{2 \cdot R_A}{UDL_{SLS}} = 43.132 \text{ m}$$

$$l_b := L_a - l_0 = 16.868 \text{ m}$$

$$z_c := l_b \cdot \frac{\frac{l_0}{3} + \frac{l_b}{4}}{\frac{l_0}{2} + \frac{l_b}{3}} = 11.536 \text{ m}$$

$$\Theta_{B1self} := \frac{\frac{2}{3} \cdot \frac{M_1}{EI_{span}} \cdot l_0 \cdot \frac{l_0}{2} + \frac{UDL_{SLS}}{2EI_{support}} \cdot \left(l_0 \cdot \frac{l_b^2}{2} + \frac{l_b^3}{3} \right) (l_0 + z_c)}{L_a} = 1.977 \times 10^{-3}$$

This way the total deflection can be calculated by considering the three contributions to the support rotation and multiplying for half the side span.

$$\delta_{span1} := \Theta_{B1conc} \cdot (30\text{m}) + \Theta_{B1dist} \cdot (30\text{m}) + \Theta_{B1self} \cdot (30\text{m}) = 113.375 \cdot \text{mm} \quad \text{Total deflection}$$

$$\mu_{5s} := \frac{\delta_{span1}}{\frac{L_a}{400}} = 0.756 \quad \text{Utilization factor in deflection}$$

A.3.8.2 Deflection in the middle span

Center span: the maximum deflection is obtained when the axel loads are in the middle of the span. In addition the distributed loads coming from the traffic and selfweight are added.

The actions deriving from the axel loads in the middle of the span are as follows:

$$F := R_{1c} \cdot 0.75 = 306.975 \cdot \text{kN}$$

$$M_1 := 4.09 \text{MN} \cdot \text{m} \quad M_2 := 7.88 \text{MN} \cdot \text{m}$$

$$l_0 := 39 \text{m} \cdot \frac{M_2}{M_1 + M_2} \cdot 2 + 2 \text{m} = 53.348 \text{m}$$

$$l_b := \frac{L_b - l_0}{2} = 13.326 \text{m}$$

$$\Theta_{B2\text{conc}} := \frac{1}{2} \cdot \frac{M_2}{EI_{\text{span}}} \cdot \frac{l_0}{2} + \frac{M_2}{EI_{\text{span}}} \cdot 1 \text{m} - \frac{1}{2} \cdot \frac{M_1}{EI_{\text{support}}} \cdot l_b = 8.739 \times 10^{-4}$$

The actions deriving from the distributed traffic load in the middle of the span are as follows

$$q := R_{1d} \cdot 0.75 = 20.025 \cdot \frac{\text{kN}}{\text{m}}$$

$$M_1 := 10.11 \text{MN} \cdot \text{m} \quad M_2 := 5.89 \text{MN} \cdot \text{m}$$

$$l_0 := \sqrt{\frac{8 \cdot M_2}{q}} = 48.508 \text{m}$$

$$l_b := \frac{L_b - l_0}{2} = 15.746 \text{m}$$

$$\Theta_{B2\text{dist}} := \frac{2}{3} \cdot \frac{M_1}{EI_{\text{span}}} \cdot \frac{l_0}{2} - \frac{q}{2EI_{\text{support}}} \cdot \left(l_0 \cdot \frac{l_b^2}{2} + \frac{l_b^3}{3} \right) = 9.847 \times 10^{-4}$$

The actions deriving from the distributed selfweight in the middle of the span are as follows, regardless of the variation due to the dimensions of the girders. Such variation is small and can be neglected.

$$M_1 := 19\text{MN}\cdot\text{m} \quad M_2 := 11.07\text{MN}\cdot\text{m}$$

$$l_0 := \sqrt{\frac{8 \cdot M_2}{\text{UDL}_{\text{SLS}}}} = 48.528 \text{ m}$$

$$l_b := \frac{L_b - l_0}{2} = 15.736 \text{ m}$$

$$\Theta_{\text{B2self}} := \frac{2}{3} \cdot \frac{M_1}{EI_{\text{span}}} \cdot \frac{l_0}{2} - \frac{\text{UDL}_{\text{SLS}}}{2EI_{\text{support}}} \cdot \left(l_0 \cdot \frac{l_b^2}{2} + \frac{l_b^3}{3} \right) = 1.854 \times 10^{-3}$$

This way the total deflection can be calculated by considering the three contributions to the support rotation and multiplying for half the center span.

$$\delta_{\text{span2}} := \Theta_{\text{B2conc}} \cdot (40\text{m}) + \Theta_{\text{B2dist}} \cdot (40\text{m}) + \Theta_{\text{B2self}} \cdot (40\text{m}) = 148.498 \cdot \text{mm}$$

$$\mu_{5c} := \frac{\delta_{\text{span2}}}{\frac{L_b}{400}} = 0.742$$

Utilization factor in deflection

So the SLS limitation will be given by the most affected span:

$$\mu_5 := \max(\mu_{5c}, \mu_{5s}) = 0.756$$

A.3.9 Web breathing

According to Eurocode, we make sure that the limits for web breathing are met

$$\text{Webbreathing} := \begin{cases} \text{"OK"} & \text{if } \frac{h_{\text{web1}} + t_{\text{bottom1}} - y_{\text{gc1final}}}{t_{\text{web1}}} \leq 30 + 4 \cdot \frac{L_b}{m} \\ \text{"NOT OK"} & \text{otherwise} \end{cases}$$

A.3.10 Buckling bottom flange during casting: support

We here consider that the bottom flange could buckle during casting since it will not be restrained by the concrete deck. We assume a load combination with only the weight of the concrete acting and we recalculated the properties of the cross section.

Gravity center from bottom of the bridge

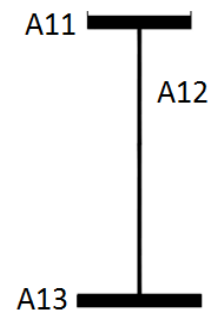
$$y_{gc1LT} := \frac{A_{11} \cdot z_{11} + A_{12} \cdot z_{12} + A_{13} \cdot z_{13}}{A_{11} + A_{12} + A_{13}} = 1.303 \text{ m}$$

Distance from local and global gravity center

$$a_{11LT} := y_{gc1LT} - z_{11} = -1.437 \text{ m}$$

$$a_{12LT} := y_{gc1LT} - z_{12} = -0.097 \text{ m}$$

$$a_{13LT} := y_{gc1LT} - z_{13} = 1.243 \text{ m}$$



Moment of inertia

$$I_{tot1LT} := \frac{b_{top1} \cdot t_{top1}^3}{12} + A_{11} \cdot a_{11LT}^2 + \frac{t_{web1} \cdot h_{web1}^3}{12} \dots = 5.076 \times 10^{11} \cdot \text{mm}^4$$

$$+ A_{12} \cdot a_{12LT}^2 + \frac{b_{bottom1} \cdot t_{bottom1}^3}{12} + A_{13} \cdot a_{13LT}^2$$

A.3.10.1 Cross-sectional constants if top flange buckles

$$c_{bottomLT} := \frac{b_{bottom1} - t_{web1}}{2} = 0.587 \text{ m}$$

Width of the top flange

$$\text{bottomflangeLT} := \frac{c_{bottomLT}}{t_{bottom1}} = 4.892$$

c/t

$$\text{Class}_{\text{bottomflangeLT}} := \begin{cases} 1 & \text{if } \text{bottomflangeLT} \leq 9\epsilon_{\text{top1}} \\ 2 & \text{if } 9\epsilon_{\text{top1}} < \text{bottomflangeLT} \leq 10\epsilon_{\text{top1}} \\ 3 & \text{if } 10\epsilon_{\text{top1}} < \text{bottomflangeLT} \leq 14\epsilon_{\text{top1}} \\ 4 & \text{otherwise} \end{cases}$$

$$\text{Class}_{\text{bottomflangeLT}} = 1$$

Cross sectional class

$$k_{\sigma\text{bottomLT}} := 0.43$$

$$\psi_{\text{bottomLT}} := 1$$

$$\lambda_{\text{pbottomLT}} := \frac{\text{bottomflangeLT}}{28.4\epsilon_{\text{bottom1}}\sqrt{k_{\sigma\text{bottomLT}}}} = 0.294$$

$$\rho_{\text{bottom1LT}} := \begin{cases} 1 & \text{if } \lambda_{\text{pbottomLT}} \leq 0.748 \\ \frac{\lambda_{\text{pbottomLT}} - 0.188}{\lambda_{\text{pbottomLT}}^2} & \text{if } \lambda_{\text{pbottomLT}} > 0.748 \end{cases}$$

$$\rho_{\text{bottomLT}} := \min(\rho_{\text{bottom1LT}}, 1) = 1$$

$$b_{\text{bottomLTeff}} := 2\rho_{\text{bottomLT}}c_{\text{bottomLT}} + t_{\text{web1}} = 1.2 \text{ m}$$

Effective width

The new cross sectional constants are calculated for one of the girders, given the symmetry.

$$A_{13\text{LT}} := \begin{cases} b_{\text{bottomLTeff}} \cdot t_{\text{top1}} & \text{if } \text{Class}_{\text{bottomflangeLT}} = 4 \\ A_{13} & \text{otherwise} \end{cases}$$

New distance of gravity center from bottom of the bridge

$$y_{\text{gc1newLT}} := \frac{A_{11} \cdot z_{11} + A_{12} \cdot z_{12} + A_{13\text{LT}} \cdot z_{13}}{A_{11} + A_{12} + A_{13\text{LT}}} = 1.303 \text{ m}$$

New distance from local and global gravity center

$$a_{11\text{newLT}} := y_{\text{gc1newLT}} - z_{11} = -1.437 \text{ m}$$

$$a_{12\text{newLT}} := y_{\text{gc1newLT}} - z_{12} = -0.097 \text{ m}$$

$$a_{13\text{newLT}} := y_{\text{gc1newLT}} - z_{13} = 1.243 \text{ m}$$

New moment of inertia

$$I_{\text{tot1newLT1}} := \frac{b_{\text{top}} \cdot t_{\text{top1}}^3}{12} + A_{11} \cdot a_{11\text{newLT}}^2 + \frac{t_{\text{web1}} \cdot h_{\text{web1}}^3}{12} \dots = 0.50757701 \cdot \text{m}^4$$

$$+ A_{12} \cdot a_{12\text{newLT}}^2 + \frac{b_{\text{bottomLTeff}} \cdot t_{\text{bottom1}}^3}{12} + A_{13\text{LT}} \cdot a_{13\text{newLT}}^2$$

$$I_{\text{tot1newLT2}} := I_{\text{tot1LT}} = 0.50757701 \text{ m}^4$$

$$I_{\text{tot1newLT}} := \begin{cases} I_{\text{tot1newLT1}} & \text{if } \text{Class}_{\text{bottomflangeLT}} = 4 \\ I_{\text{tot1newLT2}} & \text{if } \text{Class}_{\text{bottomflangeLT}} \neq 4 \end{cases}$$

$$I_{\text{tot1newLT}} = 0.508 \text{ m}^4$$

A.3.10.2 Cross-sectional constants if web buckles

$$\sigma_{\text{c1LTw}} := \frac{M_{\text{ULSLT1}}}{I_{\text{tot1newLT}}} \cdot (y_{\text{gc1newLT}}) = 79.152 \cdot \text{MPa} \quad \text{Compressive stress in the web}$$

$$\sigma_{\text{t1LTw}} := \frac{-M_{\text{ULSLT1}}}{I_{\text{tot1newLT}}} \cdot (h_{\text{tot}} - y_{\text{gc1newLT}}) = -90.974 \cdot \text{MPa} \quad \text{Tensile stress in the web}$$

$$\text{web1LT} := \frac{h_{\text{web1}} - (\text{weld} + \text{butt weld})}{t_{\text{web1}}} = 98.077 \quad \text{c/t}$$

$$\alpha_{\text{gc1LT}} := \frac{y_{\text{gc1newLT}} - t_{\text{bottom1}}}{h_{\text{web1}}} = 0.462 \quad \psi_{\text{gc1LT}} := \frac{\sigma_{\text{t1LTw}}}{\sigma_{\text{c1LTw}}} = -1.149$$

$$\text{Class}_{\text{web1LT1}} := \begin{cases} 1 & \text{if } \text{web1LT} \leq \frac{36\epsilon_{\text{web1}}}{\alpha_{\text{gc1LT}}} \\ 2 & \text{if } \frac{36\epsilon_{\text{web1}}}{\alpha_{\text{gc1LT}}} < \text{web1LT} \leq \frac{41.5\epsilon_{\text{web1}}}{\alpha_{\text{gc1LT}}} \\ 3 & \text{if } \frac{41.5\epsilon_{\text{web1}}}{\alpha_{\text{gc1LT}}} < \text{web1LT} \leq 62\epsilon_{\text{web1}} \cdot (1 - \psi_{\text{gc1LT}}) \cdot \sqrt{-\psi_{\text{gc1LT}}} \\ 4 & \text{otherwise} \end{cases}$$

$$\text{Class}_{\text{web1LT2}} := \begin{cases} 1 & \text{if } \text{web1LT} \leq \frac{396\epsilon_{\text{web1}}}{13\alpha_{\text{gc1LT}} - 1} \\ 2 & \text{if } \frac{396\epsilon_{\text{web1}}}{13\alpha_{\text{gc1LT}} - 1} < \text{web1LT} \leq \frac{456\epsilon_{\text{web1}}}{13\alpha_{\text{gc1LT}} - 1} \\ 3 & \text{if } \frac{456\epsilon_{\text{web1}}}{13\alpha_{\text{gc1LT}} - 1} < \text{web1LT} \leq \frac{42\epsilon_{\text{web1}}}{0.67 + 0.33 \cdot \psi_{\text{gc1LT}}} \\ 4 & \text{otherwise} \end{cases}$$

$$\text{Class}_{\text{web1LT}} := \begin{cases} \text{Class}_{\text{web1LT2}} & \text{if } \alpha_{\text{gc1LT}} > 0.5 \\ \text{Class}_{\text{web1LT1}} & \text{if } \alpha_{\text{gc1LT}} \leq 0.5 \end{cases}$$

$$\text{Class}_{\text{web1LT}} = 3$$

Cross sectional class

$$k_{\sigma\text{web1LT}} := \begin{cases} 7.81 - 6.29\psi_{\text{gc1LT}} + 9.78\psi_{\text{gc1LT}}^2 & \text{if } 0 > \psi_{\text{gc1LT}} > -1 \\ 23.9 & \text{if } \psi_{\text{gc1LT}} = -1 \\ 5.98 \cdot (1 - \psi_{\text{gc1LT}})^2 & \text{if } -1 > \psi_{\text{gc1LT}} > -3 \end{cases}$$

$$k_{\sigma\text{web1LT}} = 27.626$$

$$\lambda_{\text{pweb1LT}} := \frac{\text{web1LT}}{28.4\epsilon_{\text{web1}} \cdot \sqrt{k_{\sigma\text{web1LT}}}} = 0.796$$

$$\rho_{\text{web1LT1}} := \begin{cases} 1 & \text{if } \lambda_{\text{pweb1LT}} \leq 0.673 \\ \frac{\lambda_{\text{pweb1LT}} - 0.055 \cdot (3 + \psi_{\text{gc1LT}})}{\lambda_{\text{pweb1LT}}^2} & \text{if } \lambda_{\text{pweb1LT}} > 0.673 \end{cases}$$

$$\rho_{\text{web1LT}} := \min(\rho_{\text{web1LT1}}, 1) = 1$$

$$b_{\text{web1effLT}} := \rho_{\text{web1LT}} \cdot (y_{\text{gc1newLT}} - t_{\text{bottom1}}) = 1.183 \times 10^3 \cdot \text{mm}$$

$$b_{\text{web1LT1}} := b_{\text{web1effLT}} \cdot 0.4 = 473.084 \cdot \text{mm}$$

$$b_{\text{web1LT2}} := b_{\text{web1effLT}} \cdot 0.6 = 709.626 \cdot \text{mm}$$

$$b_{\text{web1gapLT}} := y_{\text{gc1newLT}} - t_{\text{bottom1}} - b_{\text{web1LT1}} - b_{\text{web1LT2}} = 0 \cdot \text{mm}$$

The final distance from bottom to gravity center.

$$z_{12aLT} := \frac{b_{\text{web1LT1}}}{2} + t_{\text{bottom1}} = 0.357 \text{ m}$$

$$z_{12bLT} := y_{\text{gc1newLT}} - \frac{b_{\text{web1LT2}}}{2} = 0.948 \text{ m}$$

$$z_{12cLT} := y_{\text{gc1newLT}} + \frac{h_{\text{tot}} - t_{\text{top1}} - y_{\text{gc1newLT}}}{2} = 1.991 \text{ m}$$

$$z_{12aLT\text{new}} := \begin{cases} z_{12aLT} & \text{if } \text{Class}_{\text{web1LT}} = 4 \\ 0 & \text{otherwise} \end{cases}$$

$$z_{12bLTnew} := \begin{cases} z_{12bLT} & \text{if } Class_{web1LT} = 4 \\ 0 & \text{otherwise} \end{cases}$$

$$z_{12cLTnew} := \begin{cases} z_{12cLT} & \text{if } Class_{web1LT} = 4 \\ \frac{h_{web1}}{2} + t_{bottom1} & \text{otherwise} \end{cases}$$

The final cross sectional constants are calculated for one of the girders, given the symmetry.

$$A_{12aLT} := b_{web1LT1} \cdot t_{web1} = 0.012 \text{ m}^2$$

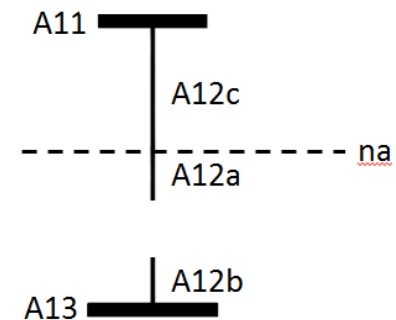
$$A_{12bLT} := b_{web1LT2} \cdot t_{web1} = 0.018 \text{ m}^2$$

$$A_{12cLT} := (h_{web1} - y_{gc1newLT} + t_{bottom1}) \cdot t_{web1} = 0.036 \text{ m}^2$$

$$A_{12aLTnew} := \begin{cases} A_{12aLT} & \text{if } Class_{web1LT} = 4 \\ 0 & \text{otherwise} \end{cases}$$

$$A_{12bLTnew} := \begin{cases} A_{12bLT} & \text{if } Class_{web1LT} = 4 \\ 0 & \text{otherwise} \end{cases}$$

$$A_{12cLTnew} := \begin{cases} A_{12cLT} & \text{if } Class_{web1LT} = 4 \\ h_{web1} \cdot t_{web1} & \text{otherwise} \end{cases}$$



The final gravity center from bottom of the bridge

$$y_{gc1finalLT} := \frac{A_{11} \cdot z_{11} + A_{12aLTnew} \cdot z_{12aLTnew} + \dots + A_{12bLTnew} \cdot z_{12bLTnew} + A_{12cLTnew} \cdot z_{12cLTnew} + A_{13LT} \cdot z_{13}}{A_{11} + A_{12aLTnew} + A_{12bLTnew} + A_{12cLTnew} + A_{13LT}} = 1.303 \text{ m}$$

The final moment of inertia

$$I_{tot1finalLT1} := I_{tot1newLT1} = 5.076 \times 10^{11} \cdot \text{mm}^4$$

$$I_{tot1finalLT2} := I_{tot1newLT2} = 5.076 \times 10^{11} \cdot \text{mm}^4$$

$$\begin{aligned}
I_{\text{tot1finalLT3}} := & \frac{b_{\text{top1}} \cdot t_{\text{top1}}^3}{12} + A_{111} \cdot \left(h_{\text{tot}} - y_{\text{gc1finalLT}} - \frac{t_{\text{top1}}}{2} \right)^2 \dots & = 5.088 \times 10^{11} \cdot \text{mm}^4 \\
& + \frac{t_{\text{web1}} \cdot b_{\text{web1LT1}}^3}{12} \dots \\
& + A_{12aLT\text{new}} \cdot \left(\frac{b_{\text{web1LT1}}}{2} + b_{\text{web1gapLT}} + b_{\text{web1LT2}} \right)^2 \dots \\
& + \frac{t_{\text{web1}} \cdot b_{\text{web1LT2}}^3}{12} + A_{12bLT\text{new}} \cdot \left(\frac{b_{\text{web1LT2}}}{2} \right)^2 \dots \\
& + \frac{t_{\text{web1}} \cdot (h_{\text{tot}} - y_{\text{gc1finalLT}} - t_{\text{top1}})^3}{12} \dots \\
& + A_{12cLT\text{new}} \cdot \left(\frac{h_{\text{tot}} - y_{\text{gc1finalLT}} - t_{\text{top1}}}{2} \right)^2 \dots \\
& + \frac{b_{\text{bottom1}} \cdot t_{\text{bottom1}}^3}{12} + A_{13LT} \cdot \left(y_{\text{gc1finalLT}} - \frac{t_{\text{bottom1}}}{2} \right)^2
\end{aligned}$$

$$\begin{aligned}
I_{\text{tot1finalLT4}} := & \frac{b_{\text{top1}} \cdot t_{\text{top1}}^3}{12} + A_{111} \cdot \left(h_{\text{tot}} - y_{\text{gc1finalLT}} - \frac{t_{\text{top1}}}{2} \right)^2 \dots & = 5.088 \times 10^{11} \cdot \text{mm}^4 \\
& + \frac{t_{\text{web1}} \cdot b_{\text{web1LT1}}^3}{12} \dots \\
& + A_{12aLT\text{new}} \cdot \left(\frac{b_{\text{web1LT1}}}{2} + b_{\text{web1gapLT}} + b_{\text{web1LT2}} \right)^2 \dots \\
& + \frac{t_{\text{web1}} \cdot b_{\text{web1LT2}}^3}{12} + A_{12bLT\text{new}} \cdot \left(\frac{b_{\text{web1LT2}}}{2} \right)^2 \dots \\
& + \frac{t_{\text{web1}} \cdot (h_{\text{tot}} - y_{\text{gc1finalLT}} - t_{\text{top1}})^3}{12} \dots \\
& + A_{12cLT\text{new}} \cdot \left(\frac{h_{\text{tot}} - y_{\text{gc1finalLT}} - t_{\text{top1}}}{2} \right)^2 \dots \\
& + \frac{b_{\text{bottomLTeff}} \cdot t_{\text{bottom1}}^3}{12} + A_{13LT} \cdot \left(y_{\text{gc1finalLT}} - \frac{t_{\text{bottom1}}}{2} \right)^2
\end{aligned}$$

$$I_{\text{tot1finalLT}} := \begin{cases} I_{\text{tot1finalLT1}} & \text{if } \begin{cases} \text{Class}_{\text{bottomflangeLT}} \neq 4 \\ \text{Class}_{\text{web1LT}} \neq 4 \end{cases} \\ I_{\text{tot1finalLT2}} & \text{if } \begin{cases} \text{Class}_{\text{bottomflangeLT}} = 4 \\ \text{Class}_{\text{web1LT}} \neq 4 \end{cases} \\ I_{\text{tot1finalLT3}} & \text{if } \begin{cases} \text{Class}_{\text{bottomflangeLT}} \neq 4 \\ \text{Class}_{\text{web1LT}} = 4 \end{cases} \\ I_{\text{tot1finalLT4}} & \text{if } \begin{cases} \text{Class}_{\text{bottomflangeLT}} = 4 \\ \text{Class}_{\text{web1LT}} = 4 \end{cases} \end{cases}$$

$$I_{\text{tot1finalLT}} = 5.076 \times 10^{11} \cdot \text{mm}^4$$

A.3.10.3 Buckling during casting verification

The verification is done considering a fictitious compressed column.

$$\sigma_{c1LT} := \frac{M_{\text{ULSLT1}}}{I_{\text{tot1finalLT}}} \cdot (y_{gc1finalLT}) = 79.152 \cdot \text{MPa} \quad \text{Maximum compressive stress}$$

$$l_{\text{cr}} := a_{\text{stiff}} = 8 \text{ m} \quad \text{Length of column}$$

$$A_{\text{bottom}} := b_{\text{bottom}} \cdot t_{\text{bottom1}} = 0.144 \text{ m}^2 \quad \text{Area of top flange}$$

$$N_{\text{Ed1}} := A_{\text{bottom}} \cdot \sigma_{c1LT} = 1.14 \times 10^4 \cdot \text{kN} \quad \text{Compressive force}$$

$$I_{\text{bottom}} := \frac{b_{\text{bottom}}^3 \cdot t_{\text{bottom1}}}{12} = 0.017 \text{ m}^4 \quad \text{Moment of inertia of bottom flange}$$

$$N_{\text{cr1}} := \frac{\pi^2 \cdot E_s \cdot I_{\text{bottom}}}{l_{\text{cr}}^2} = 5.596 \times 10^5 \cdot \text{kN} \quad \text{Critical buckling force}$$

$$\lambda_{\text{top1}} := \sqrt{\frac{A_{\text{bottom}} \cdot f_{y\text{bottom1}}}{N_{\text{cr1}}}} = 0.276 \quad \text{Slenderness}$$

$$\alpha_{\text{LT1}} := \begin{cases} 0.49 & \text{if } t_{\text{bottom1}} \leq 40 \text{ mm} \\ 0.76 & \text{otherwise} \end{cases}$$

$$\alpha_{\text{LT1}} = 0.76$$

$$\Phi_{LT1} := 0.5 \cdot \left[1 + \alpha_{LT1} \cdot (\lambda_{top1} - 0.2) + \lambda_{top1}^2 \right] = 0.567$$

$$\chi_{LT1} := \frac{1}{\Phi_{LT1} + \left(\Phi_{LT1}^2 - \lambda_{top1}^2 \right)^{0.5}} = 0.942$$

$$N_{Rd1} := \chi_{LT1} \cdot A_{bottom} \cdot \frac{f_{ybottom1}}{\gamma_{M1}} = 3.637 \times 10^4 \cdot \text{kN} \quad \text{Compressive resistance}$$

$$\mu_{16} := \frac{N_{Ed1}}{N_{Rd1}} = 0.313 \quad \text{Utilization ratio in buckling during casting}$$

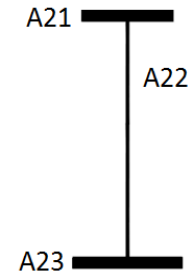
A.3.11 Buckling top flange during casting: span

We here consider that the top flange could buckle during casting since it will not be restrained by the concrete deck. We assume a load combination with only the weight of the concrete acting and we recalculated the properties of the cross section.

$$\epsilon_{\text{top2}} := \sqrt{\frac{235\text{MPa}}{f_{y\text{top2}}}} = 0.825$$

Gravity center from bottom of the bridge

$$y_{\text{gc2LT}} := \frac{A_{21} \cdot z_{21} + A_{22} \cdot z_{22} + A_{23} \cdot z_{23}}{A_{21} + A_{22} + A_{23}} = 1.319\text{m}$$



Distance from local and global gravity center

$$a_{21\text{LT}} := y_{\text{gc2LT}} - z_{21} = -1.461\text{m}$$

$$a_{22\text{LT}} := y_{\text{gc2LT}} - z_{22} = -0.081\text{m}$$

$$a_{23\text{LT}} := y_{\text{gc2LT}} - z_{23} = 1.299\text{m}$$

Moment of inertia

$$I_{\text{tot2LT}} := \frac{b_{\text{top}} \cdot t_{\text{top2}}^3}{12} + A_{21} \cdot a_{21\text{LT}}^2 + \frac{t_{\text{web2}} \cdot h_{\text{web2}}^3}{12} \dots = 1.969 \times 10^{11} \cdot \text{mm}^4$$

$$+ A_{22} \cdot a_{22\text{LT}}^2 + \frac{b_{\text{bottom}} \cdot t_{\text{bottom2}}^3}{12} + A_{23} \cdot a_{23\text{LT}}^2$$

A.3.11.1 Cross-sectional constants if bottom flange buckles

$$c_{\text{topLT}} := \frac{b_{\text{top}} - t_{\text{web2}}}{2} = 0.491\text{m}$$

Width of the top flange

$$\text{topflangeLT} := \frac{c_{\text{topLT}}}{t_{\text{top2}}} = 12.275$$

c/t

$$\text{Class}_{\text{topflangeLT}} := \begin{cases} 1 & \text{if } \text{topflangeLT} \leq 9\epsilon_{\text{top2}} \\ 2 & \text{if } 9\epsilon_{\text{top2}} < \text{topflangeLT} \leq 10\epsilon_{\text{top2}} \\ 3 & \text{if } 10\epsilon_{\text{top2}} < \text{topflangeLT} \leq 14\epsilon_{\text{top2}} \\ 4 & \text{otherwise} \end{cases}$$

$$\text{Class}_{\text{topflangeLT}} = 4$$

Cross sectional class

$$k_{\sigma\text{topLT}} := 0.43$$

$$\psi_{\text{topLT}} := 1$$

$$\lambda_{\text{ptopLT}} := \frac{\text{topflangeLT}}{28.4 \epsilon_{\text{top2}} \sqrt{k_{\sigma\text{topLT}}}} = 0.799$$

$$\rho_{\text{top1LT}} := \begin{cases} 1 & \text{if } \lambda_{\text{ptopLT}} \leq 0.748 \\ \frac{\lambda_{\text{ptopLT}} - 0.188}{\lambda_{\text{ptopLT}}^2} & \text{if } \lambda_{\text{ptopLT}} > 0.748 \end{cases}$$

$$\rho_{\text{topLT}} := \min(\rho_{\text{top1LT}}, 1) = 0.957$$

$$b_{\text{topLTEff}} := 2\rho_{\text{topLT}} \cdot c_{\text{topLT}} + t_{\text{web2}} = 0.958 \text{ m}$$

Effective width

The new cross sectional constants are calculated for one of the girders, given the symmetry.

$$A_{21\text{LT}} := \begin{cases} b_{\text{topLTEff}} \cdot t_{\text{top2}} & \text{if } \text{Class}_{\text{topflangeLT}} = 4 \\ A_{21} & \text{otherwise} \end{cases}$$

New distance of gravity center from bottom of the bridge

$$y_{\text{gc2newLT}} := \frac{A_{21\text{LT}} \cdot z_{21} + A_{22} \cdot z_{22} + A_{23} \cdot z_{23}}{A_{21\text{LT}} + A_{22} + A_{23}} = 1.301 \text{ m}$$

New distance from local and global gravity center

$$a_{21\text{newLT}} := y_{\text{gc2newLT}} - z_{21} = -1.479 \text{ m}$$

$$a_{22\text{newLT}} := y_{\text{gc2newLT}} - z_{22} = -0.099 \text{ m}$$

$$a_{23\text{newLT}} := y_{\text{gc2newLT}} - z_{23} = 1.281 \text{ m}$$

New moment of inertia

$$I_{\text{tot2newLT1}} := \frac{b_{\text{topLTEff}} \cdot t_{\text{top2}}^3}{12} + A_{21\text{LT}} \cdot a_{21\text{newLT}}^2 + \frac{t_{\text{web2}} \cdot h_{\text{web2}}^3}{12} \dots = 1.93279191 \times 10^{11} \cdot \text{mm}^4$$

$$+ A_{22} \cdot a_{22\text{newLT}}^2 + \frac{b_{\text{bottom}} \cdot t_{\text{bottom2}}^3}{12} + A_{23} \cdot a_{23\text{newLT}}^2$$

$$I_{\text{tot2newLT2}} := I_{\text{tot2LT}} = 0.1968945 \text{ m}^4$$

$$I_{\text{tot2newLT}} := \begin{cases} I_{\text{tot2newLT1}} & \text{if } \text{Class}_{\text{topflangeLT}} = 4 \\ I_{\text{tot2newLT2}} & \text{if } \text{Class}_{\text{topflangeLT}} \neq 4 \end{cases}$$

$$I_{\text{tot2newLT}} = 0.193 \text{ m}^4$$

A.3.11.2 Cross-sectional constants if web buckles

$$\sigma_{\text{c2LTw}} := \frac{M_{\text{ULSLT2}}}{I_{\text{tot2newLT}}} \cdot (h_{\text{tot}} - y_{\text{gc2newLT}}) = 139.261 \cdot \text{MPa} \quad \text{Compressive stress in the web}$$

$$\sigma_{\text{t2LTw}} := \frac{M_{\text{ULSLT2}}}{I_{\text{tot2newLT}}} \cdot (-y_{\text{gc2newLT}}) = -120.922 \cdot \text{MPa} \quad \text{Tensile stress in the web}$$

$$\text{web2LT} := \frac{h_{\text{web2}} - (\text{weld} + \text{butt weld})}{t_{\text{web2}}} = 150.556 \quad \text{c/t}$$

$$\alpha_{\text{gc2LT}} := \frac{y_{\text{gc2newLT}} - t_{\text{bottom2}}}{h_{\text{web2}}} = 0.464 \quad \psi_{\text{gc2LT}} := \frac{\sigma_{\text{t2LTw}}}{\sigma_{\text{c2LTw}}} = -0.868$$

$$\text{Class}_{\text{web2LT1}} := \begin{cases} 1 & \text{if } \text{web2LT} \leq \frac{36\epsilon_{\text{web2}}}{\alpha_{\text{gc2LT}}} \\ 2 & \text{if } \frac{36\epsilon_{\text{web2}}}{\alpha_{\text{gc2LT}}} < \text{web2LT} \leq \frac{41.5\epsilon_{\text{web2}}}{\alpha_{\text{gc2LT}}} \\ 3 & \text{if } \frac{41.5\epsilon_{\text{web2}}}{\alpha_{\text{gc2LT}}} < \text{web2LT} \leq 62\epsilon_{\text{web2}} \cdot (1 - \psi_{\text{gc2LT}}) \cdot \sqrt{-\psi_{\text{gc2LT}}} \\ 4 & \text{otherwise} \end{cases}$$

$$\text{Class}_{\text{web2LT2}} := \begin{cases} 1 & \text{if } \text{web2LT} \leq \frac{396\epsilon_{\text{web2}}}{13\alpha_{\text{gc2LT}} - 1} \\ 2 & \text{if } \frac{396\epsilon_{\text{web2}}}{13\alpha_{\text{gc2LT}} - 1} < \text{web2LT} \leq \frac{456\epsilon_{\text{web2}}}{13\alpha_{\text{gc2LT}} - 1} \\ 3 & \text{if } \frac{456\epsilon_{\text{web2}}}{13\alpha_{\text{gc2LT}} - 1} < \text{web2LT} \leq \frac{42\epsilon_{\text{web2}}}{0.67 + 0.33 \cdot \psi_{\text{gc2LT}}} \\ 4 & \text{otherwise} \end{cases}$$

$$\text{Class}_{\text{web2LT}} := \begin{cases} \text{Class}_{\text{web2LT2}} & \text{if } \alpha_{\text{gc2LT}} > 0.5 \\ \text{Class}_{\text{web2LT1}} & \text{if } \alpha_{\text{gc2LT}} \leq 0.5 \end{cases}$$

$$\text{Class}_{\text{web2LT}} = 4$$

Cross sectional class

$$k_{\sigma\text{web2LT}} := \begin{cases} 7.81 - 6.29\psi_{\text{gc2LT}} + 9.78\psi_{\text{gc2LT}}^2 & \text{if } 0 > \psi_{\text{gc2LT}} > -1 \\ 23.9 & \text{if } \psi_{\text{gc2LT}} = -1 \\ 5.98 \cdot (1 - \psi_{\text{gc2LT}})^2 & \text{if } -1 > \psi_{\text{gc2LT}} > -3 \end{cases}$$

$$k_{\sigma\text{web2LT}} = 20.645$$

$$\lambda_{\text{pweb2LT}} := \frac{\text{web2LT}}{28.4\epsilon_{\text{web2}} \cdot \sqrt{k_{\sigma\text{web2LT}}}} = 1.414$$

$$\rho_{\text{web2LT1}} := \begin{cases} 1 & \text{if } \lambda_{\text{pweb2LT}} \leq 0.673 \\ \frac{\lambda_{\text{pweb2LT}} - 0.055 \cdot (3 + \psi_{\text{gc2LT}})}{\lambda_{\text{pweb2LT}}^2} & \text{if } \lambda_{\text{pweb2LT}} > 0.673 \end{cases}$$

$$\rho_{\text{web2LT}} := \min(\rho_{\text{web2LT1}}, 1) = 0.649$$

$$b_{\text{web2effLT}} := \rho_{\text{web2LT}} \cdot (h_{\text{tot}} - y_{\text{gc2newLT}} - t_{\text{top2}} - \text{butt weld}) = 943.032 \cdot \text{mm}$$

$$b_{\text{web2LT1}} := b_{\text{web2effLT}} \cdot 0.4 = 377.213 \cdot \text{mm}$$

$$b_{\text{web2LT2}} := b_{\text{web2effLT}} \cdot 0.6 = 565.819 \cdot \text{mm}$$

$$b_{\text{web2gapLT}} := h_{\text{tot}} - y_{\text{gc2newLT}} - t_{\text{top2}} - \text{butt weld} - b_{\text{web2LT1}} - b_{\text{web2LT2}} = 510.647 \cdot \text{mm}$$

The final distance from bottom to gravity center.

$$z_{22aLT} := h_{\text{tot}} - t_{\text{top2}} - \text{butt weld} - \frac{b_{\text{web2LT1}}}{2} = 2.566 \text{ m}$$

$$z_{22bLT} := y_{\text{gc2newLT}} + \frac{b_{\text{web2LT2}}}{2} = 1.584 \text{ m}$$

$$z_{22cLT} := y_{\text{gc2newLT}} - \left(\frac{y_{\text{gc2newLT}} - t_{\text{bottom2}}}{2} \right) = 0.671 \text{ m}$$

$$z_{22aLT\text{new}} := \begin{cases} z_{22aLT} & \text{if } \text{Class}_{\text{web2LT}} = 4 \\ 0 & \text{otherwise} \end{cases}$$

$$z_{22bLT\text{new}} := \begin{cases} z_{22bLT} & \text{if } \text{Class}_{\text{web2LT}} = 4 \\ 0 & \text{otherwise} \end{cases}$$

$$z_{22cLTnew} := \begin{cases} z_{22cLT} & \text{if } Class_{web2LT} = 4 \\ \frac{h_{web2}}{2} + t_{bottom2} & \text{otherwise} \end{cases}$$

The final cross sectional constants are calculated for one of the girders, given the symmetry.

$$A_{22aLT} := b_{web2LT1} \cdot t_{web2} = 6.79 \times 10^{-3} \text{ m}^2$$

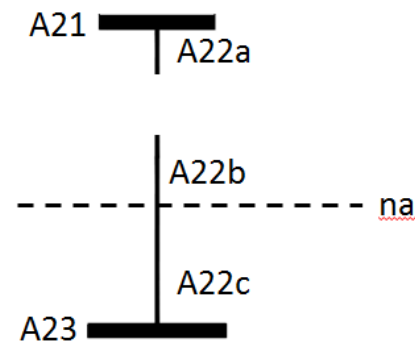
$$A_{22bLT} := b_{web2LT2} \cdot t_{web2} = 0.01 \text{ m}^2$$

$$A_{22cLT} := (y_{gc2newLT} - t_{bottom2}) \cdot t_{web2} = 0.023 \text{ m}^2$$

$$A_{22aLTnew} := \begin{cases} A_{22aLT} & \text{if } Class_{web2LT} = 4 \\ 0 & \text{otherwise} \end{cases}$$

$$A_{22bLTnew} := \begin{cases} A_{22bLT} & \text{if } Class_{web2LT} = 4 \\ 0 & \text{otherwise} \end{cases}$$

$$A_{22cLTnew} := \begin{cases} A_{22cLT} & \text{if } Class_{web2LT} = 4 \\ h_{web2} \cdot t_{web2} & \text{otherwise} \end{cases}$$



The final gravity center from bottom of the bridge

$$y_{gc2finalLT} := \frac{A_{21LT} \cdot z_{21} + A_{22aLTnew} \cdot z_{22aLTnew} + A_{22bLTnew} \cdot z_{22bLTnew} + A_{22cLTnew} \cdot z_{22cLTnew} + A_{23} \cdot z_{23}}{A_{21LT} + A_{22aLTnew} + A_{22bLTnew} + A_{22cLTnew} + A_{23}} = 1.24 \text{ m}$$

The final moment of inertia

$$I_{tot2finalLT1} := I_{tot2newLT1} = 1.933 \times 10^{11} \cdot \text{mm}^4$$

$$I_{tot2finalLT2} := I_{tot2newLT2} = 1.969 \times 10^{11} \cdot \text{mm}^4$$

$$\begin{aligned}
I_{\text{tot2finalLT3}} := & \frac{b_{\text{top}} \cdot t_{\text{top2}}^3}{12} + A_{21\text{LT}} \cdot \left(h_{\text{tot}} - y_{\text{gc2finalLT}} - \frac{t_{\text{top2}}}{2} \right)^2 \dots = 1.852 \times 10^{11} \cdot \text{mm}^4 \\
& + \frac{t_{\text{web2}} \cdot b_{\text{web2LT1}}^3}{12} \dots \\
& + A_{22\text{aLTnew}} \cdot \left(\frac{b_{\text{web2LT1}}}{2} + b_{\text{web2gapLT}} + b_{\text{web2LT2}} \right)^2 \dots \\
& + \frac{t_{\text{web2}} \cdot b_{\text{web2LT2}}^3}{12} + A_{22\text{bLTnew}} \cdot \left(\frac{b_{\text{web2LT2}}}{2} \right)^2 \dots \\
& + \frac{t_{\text{web2}} \cdot (y_{\text{gc2finalLT}} - t_{\text{bottom2}})^3}{12} \dots \\
& + A_{22\text{cLTnew}} \cdot \left(\frac{y_{\text{gc2finalLT}} - t_{\text{bottom2}}}{2} \right)^2 \dots \\
& + \frac{b_{\text{bottom}} \cdot t_{\text{bottom2}}^3}{12} + A_{23} \cdot \left(y_{\text{gc2finalLT}} - \frac{t_{\text{bottom2}}}{2} \right)^2 \\
I_{\text{tot2finalLT4}} := & \frac{b_{\text{topLTeff}} \cdot t_{\text{top2}}^3}{12} + A_{21\text{LT}} \cdot \left(h_{\text{tot}} - y_{\text{gc2finalLT}} - \frac{t_{\text{top2}}}{2} \right)^2 \dots = 1.852 \times 10^{11} \cdot \text{mm}^4 \\
& + \frac{t_{\text{web2}} \cdot b_{\text{web2LT1}}^3}{12} \dots \\
& + A_{22\text{aLTnew}} \cdot \left(\frac{b_{\text{web2LT1}}}{2} + b_{\text{web2gapLT}} + b_{\text{web2LT2}} \right)^2 \dots \\
& + \frac{t_{\text{web2}} \cdot b_{\text{web2LT2}}^3}{12} + A_{22\text{bLTnew}} \cdot \left(\frac{b_{\text{web2LT2}}}{2} \right)^2 \dots \\
& + \frac{t_{\text{web2}} \cdot (y_{\text{gc2finalLT}} - t_{\text{bottom2}})^3}{12} \dots \\
& + A_{22\text{cLTnew}} \cdot \left(\frac{y_{\text{gc2finalLT}} - t_{\text{bottom2}}}{2} \right)^2 \dots \\
& + \frac{b_{\text{bottom}} \cdot t_{\text{bottom2}}^3}{12} + A_{23} \cdot \left(y_{\text{gc2finalLT}} - \frac{t_{\text{bottom2}}}{2} \right)^2
\end{aligned}$$

$$I_{\text{tot2finalLT}} := \begin{cases} I_{\text{tot2finalLT1}} & \text{if } \begin{cases} \text{Class}_{\text{topflangeLT}} \neq 4 \\ \text{Class}_{\text{web2LT}} \neq 4 \end{cases} \\ I_{\text{tot2finalLT2}} & \text{if } \begin{cases} \text{Class}_{\text{topflangeLT}} = 4 \\ \text{Class}_{\text{web2LT}} \neq 4 \end{cases} \\ I_{\text{tot2finalLT3}} & \text{if } \begin{cases} \text{Class}_{\text{topflangeLT}} \neq 4 \\ \text{Class}_{\text{web2LT}} = 4 \end{cases} \\ I_{\text{tot2finalLT4}} & \text{if } \begin{cases} \text{Class}_{\text{topflangeLT}} = 4 \\ \text{Class}_{\text{web2LT}} = 4 \end{cases} \end{cases}$$

$$I_{\text{tot2finalLT}} = 1.852 \times 10^{11} \cdot \text{mm}^4$$

A.3.11.3 Buckling during casting verification

The verification is done considering a fictitious compressed column.

$$\sigma_{c2LT} := \frac{M_{\text{ULSLT2}}}{I_{\text{tot2finalLT}}} \cdot (h_{\text{tot}} - y_{\text{gc2finalLT}}) = 151.282 \cdot \text{MPa} \quad \text{Maximum compressive stress}$$

$$l_{\text{cr}} := a_{\text{stiff}} = 8 \text{ m} \quad \text{Length of column}$$

$$A_{\text{top}} := b_{\text{top}} \cdot t_{\text{top2}} = 0.04 \text{ m}^2 \quad \text{Area of top flange}$$

$$N_{\text{Ed2}} := A_{\text{top}} \cdot \sigma_{c2LT} = 6.051 \times 10^3 \cdot \text{kN} \quad \text{Compressive force}$$

$$I_{\text{top}} := \frac{b_{\text{top}}^3 \cdot t_{\text{top2}}}{12} = 3.333 \times 10^{-3} \text{ m}^4 \quad \text{Moment of inertia of bottom flange}$$

$$N_{\text{cr2}} := \frac{\pi^2 \cdot E_s \cdot I_{\text{top}}}{l_{\text{cr}}^2} = 1.079 \times 10^5 \cdot \text{kN} \quad \text{Critical buckling force}$$

$$\lambda_{\text{top2}} := \sqrt{\frac{A_{\text{top}} \cdot f_{y\text{top2}}}{N_{\text{cr2}}}} = 0.358 \quad \text{Slenderness}$$

$$\alpha_{\text{LT2}} := \begin{cases} 0.49 & \text{if } t_{\text{top2}} \leq 40 \text{ mm} \\ 0.76 & \text{otherwise} \end{cases}$$

$$\alpha_{\text{LT2}} = 0.49$$

$$\Phi_{LT2} := 0.5 \cdot \left[1 + \alpha_{LT2} \cdot (\lambda_{top2} - 0.2) + \lambda_{top2}^2 \right] = 0.603$$

$$\chi_{LT2} := \frac{1}{\Phi_{LT2} + \left(\Phi_{LT2}^2 - \lambda_{top2}^2 \right)^{0.5}} = 0.92$$

$$N_{Rd2} := \chi_{LT2} \cdot A_{top} \cdot \frac{f_{ytop2}}{\gamma_{M1}} = 1.154 \times 10^4 \cdot \text{kN}$$

Compressive resistance

$$\mu_{26} := \frac{N_{Ed2}}{N_{Rd2}} = 0.525$$

Utilization ratio in buckling during castin

$$\mu_6 := \max(\mu_{16}, \mu_{26}) = 0.525$$

A.3.12 Verification Summary

SUPPORT

SPAN

$$\mu_{11} = 0.807$$

$$\mu_{21} = 0.847$$

Bending resistance

$$\mu_{14} = 0.918$$

$$\mu_{24} = 0.927$$

Shear resistance

$$\mu_5 = 0.756$$

Deflection in SLS

$$\mu_{16} = 0.313$$

$$\mu_{26} = 0.525$$

Buckling during casting

Appendix B – Parametric studies

B.1 Parametric study of railway bridges

As explained in Section 8.4, a parametric study has been performed on railway bridges with span length varying between 16m and 30m. The following tables report the results of each bridge case.

Bridge data and design verifications																
	Original	New														
Length(m)	16	16	18	18	20	20	22	22	24	24	26	26	28	28	30	30
Bending	0,43	0,47	0,47	0,58	0,50	0,74	0,57	0,79	0,66	0,77	0,72	0,79	0,76	0,77	0,78	0,75
Shear	0,53	0,75	0,58	0,72	0,59	0,70	0,60	0,77	0,59	0,72	0,68	0,67	0,66	0,68	0,56	0,59
Deflection	0,44	0,55	0,53	0,67	0,61	0,81	0,71	0,95	0,79	0,99	0,88	1,00	0,97	0,97	0,97	0,99
Fatigue before PWT	0,99	3,79	0,99	3,61	0,99	3,29	1,00	3,19	0,99	3,01	0,99	3,00	1,00	2,92	0,85	2,30
Fatigue after PWT		0,95		0,99		0,97		0,98		0,99		0,99		0,97		1,00
A of I-sections (m²)	0,17	0,15	0,18	0,16	0,19	0,15	0,20	0,16	0,21	0,17	0,22	0,18	0,23	0,19	0,25	0,21

Bridge cost analysis

	16	18	20	22	24	26	28	30
Length(m)								
Material saving (%)	0,16	0,15	0,22	0,21	0,18	0,18	0,18	0,16
Cost saving (SEK)	22671	24697	44834	47076	46299	53069	60269	61433
Cost saving (%)	15%	14%	22%	20%	17%	18%	17%	16%

B.2 Parametric study of highway bridges

As explained in Section 9.4, a parametric study has been performed on highway bridges with span length varying between 16m and 44m. The following tables report the results of each bridge case.

Bridge data and design verifications																
	Original	New														
Lenght(m)	16	16	20	20	24	24	28	28	32	32	36	36	40	40	44	44
Bending	0,95	0,928	0,953	0,948	0,954	0,938	0,954	0,954	0,95	0,901	0,952	0,952	0,955	0,933	0,906	0,771
Shear	0,87	0,761	0,801	0,795	0,837	0,809	0,861	0,861	0,771	0,743	0,805	0,805	0,842	0,707	0,773	0,752
Deflection	0,769	0,954	0,798	0,956	0,853	0,956	0,874	0,874	0,895	0,954	0,922	0,922	0,948	0,951	0,951	0,957
Fatigue before PWT	0,99	2,08	0,87	1,92	0,73	1,5	0,61	0,61	0,5	0,85	0,41	0,41	0,34	0,42	0,2	0,21
Fatigue after PWT		1		0,8		0,61		0,48		0,85				0,42		0,21
A of I-sections (m²)	0,057	0,047	0,071	0,057	0,081	0,064	0,091	0,091	0,1	0,083	0,11	0,11	0,118	0,108	0,134	0,126

Bridge cost analysis

Length(m)	16	20	24	28	32	36	40	44
Material saving (%)	0,18	0,20	0,21	0,19	0,17	0,14	0,08	0,06
Cost saving (SEK)	2226	6111	10374	10487	11938	6722	-6714	-17313
Cost saving (%)	5%	8%	10%	8%	7%	3%	-3%	-5%